Miguel Alexandre Castanheira Marques

Licenciado em Ciências da Engenharia Electrotécnica e de Computadores

Sistema on-line de detecção de avarias em motores de indução baseado em PCA

Dissertação para obtenção do Grau de Mestre em Engenharia Electrotécnica e de Computadores

Orientador: Doutor João Francisco Alves Martins, Professor Auxiliar, Faculdade de Ciências e Tecnologia da Universidade Nova de Lisboa

Co-orientador: Mestre Rui Dias Jorge, EFACEC

Júri:

Presidente: Doutor João Miguel Murta Pina
Arguentes: Doutor Duarte de Mesquita e Sousa
Doutor Vitor Manuel de Carvalho Fernão Pires

FACULDADE DE CIÊNCIAS E TECNOLOGIA
UNIVERSIDADE NOVA DE LISBOA

Setembro 2012

Miguel Alexandre Castanheira Marques

BSc in Electrical and Computer Engineering

On-line system for faults detection in induction motors based on PCA

Dissertation to obtain the degree of Master in Electrical and Computer Engineering

Supervisor: João Francisco Alves Martins, PhD, Science and Tecnology Faculty from Universidade Nova de Lisboa

Co-supervisor: Rui Dias Jorge, MSc, EFACEC

Evaluation Board:

President: Professor João Miguel Murta Pina
Opponents: Professor Duarte de Mesquita e Sousa
Professor Vitor Manuel de Carvalho Fernão Pires

FACULDADE DE CIÊNCIAS E TECNOLOGIA
UNIVERSIDADE NOVA DE LISBOA

September 2012

Copyright

Acknowledgments

I express my deep thanks to the Department of Electrotechnical Engineering from Science and Technology Faculty who contributed to this work and for my personal and professional formation.

To *UNINOVA*, Instituto de Desenvolvimento de Novas Tecnologias for financial and institutional support in the acquisition of the electric motors.

My sincere thanks to my advisor, Prof. João Martins, for his singular personality and the technical and scientific teachings that collaborated to this work.

To Eng. Rui Dias Jorge for the attention, help and openness that always showed when I needed.

To Eng. Luís Filipe Mendes for the precious help and support throughout this work. To the rest of *EFACEC*'s working group by the goodwill and support.

My deep thanks to my friends Bruno Valente, Fábio Júlio, Flávio Diniz, Paulo Pereira and Pedro Gomes my thanks for your friendship, support and for having accompanied me during this years.

I wish to thank to Bruno Caixinha, Bruno Duarte, Carlos Calmeiro, Carlos Carvalho, Catarina Domingues, Catarina Lucena, Fábio Alves, Gonçalo Azevedo, João Chalaça, Luís Lopes, Luís Miranda, Micael Simões, Pedro Almeida, Pedro Oliveira, Raquel Melo, Ricardo Legas, Ricardo Mendonça, Vanessa Chamorrinha, Vitor Astúcia, my faculty friends and colleagues for their assistance and the funny moments that we passed in these years.

To my friends from the Department of Electrotechnical Engineering and the *IEEE* Student Branch, David Inácio and Pedro Pereira, for their friendship and support.

After completing this work could not fail to deeply thanks to my parents, my sister and my grandparents Margarida and Frutuoso for everything they did for me and the way it contributed to my education and happiness.

Finally, I want to thank in a very special way to Rita, for the love, encouragement and understanding that has always shown.

Sumário

Actualmente na indústria existem muitos processos onde a intervenção humana é substituída por máquinas eléctricas, especialmente máquinas de indução devido ao seu baixo custo, elevado desempenho e robustez. Embora, a máquina de indução seja um dispositivo altamente fiável, também é susceptível a falhas. Portanto, o estudo do estado da máquina de indução é essencial para reduzir custos financeiros e humanos.

As falhas em máquinas de indução podem ser divididas basicamente em dois tipos: falhas eléctricas e falhas mecânicas. As falhas eléctricas representam entre 40% e 50% das falhas reportadas e também podem ser divididas basicamente em dois tipos: desequilíbrios no estator e barras quebradas no rotor.

Tendo em conta a elevada dependência das máquinas eléctricas, é necessário dispor de sistemas de diagnóstico e monitorização para máquinas de indução. É apresentado neste trabalho um sistema on-line para detecção e diagnóstico de falhas eléctricas em motores de indução com base na monitorização das correntes de alimentação da máquina. O objectivo principal é detectar e identificar a presença de barras quebradas no rotor e curto-circuitos no estator da máquina. A presença de falhas na máquina provoca diferentes perturbações nas correntes de alimentação. Portanto através do uso de um referencial fixo, como é o caso da transformada αβ é possível extrair e manipular os resultados obtidos a partir das correntes de alimentação utilizando a decomposição em valores e vectores próprios.

Palavras-Chave: máquina de indução, diagnóstico, detecção de falhas, monitorização de condição, análise dos componentes principais, PCA, valor próprio, vector próprio

Abstract

Nowadays in the industry there many processes where human intervention is replaced by electrical machines, especially induction machines due to his robustness, performance and low cost. Although, induction machines are a high reliable device, they are also susceptible to faults. Therefore, the study of induction machine state is essential to reduce human and financial costs.

The faults in induction machines can be divided mainly into two types: electrical faults and mechanical faults. Electrical faults represent between 40% and 50% of the reported faults and can be divided essentially in 2 types: stator unbalances and broken rotor bars.

Taking into account the high dependency of induction machines and the massive use of automatic processes the industrial level, it is necessary to have diagnostic and monitoring systems these machines. It is presented in this work an on-line system for detection and diagnosis of electrical faults in induction motors based on computer-aided monitoring of the supply currents. The main objective is to detect and identify the presence of broken rotor bars and stator short-circuits in the induction motor. The presence of faults in the machine causes different disturbances in the supply currents. Through a stationary reference frame, such as αβ transform it is possible to extract and manipulate the results obtained from the supply currents using Eigen decomposition.

Keywords: induction motor, diagnosis, fault detection, condition monitoring, principal component analysis, PCA, eigenvalue, eigenvector

Table of Contents

List of Figures

List of Tables

List of Symbols

Symbol	Description	Units
A,B,C	Symbology used to identify the phases of a three-phase current system	
bd	Ball diameter	mm
E	Correlation matrix	
f_1	Electrical supply frequency	Hz
$f_{b,o}$, $f_{b,i}$, $f_{b,r}$	Bearing damages fault frequency	Hz
f_{ecc}, $f_{slot+ecc}$	Air-gap eccentricities fault frequency	Hz
f_{sc}	Stator windings fault frequency	Hz
f_r	Mechanical rotor speed	Hz
I	Identity matrix	
i_a, i_b, i_c	Motor supply currents	A

i_M	Maximum value of the supply phase current	A
i_α, i_β	αβ stator current components	A
I_{nom}	Nominal Current of dc generator	A
k, m	Positive integer number	
n	Number of bearing balls	
N	Motor Rated Speed	RPM
n_d	Rotating eccentricity order	
n_w	Stator MMF harmonic order	
p	Number of pole pairs	
pd	Bearing pitch diameter	mm
P_{el}	Electrical Power	kW, MW
P_{mec}	Mechanical Power	HP
R	Rotor slots number	
s	Slip per unit	%
S	Apparent Power	kVA
SF, SF_{1BB}, SF_{6BB}	Fault Severity Factor	%
t	Time variable	s, ms
u	Eigenvectors	
X	Data matrix	
β	Contact angle of the balls on the races	
λ	Eigenvalues	
ω	Angular supply frequency	rad/s
V_{rms} ,V_{nom}	Motor nominal voltage	V

Acronyms

AC	Alternate Current
ADC	Analog-Digital Converter
AI	Artificial Intelligence
ARM	Advanced RISC Machine
BM	Breakdown Maintenance
C#	C Sharp
CBM	Condition Based Maintenance
CCS	Code Composer Studio
Cerberus	Framework of TPU x220
CM	Condition Monitoring
CMS	Condition Monitoring System
CPU	Central Processing Unit
CT	Current Transformer
DC	Direct Current
De Lorenzo	Italian company that develop educational systems
DLL	Dynamic Link Library
DMA	Direct Memory Access
DNP	Distributed Network Protocol
DSP	Digital Signal Processor
DTC	Direct Torque Control
EFACEC	Portuguese company
EMIF	External Memory Interface

EPRI	Electric Power Research Institute
FDD	Fault Detection and Diagnosis
FFT	Fast Fourier Transform
GOOSE	Generic Object Oriented Substation Events
GPIO	General Purpose Input/Output
HMI	Human Machine Interface
HP	Horse Power
HV	High Voltage
I/O	Input/Ouput
IAS	Industry Applications Society
IDE	Integrated Development Environment
IEC	Internacional Electrotechnical Commission
IEEE	Institute of Electrical and Electronic Engineers
IFAC	International Federation of Automatic Control
IMS	Intelligent Maintenance System Group
IRIG	Inter-Range Instrumentation Group
ISO	Internacional Organization for Standardization
ISR	Interrupt Service Routine
LCD	Liquid Crystal Display
LED	Light-Emitting Diode
MATLAB	MATrix LABoratory
MCSA	Motor Current Signature Analysis
MMoDiS	Machine Monitoring and Diagnosis System
MV	Medium Voltage

OMAP	Open Multimedia Applications Platform
OOL	Object Oriented Language
PC	Principal Components
PCA	Principal Component Analysis
PdM	Predictive Maintenance
PLC	Programmable Logic Controller
PM	Preventive Maintenance
PWM	Pulse Width Modulation
RCM	Reliability-Centered Maintenance
RISC	Reduced Instruction Set Computing
RMS	Root Mean Square
RPM	Revolutions per Minute
RTDB	Real-Time Data Base
SDRAM	Synchronous Dynamic Random Access Memory
SNTP	Simple Network Time Protocol
SVD	Single Value Decomposition
Syrius	Framework of TPU x220
TCP/IP	Transmission Control Protocol/Internet Protocol
TPU	Terminal Protection Unit
UML	Unified Modelation Language
UMP	Unbalanced Magnetic Pull
VMM	Vienna Monitoring Method
VT	Voltage Transformer
x220	Line of products from TPU developed by EFACEC

XML	eXtensible Markup Language

Chapter 1

Introduction

In this introductory chapter, it is presented the context of the work that resulted in this thesis. The Section 1.1 refers to the motivation for the theme of this work and in Section 1.2 is made a general description of the state-of-the-art. In Section 1.3 are listed the objectives and the contributions of this research work and in Section 1.4 it is made reference to the organization of the thesis.

1.1 Motivation

Rotating electrical machines, especially three-phase induction machines, perform critical functions as part of industrial processes, mainly due to its simplicity of construction, low production cost, robustness and reduced maintenance compared for example, with *dc* machines or synchronous machines. It is estimated that about 60% of the electrical energy produced in the United States is consumed by electrical machines, such as synchronous machines, *dc* machines or induction machines [1]. In addition, induction motors typically consume 40 % to 50 % of all electrical energy produced in a country [2]. Therefore induction motors have a special role in the economy of the industrialized countries.

However despite the robustness of the induction motor, any electromechanical device presents erosion and need maintenance to prevent that faults put in risk the equipment and manufacturing processes. The task of discovering the state of the machine's components is complicated and a time consuming task, because it is necessary the presence of technical experts and sometimes it is necessary to replace the failed machine for an healthy machine to proceed to its repair. In the case of large-sized machines this task becomes even more complicated by the fact that sometimes it is not possible to replace the machine and the tools necessary to perform the repairs are expansive and not easy to carry. All these mentioned difficulties have human and economic costs, such as the need to stop industrial processes and the waste of raw materials. Due to its importance, such equipment needs special attention to assure his performance, reliability and efficiency and to avoid human and economic costs [3].

According to Tavner *et al*. [3], the annual investment per employee in machinery in certain areas, such as oil and gas is growing. The same authors stated that the average annual costs on maintenance were 80% of the amount annually invested in plant and machinery.

Taking into account the reports published in [3] is urgent to develop intelligent systems that detect the presence of faults in the machines in order to reduce maintenance costs. These systems will allow the possibility of scheduled maintenance and predict the need for maintenance before serious deterioration or fault occurs, making it possible to increase the reliability of equipment, the improvement of his behavior and performance [4].

1.2 Overview

The first public developments in this area came in 1935 with the deduction of expressions for induction motors with unbalances in the input voltage source [5]. In the following years the scientific activity in the area was related only to the detection of defects in squirrel-cage rotors [6-8]. In the early of the 1960s, some research works expressed a concern in studying the behavior of the induction motors in applications related to its protection [9, 10].

According to Penman and Stavrou [11], in the 1970s, was established a generalized rotating field theory with the purpose of demonstrate that the presence of asymmetries in the machine will lead to the appearance of induced currents in the stator windings at frequencies close to the supply frequency of the machine. In this decade was also proposed [12] the use of a set of thermocouples with the objective of monitoring the temperature in the rotor bars and end-rings, in order to protect them from overheating. The proposed system was implemented in high power induction and synchronous machines.

Only in the 1970s and 1980s the researchers have intensified efforts in analyzing the effects that caused the appearance of faults in induction machines. Initially the study of these causes was performed in laboratory tests based on measurements of electric or magnetic quantities. This was made only by observation of the measurements, without the intervention of any type of device with computing power [13-18].

Williamson and Smith [14] developed a rotor model with the objective of evaluating the cases related with broken rotor bars and cracked end-rings. The model is formed by two adjacent bars and two end-rings that link the bars. It is important to note that is this model the air-gap is considered small when compared with the radius of the rotor, the rotor bars and isolated from the rotor cored and the saturation of the rotor core is not considered.

In 1983, Dey [19] developed the first on-line protection system based on the measurements of the machine axial flux with the aid of a micro-computer. After this, Thomson and Stewart [20] in 1987 present an on-line fault detection system based on spectral analysis of the input current. However, the proposed system only detected broken rotor bars and air-gap eccentricities and was tested only at a laboratory level. In 1989 Kliman *et al.* [21] also developed an on-line system for fault detection, similar to the system proposed by Thomson and Stewart [20], but the difference was in the spectral analysis. This method uses input current and axial flux to make the spectral analysis. Kliman *et al.* also patented in the United States, two applications [22, 23] for fault detection and diagnosis in induction machines.

Siyambalapitiya and McLaren [4] in 1990 presented a study that suggests the use of methods to quantify the savings achieved through the implementation of a monitoring system for large induction machines in industrial environments. The study also suggests the possibility to evaluate the economic viability of using a specific monitoring system, depending on the desired reliability for the system.

During the 1990s to the present, fault detection and diagnosis (*FDD*) in induction machines is a research area that had a great evolution, as seen by the number of proposed methodologies, such as neural networks [24-26], finite element methods [27-29], current space patterns [30-35], fuzzy logic [36, 37], parameter estimation [38-40], spectral analysis [41-45], wavelets transform [46, 47], negative sequence components [48], mathematical methods [49-51], vibration monitoring [52, 53] and artificial intelligence (*AI*) techniques [54].

However, although there is a large variety of techniques for detection and diagnosis there are some gaps in this area that have not yet been filled. Firstly due to the variety of electrical machines, the application of fault detection and diagnosis (*FDD*) techniques becomes more difficult. Secondly the fact that most of the research works in this field are only implemented at laboratory level, there is no integrated product that is ready to be connected to any induction machine.

Currently the types of techniques used or developed for condition monitoring and fault detection are almost the same techniques used at 10 years ago. However, due to major developments in terms of computing power of microprocessors and communication technologies, the direction of research in the diagnosis and detection of faults in electrical machines, points to the use of *FDD* methods based on on-line non-invasive measurements. This type of measurement only uses voltage and current measurements from the motor terminals and do not require additional sensors.

1.3 Objectives and Contributions

In the context of condition monitoring systems (*CMS*), where a continuous evaluation of the equipment health during its serviceable life is made while the machine is running, the main objective of the present work is the development of an on-line system for detection and diagnosis of electrical faults in three-phase induction motors. To achieve the main objective the present work refers to the development of a software infrastructure called *Machine Monitoring and Diagnosis System* (*MMoDiS*) that will be presented throughout this document. In synthesis there were established the following objectives for this work:

1. Establish a theoretical treatment by reviewing the state-of-the-art in the field of faults in electrical machines and what techniques and methods are used for detection and identification of these faults;
2. Development of a software application based on *EFACEC*'s digital protection relay, the Terminal and Protection Unit (*TPU x220*) that detects and diagnose electrical faults in three-phase induction motors;
3. Simulation and experimental tests, using the developed software application in low power induction machines.

Concerning to the contribution of this research work, since that the existing systems for fault detection and diagnosis (*FDD*) in electrical machines are only implemented only at laboratory level, the contribution of this work is the development of a software application integrated in an industry product that makes a continuous monitoring of the machine's state.

1.4 Outline of Dissertation

The present work is composed by seven chapters and is organized in the following way:

Chapter 2

This chapter presents an overview of the faults that can be found in induction machines and a description of the possible causes and consequences produced by each fault.

Chapter 3:

In this chapter the first sections presents some terminologies and definitions that are used in the *FDD* field. There are also classified the *FDD* methods that currently exists. Secondly, it is made a survey on the different concepts of maintenance and its

importance. Then, it is made a wide description of the methods that are currently used to detect and diagnose faults in induction machines.

Chapter 4:

The fourth chapter presents a major description of the Terminal Protection Unit (*TPU*) x220 used in this work. Initially is made and introduction to the equipment, why it was developed and what is his objective. In the final sections it is made description of the hardware and software architecture.

Chapter 5:

This chapter explains the whole architecture of *MMoDiS* since the high-level representations up to the description of the routines. Firstly, *MMoDiS* is presented as a on-line condition monitoring systems and are also discussed his operational requirements. Secondly, it is described the conceptual model of the system, that basically is the idea that supports the developed solution. Then, it is explained the architectural diagram of the system and finally the description of the existing routines inside the system.

Chapter 6:

It will be shown an example of *MMoDiS* in operation, as well as several tests made to the proposed solution. First is described the experimental setup used, and finally it is shown the simulation and experimental results obtained.

Chapter 7:

This chapter provides an overview of the work, reviews the contributions of this thesis and the possible future work.

Appendix A:

In appendix A is the code used for simulation purposes.

1.5 Publications

The following publications resulted from the research work presented in this Dissertation:

"Fault Detection and Diagnosis in Induction Machines: A Case Study", Miguel Marques, João Martins, V. Fernão Pires, Rui Dias Jorge and Luís Filipe Mendes. Waiting for acceptance in the 4th Doctoral Conference on Computing, Electrical and Industrial Systems – DoCEIS 2013, Caparica, Lisbon, Portugal, 15-17 April, 2013.

Chapter 2

Induction Machines Faults

This chapter presents a major description of the types of faults and their consequences to three-phase induction motors. Moreover, it explains the causes and the physical phenomena that lead to the appearance of faults in induction motors.

2.1 Introduction

In Figure 2.1 is presented a squirrel-cage induction machine and his components. Despite of an induction motor has several parts it is basically composed by a wound stator and by a wound or squirrel-cage rotor.

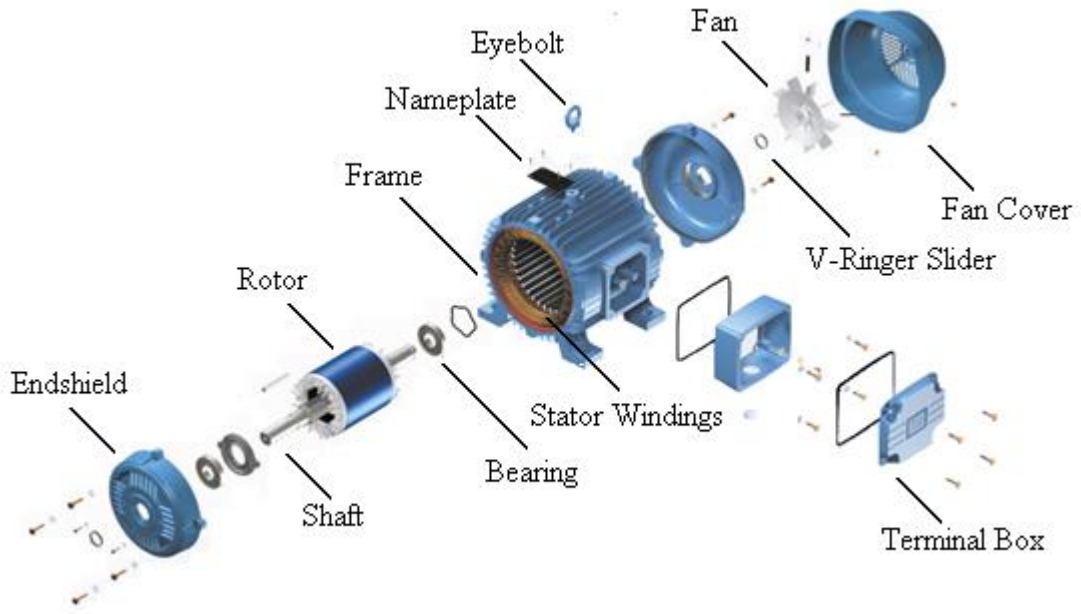

Figure 2.1 – Components of a squirrel-cage induction motor (adapted from [55]).

The stator is essentially composed by three parts: frame, lamination core and windings. The frame gives mechanical support to stator windings, the lamination core and the rotor bearings. The stator windings are composed by three coils equally distributed through the stator lamination core. The rotor is mainly composed by conductive rotor bars that are short-circuited, a shaft that gives mechanical support to the rotor and transmits the generated torque, a fan that cools the frame and bearings that reduce the friction.

Electrical machines and drive systems are subjected to many different types of faults. According to Nandi and Toliyat [56], faults in squirrel-cage induction machines can be classified as:

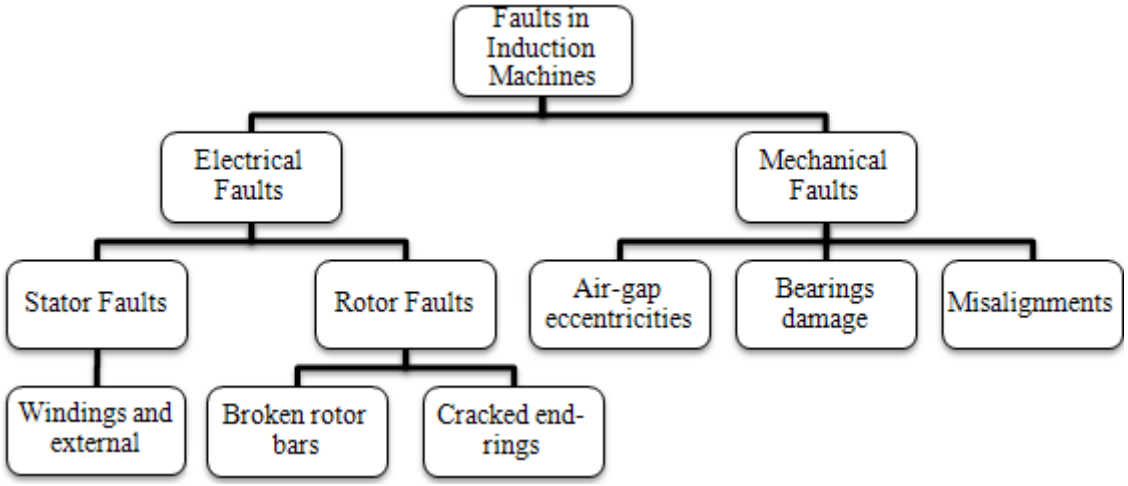

Figure 2.2 – Types of faults in induction machines (adapted from [56])

Several surveys have been carried out on the reliability of electrical machines. The distribution of faults in induction machines presented in Table 2.1 is based on published surveys [57, 58]. This table presents the surveys conducted by the Motor Reliability Working Group of the *IEEE-IAS*, which surveyed approximately 1000 motors [57] and the survey conducted by the Electric Power Research Institute (*EPRI*) that covered about 5000 motors [58], approximately 97% of the surveyed machines were three-phase induction motors.

Fault Component	Percentage of faults (%)	
	IEEE-IAS	***EPRI***
Bearings Related	44	41
Stator Windings Related	26	37
Rotor Related	8	10
Others	22	12

Table 2.1 – Comparison between surveys of faults distribution in electrical machines.

The *IEEE-IAS* survey and the *EPRI* report identified several faults mechanisms. Through the Table 2.1 it is possible to verify that both surveys converge to similar values. The majority of faults are related to mechanical causes, more specifically the bearing damages (between 41% and 44%). The electrical faults occur mainly due to faults in the stator windings (26% to 37%) and only a small percentage is related to rotor faults (about 10%). The faults referred as others, are due to shaft and coupling malfunctions or related with external devices.

It should be noted that the provided data by the *IEEE-IAS* survey does not take into account the fact that the machines work in different applications. So a fault occurrence depends on the application of the machine.

In Figure 2.3 is also reported another study published in the *EPRI* report [58] that analyses more specifically the distribution of faults for each item listed in the Table 2.1.

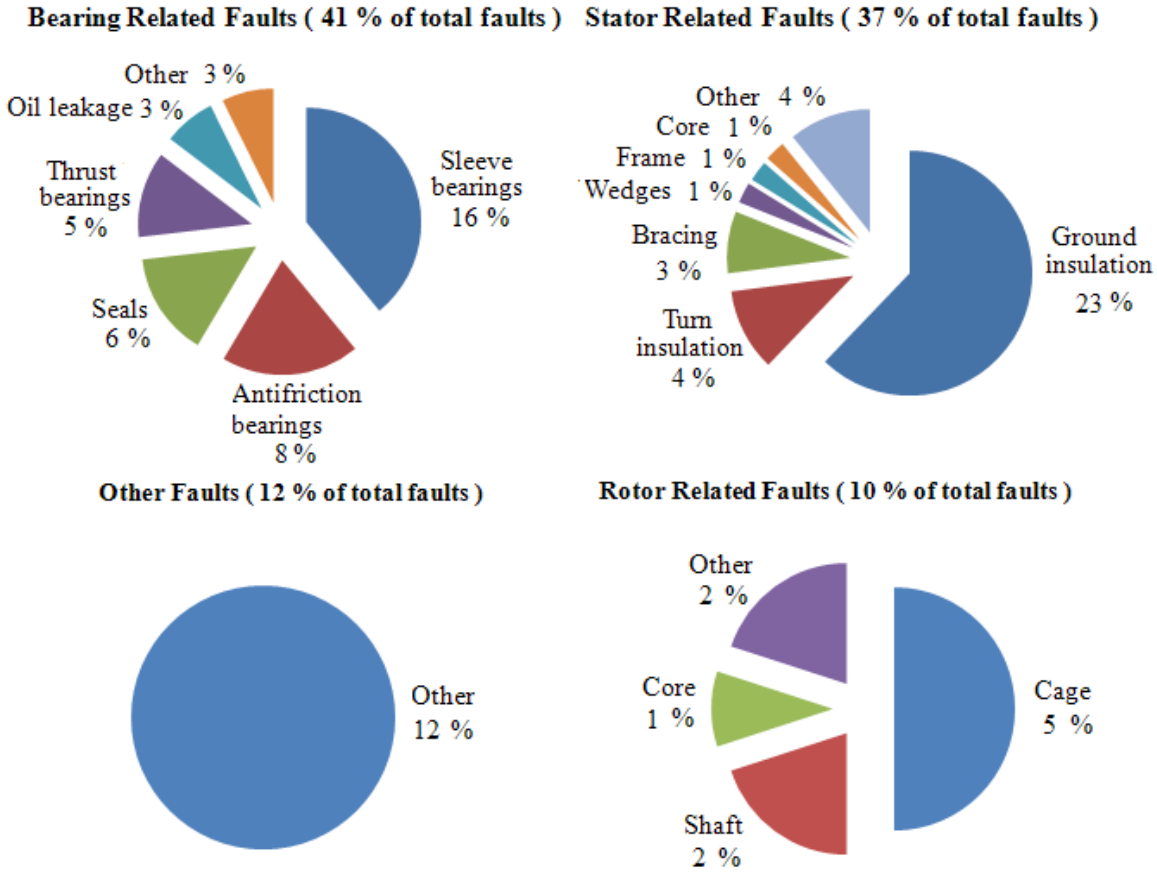

Figure 2.3 – Faults distribution in induction machines

The percentage of faults associated exclusively with bearings is more than half of the graphic events. In the case of stator related faults, it is noted that insulation faults are the most common occurrences, they represent 27% in a total of 37 %. In the rotor side the most common faults are related to problems in the cage structure.

The *IEEE-IAS* survey [57] studied the causes that contributed to the occurrence of faults and reached the following results:

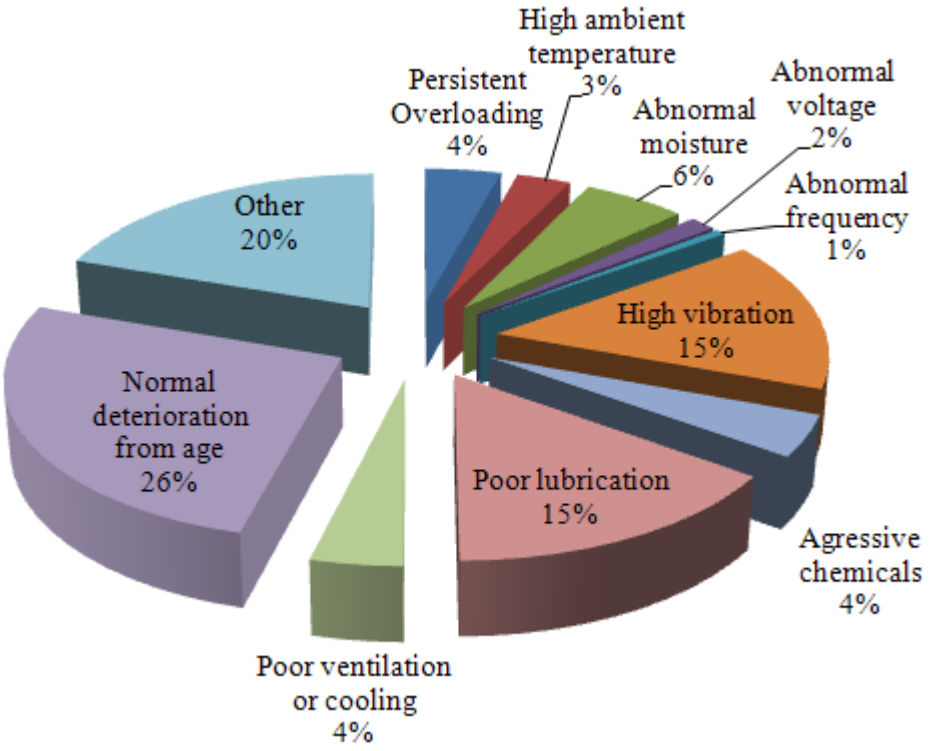

Figure 2.4 – Events that contribute for induction motor faults.

The Figure 2.4 shows that the major contributing cause reported is normal deterioration from age. High vibration and poor lubrication were also reported as major contributors for the occurrence of faults which reinforce the results from Table 2.1 and Figure 2.3 where mechanical faults, such as bearing damages are the principal cause for the occurrence of faults in induction motors.

2.2 Electrical Faults

As stated before, electrical faults can be divided in stator and rotor faults. They represent between 40% and 45% of the reported faults. This section reports the most common electrical faults and their causes in three phase induction motors.

2.2.1 Stator Faults

Nandi and Toliyat [56] affirm that these faults are usually related to insulation failures and there are two types of faults in the stator windings that can be considered: asymmetries in the stator windings as an open phase fault and short circuits in the stator windings.

The faults related to stator asymmetries are the result of unbalanced phase currents caused by a negative sequence component produced in the input current, which leads to asymmetries in

the machine impedance. As a result, the machine will operate with reduced torque. However, unbalanced current can also be caused by unbalance of the load and/or machine saturation [59].

In the case of short circuits in the stator windings they are usually related to faults in the stator insulation system that cause turn-to-turn fault that initially remain undetected but later can progress to more serious short-circuits that can damage the machine [60]. Usually short-circuits occur between turns of one phase, or between turns of two phases, or between turns of all phases. The results produced by short circuits in the stator windings are presented in the Figure 2.5 and Figure 2.6.

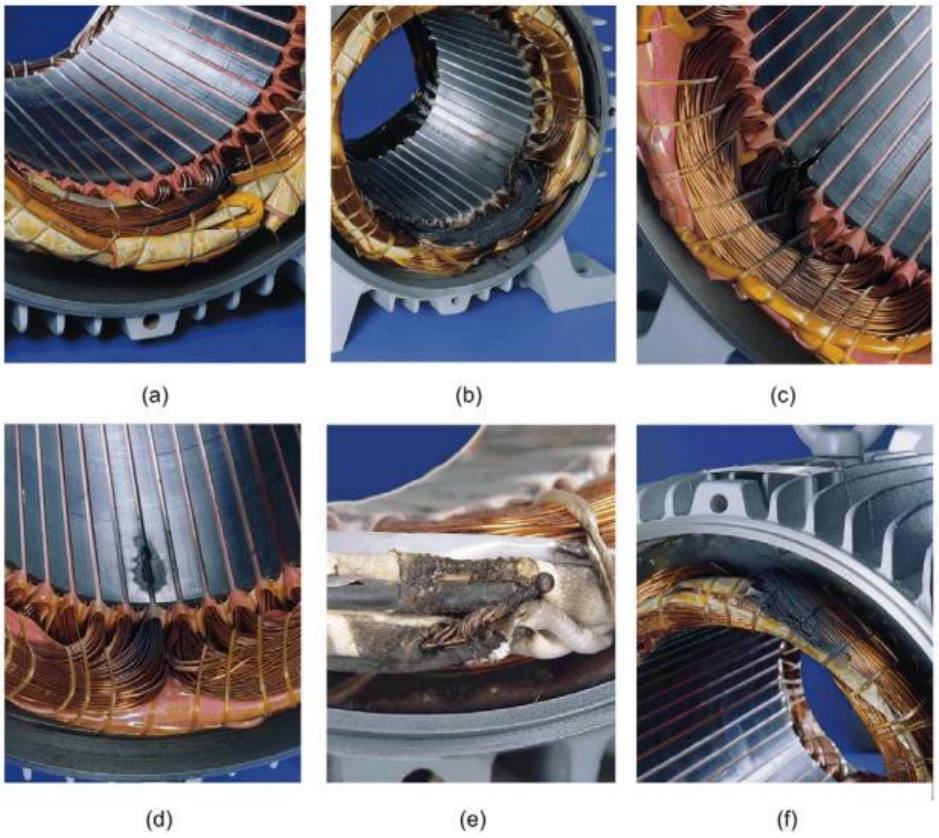

Figure 2.5 - Typical insulation damage leading to inter-turn short circuit of the stator windings in three-phase induction motors. (a) Inter-turn short circuits between turns of the same phase. (b) Winding short circuited. (c) Short circuits between winding and stator core at the end of the stator slot. (d) Short circuits between winding and stator core in the middle of the stator slot. (e) Short circuit at the leads. (f) Short circuit between phases. [61]

According to Bonnett and Soukup [62] most failures that occur in the stator are related to thermal, electrical, mechanical and environmental stresses. The physical integrity of stator windings insulation system is critical to a correct motor operation. For such there are a set of insulation subsystems that have to be considered:

- Between conductors of the same coil;
- Between different phases;
- Forehead area of the coils;

- Between the conductors and the slot where they are housed.

When the insulation system loses its physical integrity, it ceases to be resistant to stresses and occurs a situation of short circuit that later can lead to a failure situation. It is estimated that for every 10 ºC increase in the operating temperature of the windings, the lifetime of the insulation system is halved [62].

2.2.1.1 Causes for Stator Faults

Thermal Stresses

Thermal stresses are related with the incorrect use of the motor that will later cause an increase in temperature. Over time the insulating materials that constitute the insulation system are brittle and crack. These symptoms are related to the thermal stresses that causes expansion and contraction of these materials. Bonnett and Soukup [62] argue that this type of overloads can be caused by any of the following conditions:

- Voltage Variations: Nowadays the induction motors are manufactured to support variations in the supply voltage of about 10%. The operation outside these limits will cause a decrease in the lifetime of the insulation system;
- Unbalanced Phase Voltage: The existence of small unbalances in supply voltage causes an excessive increase in temperature of the windings and therefore in the insulation system. For each 3.5% unbalanced voltage per phase there is an increase of 25% in the temperature of the phase with the highest current value. The supply voltage must be kept as balanced as possible to avoid damages in the insulation system;
- Repeated and/or consecutive starts: It is well known that during the startup, the stator currents are 3 to 6 times higher than the nominal current. So if the motor is subjected to multiple starts in a short period of time, the temperature of will increase and overheat the insulation system;
- Overloading: There are situations where the total power is used, in this situation an increase in the load leads to an overload. It is estimated that the winding temperature rise will increase as the square of the load, which leads to a reduction in the lifetime of the insulation system;
- Obstructed Ventilation: The motor should be kept clean inside and outside to ensure that the cooling system works correctly. Anything that restricts the flow of air will cause a temperature increase in stator and rotor components;
- Ambient temperature: Most induction motors are designed to operate at an ambient temperature of 40 ºC. So if the ambient temperature is above 40 ºC the insulation life time of stator windings will decrease.

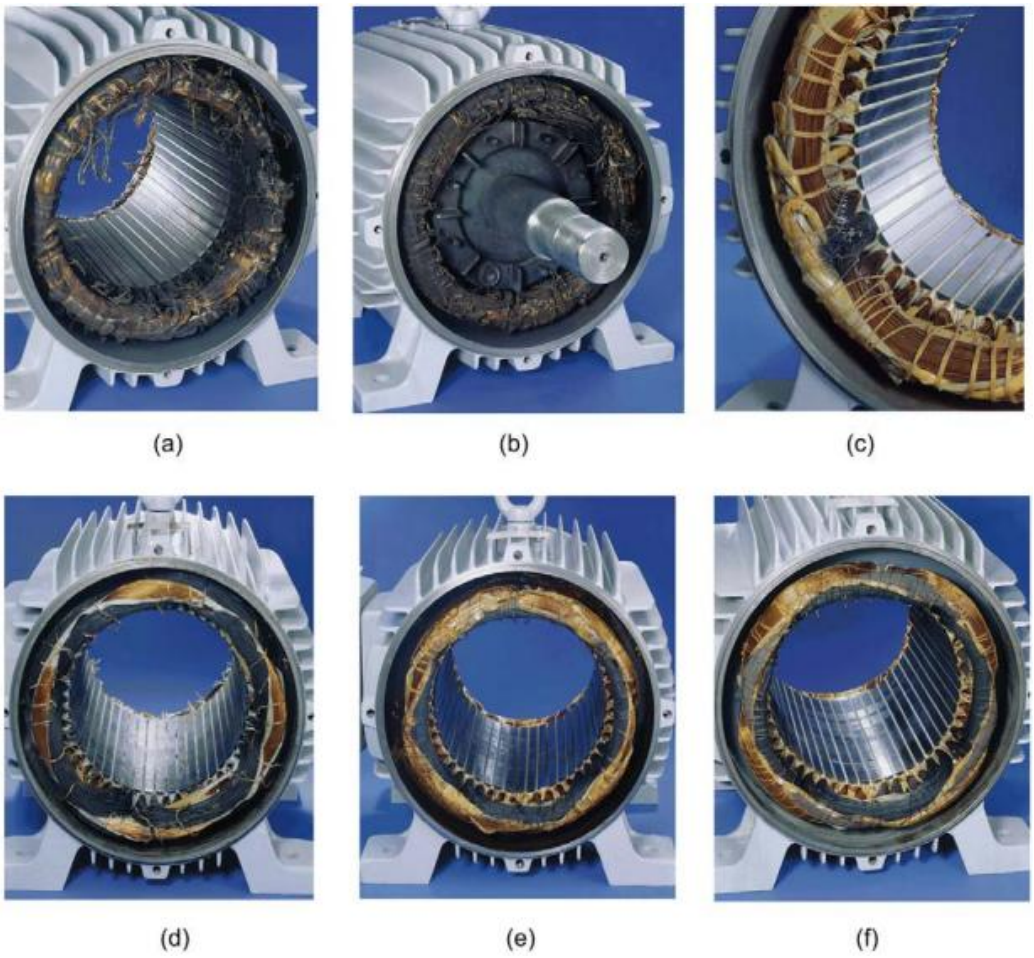

Figure 2.6 - Inter-turn short circuit of the stator winding in three-phase induction motors. (a) Short circuits in one phase due to motor overload (b) Short circuits in one phase due to blocked rotor. (c) Inter-turn short circuits are due to voltage transients. (d) Short circuits in one phase due to a phase loss in a Y-connected motor. (e) Short circuits in one phase due to a phase loss in a delta-connected motor. (f) Short circuits in one phase due to an unbalanced stator voltage. [61]

Electrical Stresses

The insulation lifetime is directly related with the electric stresses applied in the motor. When the insulation system is exposed to additional electrical efforts, to ensure the electrical integrity of devices their lifetime decreases as the effort made by the material is higher. In the case of electrical machines is necessary to ensure a proper insulation to avoid damages in the windings. Electrical stresses are directly related to transient voltage regimes and the occurrence of partial discharges in the stator windings.

According to Olyphant [63] partial discharges occur from a transient gaseous ionization in the insulation system where the voltage stresses exceeds a certain threshold. This phenomenon is a serious problem for the insulation system especially in high-voltage machines. The occurrence of these discharges is affected by factors such as frequency, dielectric thickness, humidity and

temperature. The consequences of these discharges result in heating, eroding or chemical reactions that causes the deterioration of winding insulation.

In [62] Bonnett and Soukup holds the view that the exposure of electrical motors to transient voltage condition causes a reduction in the lifetime of the windings and subsequently cause faults such as turn-to-turn or turn-to-ground short circuits. The existence of this type of transient voltages is related to a wide range of factors which are the following:

- Supply overvoltage that sometimes reach 3,5 times their normal peak value in small ranges of time;
- High voltage oscillations caused by bad connection to the ground;
- Circuit breakers such as current limiting fuses that when interrupt the current in the circuit cause voltage oscillations;
- Insulation failures can cause increases in the voltage that will exceed the normal operation voltages;
- The use of capacitors connected to the stator windings to improve the power factor. When the capacitors and the motor are shutdown can cause magnetic resonance between the capacitors and the leakage inductances, resulting in transient regimes in stator windings;
- The advent of variable frequency drives such as Pulse Width Modulation (*PWM*) drives has simplified the motor control, but unfortunately it is known that the use of such equipments causes large electric efforts in the stator windings that lead to premature aging of the machine [64].

Mechanical and Environmental Stresses

There are a few mechanical and environmental problems that cause insulation degradation and therefore the appearance of stator faults. Theses stresses include coil movement resulting from vibrations, rotor strikes due to rotor unbalances and contaminations from foreign materials [62].

In the case of mechanical stresses, they are related with mechanical forces resulting from the current in the stator windings that produce a force on the coils which is proportional to the square of current. This force produces vibrations in the coils at twice the synchronous frequency which cause radial and tangential movement in the coils [62].

Another factor that can cause physical damages to the stator are the rotor collisions with the stator. There are several factors that cause such conflicts, but the most common occurrences are bearings failures, shaft deflection, rotor-to-stator misalignment or parts of the ventilation system that are released and collide with stator.

The presence of foreign material, such as dust, moisture, oils, and chemicals may have a contaminating and abrasive effect that result in a premature degradation of stator materials. In this type of stresses one of the most common is the phenomenon of condensation in the stator windings which leads to ground out in the slot. So to ensure a trouble-free engine operation is extremely important to keep the unit clean and dry, both internally and externally.

2.2.2 Rotor Faults

Currently there are two types of squirrel-cage rotor in induction machines: cast and fabricated (Figure 2.7). The cast rotors are usually used in small machines with low power and are almost impossible to repair in case of failure, due to the way they are manufactured, while the fabricated rotors are used in larger machines or specific applications and in case of failure there is the possibility of reparation.

Figure 2.7 – Two types of squirrel-cage rotors. (A) Cast rotor (B) Fabricated rotor

According to Nandi and Toliyat [56] rotor faults in this type of induction motors (squirrel-cage rotor) can be divided into two categories: broken rotor bars (Figure 2.8) and cracked end-rings. Although they are different faults they are both related because of their physical connection.

A broken rotor bar (*BRB*) or a cracked end-ring force the healthy bars to carry additional current that leads to rotor core damage due to the elevated temperatures in the vicinity of the broken bars and the additional currents pass through the core from broken to healthy bars.

Although a fault in the rotor does not cause in some cases immediate problems, this type of faults can lead to additional effects, like torque and speed oscillations, that cause increases in temperature and insulation faults that reduce the machine's lifetime.

Figure 2.8 – Fabricated rotor of a 5 *MW* rated power (P_{el}) machine with multiple broken rotor bars [65]

2.2.2.1 Causes for Rotor Faults

Thermal Stresses

Any increase in temperature during motor operation can also cause thermal overload in the rotor. Generally thermal stresses appear during acceleration, running or stall conditions. Even with the modern protection systems that limits the temperature in the machine, the rotor does not remain free of damages because usually the protection systems are implemented in the stator side. There are numerous causes for the existence of thermal overloads, the most common are the following [62, 66]:

- excessive consecutive starts that causes high temperatures in the rotor bars or end rings;
- bearing failures and/or eccentricities in the air-gap that causes strikes between rotor and stator;
- obstructed ventilation system;
- unbalanced phase voltages;
- broken rotor bars;
- rotor stalling due to oscillations in the load.

In high-speed machines there is also the occurrence of thermal oscillations due to high length to diameter ratio. As the rotor has a larger length compared with the diameter, the temperature in the entire length of the rotor has variations that cause fluctuations in temperature.

Hot Spots and Excessive Losses

This type of thermal stress is caused by incorrect manufacture, design or repair processes that can cause unexpected losses and hot spots. In relation to the symptoms that cause hot spots and losses, these are mostly related to irregularities in the lamination of the rotor, such as, improper lamination design, variations in thickness and length of the blades. The only way to reduce these symptoms is through tests and repairs made after the manufacturing process [62, 66].

Rotor Sparking

Usually rotor sparking occurs in high power machines with fabricated rotor. There are several reasons for rotor sparking, some are not harmful to the rotor and others can cause failures. In the case of non-destructive sparks, they have low intensity and are rarely observed. These sparks are primarily related to voltage drops in the rotor, load fluctuations, switching disturbances that generally occur in full load or speed regimes. During the startup period, sometimes there is a period of intensive sparking due to high currents that exists during this operation period, but does not present risks to machine's safety.

The sparks that can cause destruction of some component in the rotor depends on several factors. However, broken bars and end-ring defects are the most common causes. Despite these sparks have great intensity compared with the non-destructive sparks are also difficult to observe [62, 66].

Magnetic Stresses

The electromagnetic forces generated by the slot linkage flux are unidirectional and proportional to the square of the rotor current. These forces cause a radial displacement of the rotor bars from the inside to the outside of the rotor as can be seen in Figure 2.9. A loose rotor bar can cause a strike against the stator winding causing a catastrophic motor failure.

The period of motor operation where these electromagnetic forces are more relevant is the start, because that is where the current reaches a higher value. As time passes this kind of stress causes the appearance of gaps in the rotor bars (Figure 2.9) and consequently the appearance of vibrations in the rotor [67].

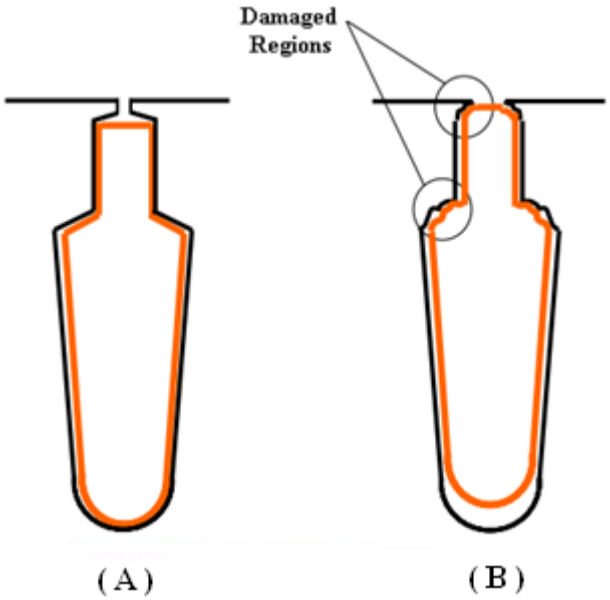

Figure 2.9 – (A) Bar housed in a slot without damage (B) Bar housed in a slot with damage (adapted from [68])

Besides electromagnetic forces, there are other magnetic stresses that affect the machine, for example the case of unbalanced magnetic pulls (*UMP*). Ideally an electric machine must have the rotor centered in the air-gap, resulting in a balance of the magnetic forces that does not cause deflection in the rotor. However, in a "real" machine, the rotor is not centered in the air-gap due to situations such as eccentricities, belt loading, bearing wear and others that affect the position of the rotor in the air-gap.

According to [67] for these stresses, there is an area where the distance between the rotor and stator decreases and there will be another area where the distance between the rotor and stator will increase. The occurrence of changes in the air-gap also causes changes in magnetic reluctance, for example in the case where the distance between the rotor and stator decreases, the magnetic reluctance also decreases, unlike the magnetic force that increases and force the rotor to move in the direction where this attraction have more intensity, until the distance between the rotor and stator tends to zero, which means a strike between the rotor and stator.

Residual Stresses

This type of stress normally is related to fabrication processes, such as casting, welding and stacking. If the geometry of the rotor does not change, this kind of stress is not harmful to the machine. When the geometry of the rotor is affected during the manufacturing process, can occur the appearance of vibrations and thermal stresses during the transition from idle to full-load regime [62, 66].

Environmental Stresses

Like in the stator side environmental stresses also affect the rotor. The presence of chemicals, oils and dust can cause contamination and corrosion. These environmental stresses usually affect the ventilation system causing obstruction to airflow. Another consequence of this stress is the corrosion that can cause unbalanced weights in the rotor and consequently strikes between the rotor and stator.

2.3 Mechanical Faults

According to Table 2.1 and Figure 2.2 almost 40 to 45% of faults in inductions machines are related to mechanical faults. Zhongming and Bin [69] states there are two types of mechanical faults:

- Bearing faults;
- Air-gap eccentricity;

2.3.1 Bearing Faults

Bearing are common elements in rotating electrical machines. In fact, almost all the rotating electrical machines use either ball or rolling bearings to decrease friction between the motor frame and the shaft, which increase the machine efficiency. Motor bearings may cost between 3 and 10% of the actual cost of the motor, but the hidden costs involved in downtime and lost production combine to make bearing failure a rather expensive abnormality [70]. According to the *EPRI* report [58] and to the *IEEE-IAS* survey [57] faults in bearing elements represent the most common cause of faults in induction machines.

An either-ball bearing is composed by two rings called inner and outer race rings (Figure 2.10). A set of balls or rolling elements are placed in raceways to rotate inside of these rings. There are several reasons that cause bearing faults, the most common are the following:

1. poor lubrication;
2. improper application or installation;
3. excessive vibrations;
4. shaft misalignments;
5. mechanical overload;
6. bearing currents;
7. contamination and corrosion;

Bearing faults can be categorized as outer bearing race defects, inner bearing race defects, ball defects and train defects. These faults result in rough running that generates detectable vibrations and increase noise levels [71]. The continuous operation of the machine in a bearing fault situation causes fragments of material to break loose that produce fatigue problems known as flaking and spalling [71].

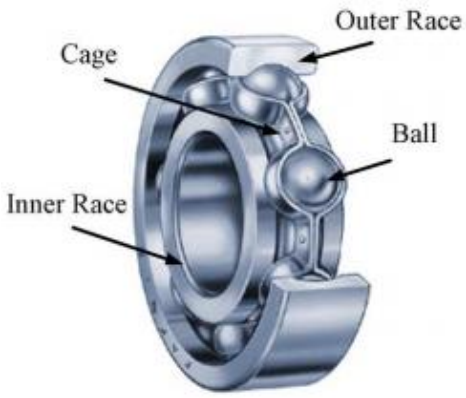

Figure 2.10 – Schematic diagram of a rolling-element bearing [72]

2.3.2 Air-gap Eccentricity

Machine eccentricity is defined by Vas as an "*asymmetric air-gap that exists between the stator and rotor*" [73]. When the rotor in not centre aligned with the stator core, the rotor stops to describe a circular trajectory which causes a variation in the air-gap thickness. This phenomenon causes the appearance of unbalanced radial forces that lead to efforts in the stator windings and at worst case may cause strikes between rotor and stator, resulting in damages to both components [66]. There are two types of air-gap eccentricity (Figure 2.11) [67]:

1 Static eccentricity;
2 Dynamic eccentricity;

In the case of static air-gap eccentricity, the rotor is displaced from the stator geometric center and turn upon its own axis. The position of the minimal air-gap length is fixed in the space. This type of eccentricity is detectable only with the use of special equipment [67]. On the other hand in dynamic eccentricity the rotor is turning upon the stator geometric center, but is not running in its own center.

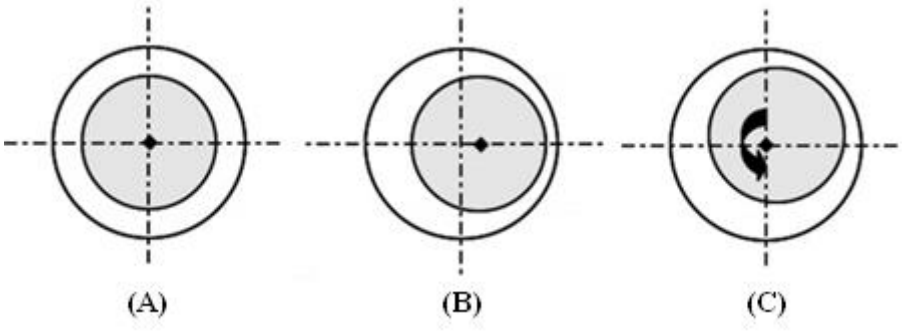

Figure 2.11 - Different types of eccentricity (border line is the stator inner ring, round rotor is in grey). (a) Without eccentricity (b) Static eccentricity (c) Dynamic eccentricity (from [60])

In reality, both static and dynamic eccentricities tend to coexist. The ideal conditions can never be assumed. Even new machines present some kind of eccentricity, some manufacturers specify a maximum air-gap variation of 5% to 10% [72].

Chapter 3

Fault Detection and Diagnosis in Induction Machines

In this chapter the first sections presents some terminologies and definitions that are used in the *FDD* field. There are also classified the *FDD* methods that currently exists. Secondly, it is made a survey on the different concepts of maintenance and its importance. Then, it is made a wide description of the methods that are currently used to detect and diagnose faults in induction machines.

3.1 Introduction

The industrial era, triggered by the industrial revolution in the eighteenth century generated an unprecedented economic growth in human history. The fact of existing large quantities of raw materials available, low cost of labor force and a continuous technological development, led mankind to believe that the paradigm of mass production, mass consumption would lead humanity to a period of exponential development and sophistication. This would not be verified due to several factors, such as shortage of raw materials, environmental problems, health problems that put in risk the human population and social problems that create more unemployment and differences between social classes.

Nowadays people and especially the companies besides the financial difficulties have to deal with labor, environmental and security problems. In the industrial field the first steps to increase the productivity, improve the robustness of processes and reduce the operation time were given through the use of machines, control systems and information technologies. These items can be clustered in a word, automation.

Automation is a significant component of modern engineering systems. Although automation brings several advantages, such as those described above, it also increases system complexity. According to [74], the increasing of the system complexity results in an overload of information and makes the system more susceptible to faults. The appearance of a fault in a process or in an industrial complex is something undesirable, system faults can lead to serious consequences, such as plant shutdown, huge economic loss, and human casualties. Therefore,

along with automation, Fault Detection and Diagnosis (*FDD*) systems have an increasing interest because it improves the reliability and availability of the system.

3.1.1 Terminology and Definitions

The terminology used in the field of *FDD* is not unique. Therefore, the used terminology tries to follow the definitions proposed in the Safeprocess Technical Committee of *IFAC* (International Federation of Automatic Control) and references such as Isermann and Ballé [75].

- *Fault*: Unaccepted deviation of at least one characteristic property or parameter of a system from its standard condition;
- *Failure*: inability of a system or a component to accomplish its function;
- *Symptoms*: A change of an observable quantity from its normal behavior;
- *Fault detection*: indication that something is wrong in the monitored system;
- *Fault isolation*: determination of the exact location, type, and time of the detected fault. Usually fault isolation is confused with fault diagnosis;
- *Fault diagnosis*: determination of the magnitude of the fault. Sometimes fault diagnosis can include, fault detection and isolation;
- *Monitoring*: Continuous (real-time) task of discovering the condition of a component or system through data acquisition;
- *Reliability*: probability of a system to perform a required function during a given period of time in normal conditions;

3.1.2 Fault classification

As mentioned in the previous section, faults are events that can influence the behavior of various components of a system. Concerning to the faults location, these can happen in actuators, sensors and in internal components of a system.

The effects of a fault can also be classified in relation to the consequences produced over time. They can be divided in three categories, as can be seen in the Figure 3.1.

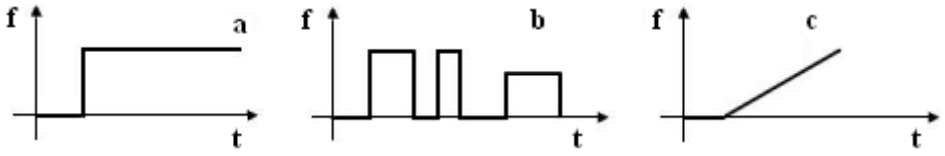

Figure 3.1 – Time-dependency of faults. (a) Abrupt fault (b) Intermittent fault (c) Incipient fault

The abrupt faults usually occur instantaneously and are persistent in time. The intermittent faults do not appear continuously and exhibit a behaviour similar to timing pulses while the incipient faults exhibit slow changes over time. Incipient faults are difficult to detect

because in an initial stage present a low severity index, but in a final stage may evolve into an abrupt fault. In this research work only incipient faults are considered.

3.1.3 Classification of the *FDD* methods

The types of methodologies used in fault detection and diagnosis are dependent of the process and the type of information available to be used for *FDD* purposes. Taking into account the variety of existing processes in today's industry, it is natural the existence of several methods for detection and diagnosis of faults. In the Figure 3.2 is represented how Isermann [76] classifies the existent fault detection methods.

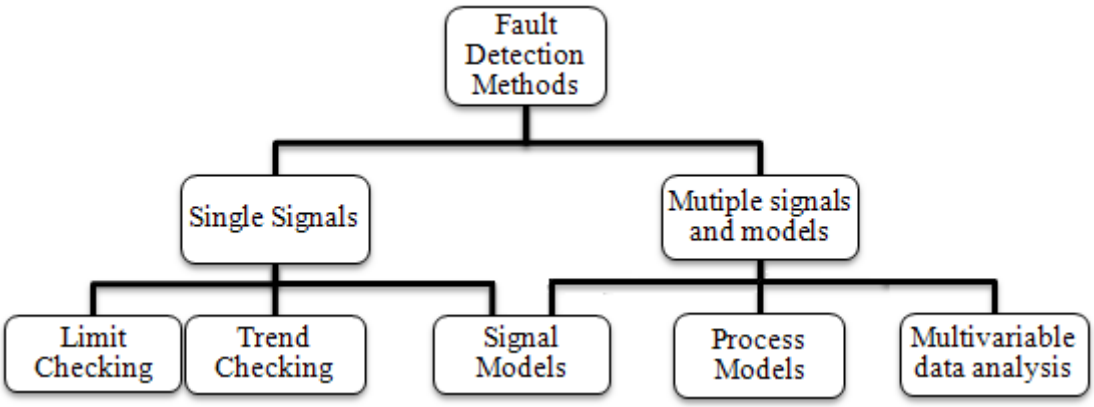

Figure 3.2 – Fault detection methods classification [76]

Fault detection methods can also be classified in three different approaches: model-based, signal-based and data-based. In fact, all the mentioned approaches use signal processing but the way as signal processing is used is different and the impact in the final result is also different. Model-based methods are based on the use of analytical redundancy, for example is provided a theoretical model of the system and the difference between the measured data and the predicted values obtained from the theoretical model are used to detect fault situations (Figure 3.3).

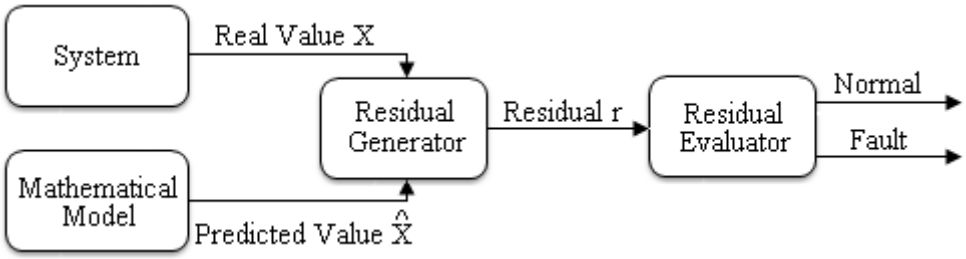

Figure 3.3 - Schematic diagram of model-based methods

Signal-based methods do not incorporate any model, these methods use the acquired signals to search for known fault signatures. Here signal processing and the acquisition system plays an important role because the results are directly dependent of the quality of the read

signals. The detection of faults in signal-based methods has two important stages. First it is necessary to recognize a deviation or a fault signature in the measured variables. This is called pattern recognition. The second stage is the decision-making, where it is classified the fault and his magnitude.

In data-based techniques the sampled data is used to extract a set of features that are clustered in order to classify them. This technique does not require any knowledge of machine parameters as Model-based or Signal-based techniques require. One form of a knowledge-based system is an expert system, which is defined by Biondo [77] as a "*computer program that uses knowledge, facts, and reasoning techniques to solve problems and make decisions.*" The schematic diagram of an expert system is shown in the Figure 3.4. The knowledge acquisition modules have the objective of acquiring new facts or rules from the human experts and specialists. The knowledge base is similar to a database where are stored all the facts and rules introduced by the humans. Regarding to the inference engine, this module is the manager of the knowledge base. In this module is processed the information provided by the knowledge base.

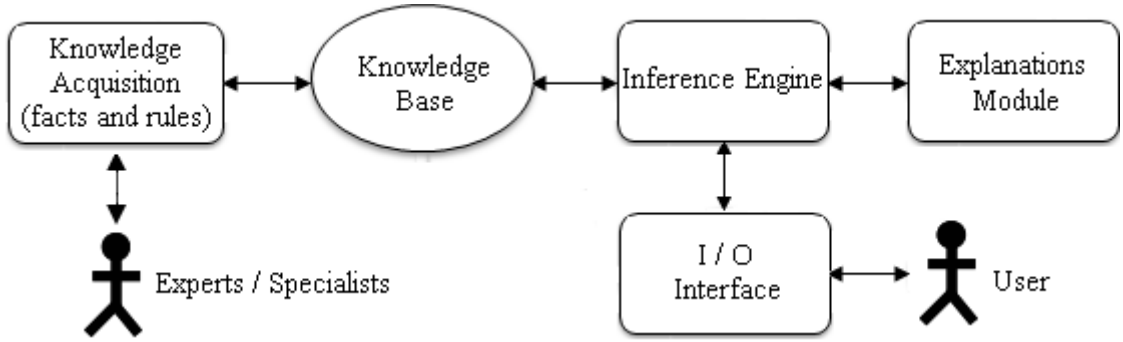

Figure 3.4 – Expert System structure (adapted from [77])

Concerning to diagnosis there are also numerous methods used currently. In Figure 3.5 is the division proposed by Isermann [76].

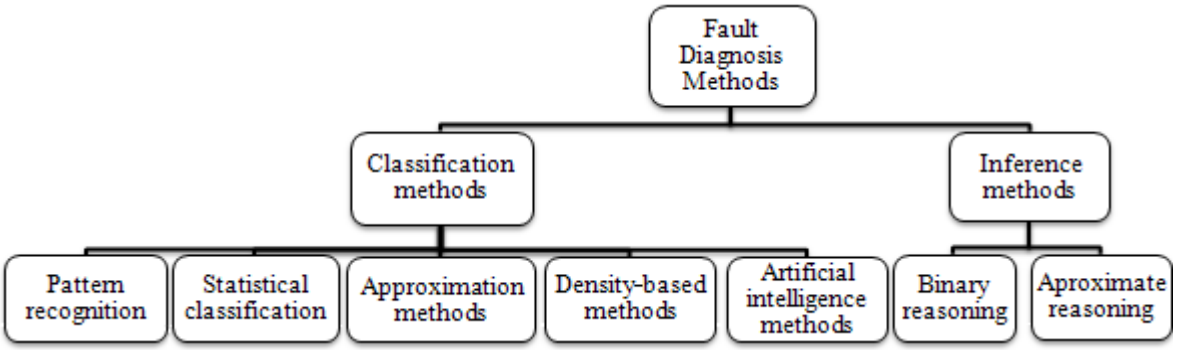

Figure 3.5 – Fault diagnosis methods classification [76]

3.1.4 Maintenance

Since the principles of mankind the human being felt the need to keep his equipment in good conditions. No matter how the equipments are designed, to keep them operating at desired reliability level, maintenance is required. According to Tsang *et al.* [78] maintenance is the act of repairing broken items.

Maintenance of electrical machines is a very popular topic, since it corresponds with industrial requests for an increasing number of applications where reliability is a keyword. It is known that an interruption in a manufacturing process causes loss of funds to a company, so a proper maintenance and an early detection of faults can result in a reduction of financial losses.

In the literature the maintenance methods are presented by different authors in different perspectives. However, the most important is to realize that maintenance methods refer to the way the maintenance tasks are planned and scheduled. According to Tavner *et al.* [3] there are three basic maintenance strategies that have to be considered:

- Breakdown maintenance;
- Planned maintenance;
- Predictive maintenance.

In breakdown maintenance (*BM*) the problems are only fixed when they occur. This type of maintenance is used when the equipment does not have significant importance to the operation or does not generate significant losses. A planned maintenance (*PM*) consists in periodic inspections to replace parts that are supposed to break after a certain number of hours. A predictive maintenance (*PdM*) or condition-based maintenance (*CBM*) consists in the evaluation of the equipment condition by performing periodic (off-line) or continuous (on-line) analysis of the device status. The main advantages and disadvantages of these three types of maintenance are presented in the Table 3.1.

Type of Maintenance	Advantages	Disadvantages
Breakdown Maintenance (*BM*)	• No over-maintenance; • Minimal management; • Requires fewer staff;	• Large spare inventory; • High cost repairs; • Intensive labor; • Safety problems; • Increased costs due to unplanned equipment downtime;

Type of Maintenance	Advantages	Disadvantages
Preventive Maintenance (*PM*)	• Increased component life cycle; • Reduced unexpected failure; • Decreased system downtime;	• Unneeded maintenance; • Catastrophic failures still likely to occur;
Condition-Based Maintenance (*CBM*)	• Improved usage efficiency and reliability of the equipment; • Decrease in costs for parts and labor; • Reduced unplanned downtimes;	• Increased investment in staff training; • Increased investment in diagnostic equipment;

Table 3.1 – Comparison of maintenance techniques

There are other two techniques of maintenance that are not referred by Tavner *et al.*, the reliability-centered maintenance (*RCM*) and E-Maintenance. The concept of *RCM* was firstly used in the 1970s in the aviation industry and later was used in nuclear plants [79]. Moubray [80] refers to reliability-centered maintenance as a process to establish the safe minimum levels of maintenance. According to [79] *RCM* is a strategy used to determine cost-optimized maintenance point that is needed to sustain the operational reliability of systems and equipment.

In *RCM* there are criteria used to distinguish which are critical components in the system. In the case of critical components, planned maintenance actions are performed in order to prevent a decrease in reliability or deterioration in safety levels. For non-critical components, the components are left to "run to failure" (*BM*). The component is replaced only when it ceases to fulfill its function. These corrective actions are only applied to low cost components that do not represent safety problems to the system.

RCM depends on the same measurements used in *CBM*, but saves additional maintenance resources by spending less effort on less important machinery. *RCM* also requires more training and software than *CBM*.

In the end of the 1990s with the spread of the Internet a new field of research emerged in the maintenance domain and the concept of E-Maintenance is introduced. In [81] there are a set of definitions for E-Maintenance, the most important are the following:

- "*The ability to monitor plant floor assets, link the production and maintenance operation systems, collect feedback from remote customer sites, and integrate it with upper level enterprise applications.*"
- "*The network that integrates and synchronizes the various maintenance and reliability applications to gather and deliver asset information where it is needed.*"

Basically E-Maintenance includes the concepts of *CBM* and *PM*, but applied in a web context. In 2006 the Intelligent Maintenance System Group (*IMS*) [82] developed the Watchdog Agent™. This platform uses the collected data from sensors to perform monitoring tasks and to detect degradations in the process.

3.2 Why Condition-Based Maintenance?

Nowadays, as equipment, plant costs and his maintenance are increasing, *CBM* plays an important role in this scenario. With *CBM* it is possible to eliminate unexpected downtimes and schedule future repair works and maintenances that will result in reduced replacement and less maintenance costs. Other advantages, such as the increase of equipment lifetime, increase of plant safety and the decrease of accidents are not directly related to *CBM* but cause an increase in the efficiency and reliability of the equipment.

On the other side, the disadvantages of using *CBM* are related to high installation costs in comparison with the equipment cost and the investment in training the company employees.

Condition Monitoring (*CM*) is the technique served for Condition-Based Maintenance (*CBM*). Han and Song [83] describes Condition Monitoring (*CM*) as the process of monitoring characteristics or parameters of a machine, in order to verify significant changes and trends that can be used to indicate a fault situation or the need for maintenance.

The first Condition Monitoring Systems (*CMS*) for rotating electrical machines have emerged in the end of 1980s, with the appearance of the first processors with enough computing power to analyze and process the acquired data [83]. Before the appearance of *CMS*, the assessment to the state of rotating electrical machines was made through the use of analog instruments for measuring electrical and magnetic quantities. Before the existence of *CMS* were used protection systems such as overcurrent, overspeed, or earth fault that acted only when there was a fault situation.

3.2.1 Main Functions and Characteristics of a *CMS*

The main function of a *CMS* is monitoring and diagnosis the state of a device by extracting features of previously acquired data. According to Thompson [84] there are several characteristics that need to be considered when selecting a *CM* technique for application in an industrial environment. The most important characteristics are listed below:

- the sensor should be non-invasive;
- the sensor must be reliable;
- the instrumentation must be reliable;
- existence of a severity factor that quantifies the problem;
- ideally, remaining run-lifetime estimation should be given;
- ideally, prediction of the cause(s) of the fault;

Advantages of Condition Monitoring Systems

The advantages of using Condition Monitoring Systems are the following [3]:

- Prediction of the equipment failure;
- Improvement of equipment reliability;
- Reduction of maintenance costs;
- Improvement of equipment efficiency.

Regarding to how the algorithms are executed there are also two types of algorithms: on-line systems and the off-line systems. On-line systems make a serial processing of the input information “piece-by-piece”, without having the entire input available from the start of the processing. No future information is available at the decision moment.

In the case of Off-line systems these systems do not make a continuous evaluation of the device and the entire input data is given and it is expected that the output solves the problem in the moment. These Off-line tests usually require the shutting down of the machine and disconnecting it from the supply.

The application of an on-line algorithm to a *CMS* has the benefit of making an easier monitoring because the machine is under constant monitoring and the machine does not have to be taken out of service. The installation of additional equipments, such as transducers and sensors are a disadvantage to the use of these systems.

In contrary, off-line algorithms do not require the installation of additional equipment, but require the direct intervention of a human operator.

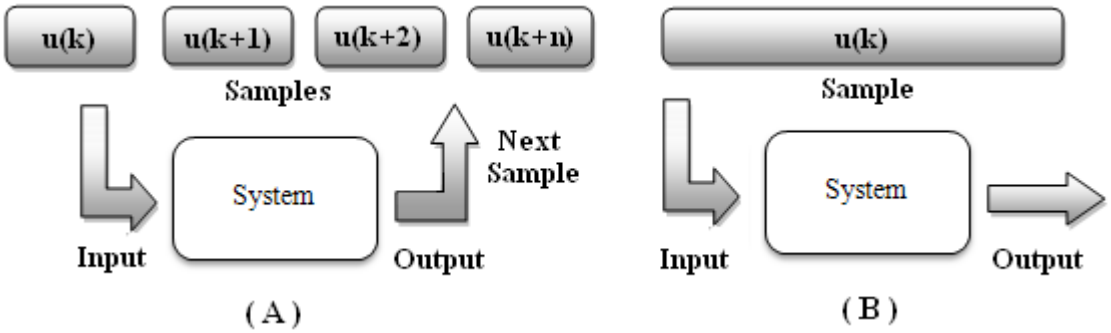

Figure 3.6 – Differences between on-line and off-line methodologies

3.3 On-line Condition Monitoring

On-line condition monitoring systems consists in monitoring and diagnosis the condition of a machine while it is running. The great advantage of these systems is the ability of detecting faults while they are still developing, when they in an initial stage. This is called incipient fault detection (Section 3.1.2). Han and Song [83] suggest that a *CMS* must contain four basic modules: sensors, data acquisition, fault detection and fault diagnosis.

Figure 3.7 – Basic modules from a *CMS* [83]

The sensors and data acquisition modules are used to measure the desired quantities, convert the measured quantities into an electrical signal. It is also in the data acquisition module that is chosen how the signal is conditioned (time domain, frequency domain or time-frequency domain). Such a conditioned signal may be a current or a voltage phasor derived from current or voltage instantaneous values, or the motor model, or a frequency spectrum computed with the Fast Fourier Transform (*FFT*). There many types of sensors used in on-line systems, such as thermal sensors, current sensors, voltage sensors, flux sensors and vibration sensors. The process of choosing the sensor depends on the used monitoring method.

The fault detection module must be able to verify in the obtained sensorial information if any type of fault occurs. Everything that occurs outside the expected must be considered a fault. Through feature extraction from the read data, this module must be able to inform the fault diagnosis module that there is a fault situation [85].

The fault diagnosis module must have the ability of detecting the exact location and the magnitude of the fault. This module should be necessarily separated from the fault detection module, because it requires a larger time interval to evaluate the obtained information. The fault

diagnosis module is only called when a fault situation occurs, unlike the fault detection that is always extracting features from the acquired data [85]. In Sin *et al.* [86] proposes an alternative to the condition monitoring process described by Han and Song [83]. In Figure 3.8 is shown the scheme proposed by Sin *et. al* [86].

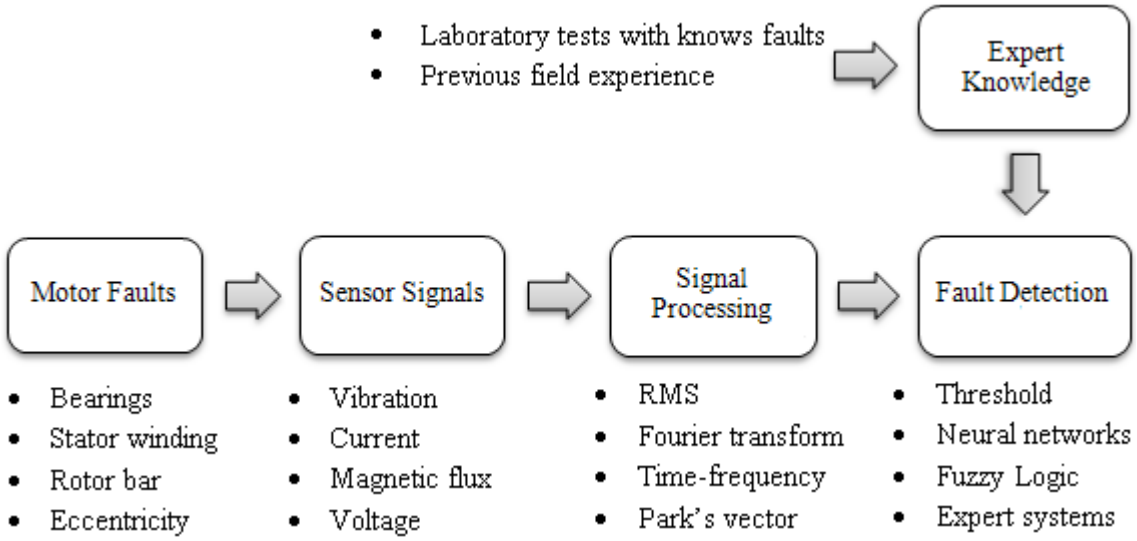

Figure 3.8 – Alternative schematic diagram for on-line condition monitoring [86]

Both proposed systems [83, 86] have obvious similarities. The sensor, signals processing and fault detection modules are present in both diagrams of Figures 3.7 and 3.8. The main differences are in terms of faults detection and diagnosis concepts. Han and Song separate the concept of fault detection and fault diagnosis (which is currently used in literature) while Sin *et al.* combine the two concepts and consider that the fault detection module is dependent from external knowledge. The architecture used in this research work is the one proposed by Han and Song.

3.4 *FDD* Techniques used in Induction Machines

There is an abundant literature in the field of condition monitoring of induction machines. Tavner in his textbook [3] describes different monitoring techniques based on vibration, chemical and electrical measurements. Vas [73] also describes the condition monitoring in induction machines but the main subject is the parameter estimation of the machine. Han and Song [83] made a general review on the condition monitoring process for electrical machines, such as motors, generators and transformers.

The *FDD* techniques used in induction machines can be divided in two types: mechanical techniques and electrical techniques. The mechanical techniques are related with methods based on temperature monitoring, vibration monitoring and chemical analysis. On the other side,

electrical techniques proceed to the measurement of electrical and magnetic quantities. Following, will be presented the most used condition monitoring methods.

3.4.1 Non-Electrical Techniques

3.4.1.1 Vibration Monitoring

In [87] Timár addresses the issue of vibration monitoring in electrical machines. It includes the description of rotating machines, the sources of the vibration and the informations provided by the vibrations. According to Tavner *et al.* [3] this kind of technique is used for many years and due to its popularity there are standards that regulate the use of this technique. An ideal rotating machine does not have vibrations. Because the machines are designed and manufactured to work within tolerances there are always vibrations that can cause high levels of acoustic noise, progressive mechanical and aerodynamic forces [3]. The principal sources of vibration in rotating electrical machines are related to the magnetic attractive forces between stator and rotor, and the response of the rotor bearings as the machine rotates. Thus by analyzing the vibration signals produced by the electrical machine, it is possible to detect various types of faults. Rotor eccentricities, bearing faults, air-gap eccentricities and bent shafts are the most common faults detected by this technique [3].

Usually to measure the vibrations in the machine are used, displacement transducers, velocity transducers and accelerometers, each one working in different frequency ranges. The choice of the transducer also depends on the machine's application.

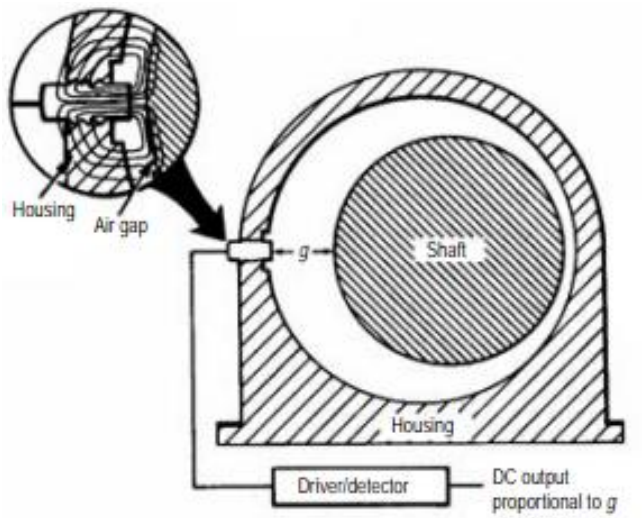

Figure 3.9 – Experimental apparatus for vibration measurements in electrical machines [3]

However, despite the proven results and the existing standards such as *ISO* 10816 [88], this technique has the disadvantage of having high costs because it is necessary to mount various

sensors in precise locations to measure the vibrations produced by the machine. Also the environment around the machine must be free of vibrations to avoid changes in the measurements. Another disadvantage is the dependence on the type of machine's application, which for certain application the transducer and his location changes.

3.4.1.2 Acoustic Noise Monitoring

When the machine operating condition changes it is common the occurrence of variations in the noise produced by the machine. The noise spectrum of induction machines is dominated by electromagnetic, ventilation, and acoustic noise. The ventilation is the result of air turbulence produced by the rotating parts due to periodic disturbances in the air pressure. The electromagnetic noise is due to electromagnetic asymmetries that act in the iron surfaces. To measure these noises are used microphones that capture the sound and then a spectral analysis is made to detect if there is any fault in the machine.

This method has the advantage of being easy to measure because it only needs a microphone. However there are more disadvantages than advantages because background noise or unwanted noise can corrupt the measurements and lead to incorrect or incomplete conclusions. This technique cannot be used in industrial environment due to the presence of many electrical machines and other equipments that corrupt the measurements. This method was applied, in gas turbines, aircraft transmissions and the result was disappointing [89].

In high-noise environments the spectral analysis of high frequencies (above 100 kHz) is the only way to use acoustic noise monitoring. The high-frequency waves produced by the machine can still provide information of the machine's state. However, the cost of sensors and the need of experienced technicians make this method unpopular.

3.4.1.3 Thermal Monitoring

The machine's temperature measurement provides important information about the machine health. Normally, a fault in a rotating electrical machine produces excessive heat (Figure 3.10) that can be detected with sensors in the stator windings or in the bearings of the machine. Although nowadays it is possible to measure the temperature without sensors inside the machine using IR monitors or optic fiber cables [90]. Usually temperature transducers are used to protect the machine (the transducer shutdown the supply source) instead of being used to monitor the machine's state. Said and Benbouzid [91] suggests the use of temperature estimation for *FDD* purposes. The system proposed is based on the thermal model and stator resistance model of the induction machine, but there are some assumptions such as, unobstructed ventilation and ambient temperature that must be ensured.

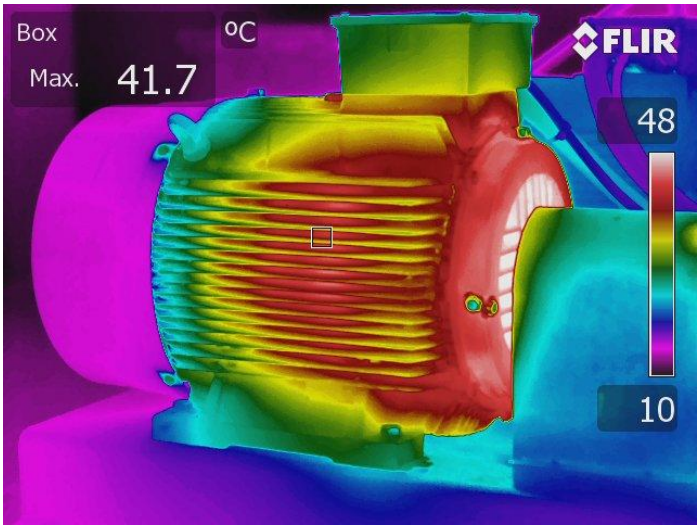

Figure 3.10 - Thermography of an electrical motor [92]

The disadvantage of using temperature to detect faults in electrical machines is that it takes effort to place embedded temperature sensors and ambient temperature can cause variations in the measurement. In the case of a detected fault by an abnormal temperature raising it is necessary to stop the machine and investigate what caused the temperature raising. It is also possible to detect the origin of a fault through thermal models of the machine, but the process is too complex and expensive. Due to its complexity this diagnosis method is not very popular currently.

3.4.1.4 Chemical Monitoring

Chemical analysis is a traditional way to monitor insulation condition. For example, when the bearings and the lubricating oils are degraded, they produce chemical gases in several forms, such as, liquid, gas and solid [3]. There are several techniques based on the chemicals released by a machine, such as oil analysis, gas analysis and wear debris analysis. Each one of these mentioned techniques is used to detect different faults. According to Tavner *et al.* [3] dissolved gases in the oil produced by thermal ageing, can indicate the presence of bearing faults. The analysis of the gases produced by the machine can also be used to detect short circuits in the stator windings.

In [93] Skala has proposed a system for detecting faults in induction machines based on the analysis of gases released by the machine. The cooling gas of the machine enters in an ion chamber and it is ionized by a radioactive source. The charges in the gas are collected in an electrode and then through a signal amplifier, will be produced an output voltage proportional to the ion current. Carson *et al.* [94] applied the system proposed by Skala in large turbine generators. In the Figure 3.11 is presented a diagram of the proposed system.

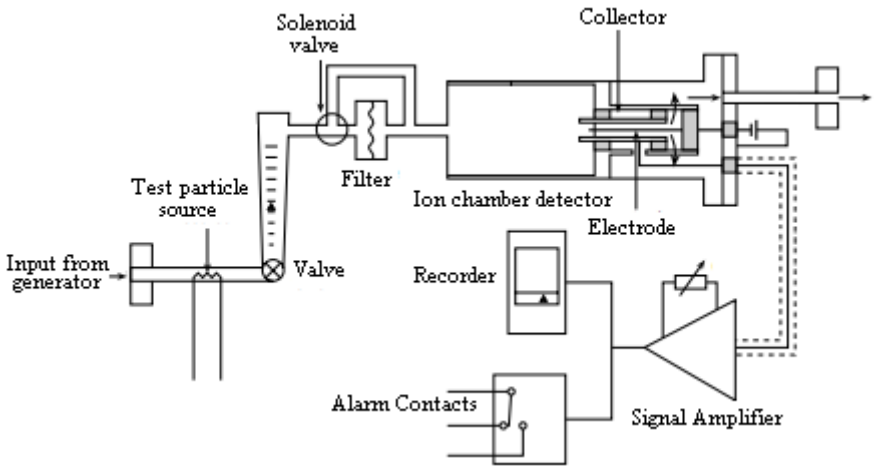

Figure 3.11 – Chemical monitoring system implemented by Carson *et al.* [94]

In the case of gas analysis the stresses exerted in the insulation system during abnormal situations of the machine operation, such as an unbalanced voltage supply or a temperature rise in the windings cause the release of carbon monoxide that can be detected by infrared sensors. Chemical monitoring is only applicable for large machines with an electric power above 50 kW and oil-lubricated bearings with a continuous oil supply. For these reasons these methods are not widely used due to the cost and complexity of the processes involved. Also environmental factors such as humidity and temperature can disturb the measurements. Currently this type of analysis is only applied in large machines and in military applications [3].

3.4.2 Electrical Techniques

Flux monitoring, current patterns recognition, current signature analysis and negative-sequence current analysis are the most used electrical techniques for condition monitoring in induction machines. In all these methods with the exception of flux monitoring, the stator currents are the used signal to extract information about the state of the machine. As a result, the data acquisition process is easier, it only needed voltage and current transformers that sometimes are already installed in the protection systems [3]. This is a major advantage because is not necessary to install additional sensors inside the machine, these techniques are non-invasive and can be implemented in a remote control center. Therefore, current monitoring can provide significant economic and implementation benefits.

3.4.2.1 Axial Magnetic Flux Monitoring

Ideally a machine should not have any type of axial flux in the air-gap [3]. However due to imperfections inherent to manufacturing process, an induction machine does not have a perfect asymmetry and therefore there is a residual axial flux that is measurable using a search coil fitted

around the shaft (Figure 3.12). Then the signal can be spectral analyzed and a decision of the machine's state is taken [95, 96].

This method has the disadvantage of depending on machine's load level, it is necessary to know the values of the axial flux before and after the occurrence of the fault and make several comparisons of different load levels. Another factor that limits the use of this method is the wide range of machines with different materials and geometries that sometimes does not allow the measurement of axial flux due to the low values of axial flux.

Figure 3.12 - Equipment used to measure the axial flux in an electrical machine [97]

3.4.2.2 Partial Discharge Monitoring

As mentioned in Section 2.2.1.1 partial discharges usually occur in high-voltage machines. This monitoring technique is used to diagnose faults in insulation systems and was used for the first time in the 1970s in large hydro generators [98]. As gaps are appearing between the coils of the motor windings and in the slots that house them, the degradation of semiconductor material that covers the coils/bars of the stator windings or the contamination of the forehead area of the coils are close to some of the causes that increase the level of activity of partial discharges, thus predicting a fault in the insulation system.

This method is based on the fact that partial discharges create voltage pulses of very short duration at the terminals of the stator windings which later can be measured by capacitors. One of the indicators of problems in the insulation system is the successive increase of partial discharges over time, so it is necessary to be done regularly measured [3, 98].

However this method of diagnosis is still limited due to the fact that require skilled technicians that are capable to interpret and analyze the results with reliability. The environmental factors such as temperature or humidity also limit the use of this method because the results may be influenced.

3.4.2.3 Negative Sequence Components Monitoring

It is known that the degradation of the insulation system and unbalances in the power supply can be measured in terms of positive and negative sequence components in the supply voltage and motor current [48, 99]. In unbalanced conditions the negative-sequence currents produce a magnetic field that opposes to the rotating magnetic field generated in the motor windings and leads to heating.

Several tests shows that the amplitude of negative-sequence component is directly proportional to the leakage currents when the leakage path has high impedance in the windings, so measuring the negative-sequence components of machine's supply current it is possible to detect fault in the machine [48, 99]. It is desirable to have a well balanced voltage source but there are always unbalances that result in the appearance of negative-sequence components which limit the use of this diagnostic method because it is difficult to distinguish if the negative-sequence component is associated to a fault or is related to the fact that the voltage supply is not ideal. It is important to note that there are also other residual asymmetries that cause the appearance of negative-sequence components in the currents that cannot be related to the existence of a fault in the machine [48, 99].

3.4.2.4 Induced Voltage Monitoring

This method was introduced due to the difficulties related to the existence of residual asymmetries in the machine and unbalances in the power supply system observed for example in negative sequence components monitoring. In healthy motors, the stator windings are receptors of voltages induced by the magnetomotive forces produced by the rotor. However, when a short circuit occurs in the stator windings, the shorted-circuit winding will capture most of the induced voltages. When the motor is switched off, the short circuit current that flows in the winding affected by the fault will induce currents in the remaining healthy motor windings. So, after turning off the motor through the measurement and the spectral analysis of the induced voltages it is possible to detect the existence of faults in the motor [100].

The results presented by the authors show that there is an immunity to the unbalances of supply voltage system and to the residual asymmetry of the motor. Moreover, it has also been shown that any damage to the core or the winding need to be substantial to produce a significant variation in the induced voltages [100].

The fact of being necessary to turn off the motor to make the diagnosis is a disadvantage of this method because there are industrial processes that cannot be stopped. Moreover, the existing voltage sensors in industrial environments are not installed at the terminals of the

electrical motors, they are installed on the frames that feed the electrical motors. To use this method it is necessary to install additional sensors at the motor terminals.

3.4.2.5 Motor Current Signature Analysis (*MCSA*)

Motor Current Signature Analysis (*MCSA*) is one of the most used diagnosis method to detect and diagnose faults in induction machines [84]. This is a non-invasive method that consists in collecting samples from the stator currents and then proceed to a spectral analysis of the stator currents in search of characteristics frequencies. There are two possible scenarios for the analysis of the current spectrum:

- perfectly symmetrical motor – Only forward-rotating field is produced, which means that the rotating magnetic field is produced only in the stator-rotor direction.
- asymmetric motor – a backward-rotating field, induces a voltage in the stator at the corresponding frequency, and a modification in the stator current appears.

When occurs a fault situation, the current spectrum becomes different from the spectrum of a healthy motor. In a healthy situation, with an induction machine supplied by a balanced three-phase and sinusoidal system with a frequency f_1 of 50 Hz the current spectrum is shown in Figure 3.13.

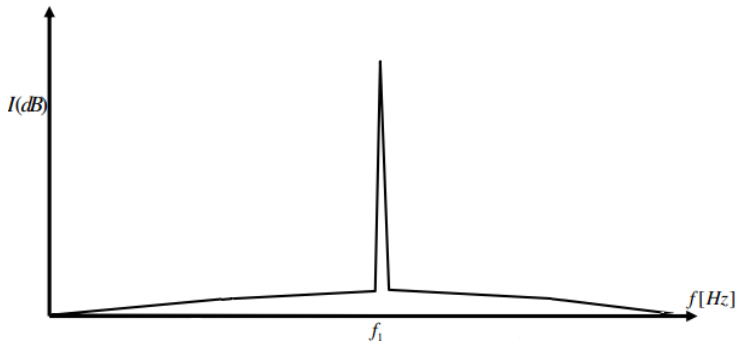

Figure 3.13 – Ideal current spectrum of a healthy machine

The faults in induction motors that this diagnosis method detects are the following [1]:

- broken rotor bars;
- air-gap eccentricities;
- short-circuits in stator windings;
- bearings damage.

Benbouzid [101] made a review that identifies the frequencies expressions that correspond to each fault. In the case of broken rotor bars, occurs the appearance of sideband components (Figure 3.13) f_b around the fundamental frequency. The expression of these sideband components is given by,

$$f_b = (1 \pm 2ks)f_1 \tag{3.1}$$

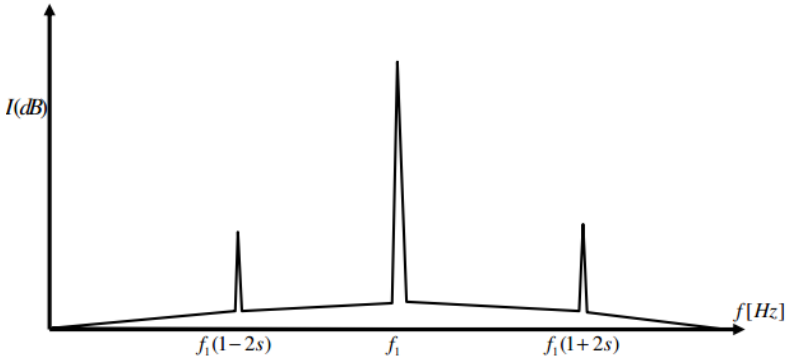

Figure 3.14 – Ideal current spectrum in a motor with broken rotor bars

The lower sideband is specifically related to broken rotor bar effects and the higher sideband is due to consequent speed oscillation [101].

The frequency components associated with short circuits in the stator windings can be identified in the spectrum by the following expression.

$$f_{sc} = \left(\frac{n}{p}(1 - s) \pm k\right) f_1 \tag{3.2}$$

Unlike the detection of broken rotor bars, to detect short circuits in the stator windings the load on the machine is minimal or even no load [102]. However, the frequencies with k=1 in expression (2) coincide with the faults related to eccentricities in the air-gap [1]. So a short circuit can be understood as an air-gap eccentricity.

Through *MCSA* it is also possible to detect the existence of static and dynamic eccentricities. There are two expressions that can be used to detect these eccentricities, the expression (3.3) is related to the behavior of the current at the sidebands of the slot frequencies and the expression (3.4) monitors the behavior of the current at the sidebands of the supply frequency. So the two expressions related to this fault are given by,

$$f_{slot+ecc} = f_1 \left[(kR \pm n_d)\left(\frac{1 - s}{p}\right) \pm n_w\right] \tag{3.3}$$

$$f_{ecc} = f_1 \left[1 \pm m\left(\frac{1 - s}{p}\right)\right] \tag{3.4}$$

Using the expression (3.3) it is possible to separate the spectral components produced by air-gap eccentricities from the spectral components created by short circuits, but to use this expression it is necessary to knows aspects related to the machine construction. Unlike expression (3.3), for the expression (3.4) it is not required any knowledge of the machine construction, it is only necessary to know the number of pole pairs of the machine.

From Table 2.1 it appears that almost 40-50% of machine related faults are due to bearing faults. According to Nandi and Toliyat [56] these faults can be categorized as outer bearing race defect, inner bearing race defect, ball defect and the frequencies related to these faults are,

$$f_{b,o} = \frac{n}{2} f_r \left[1 - \frac{bd}{pd} \cos\beta\right] \tag{3.5}$$

for an outer bearing race damage

$$f_{b,i} = \frac{n}{2} f_r \left[1 + \frac{bd}{pd} \cos\beta\right] \tag{3.6}$$

for an inner bearing race damage

$$f_{b,r} = \frac{pd}{bd} f_r \left[1 + \left(\frac{bd}{pd} \cos\beta\right)^2\right] \tag{3.7}$$

for a ball damage

It is important to note that for the previous expressions (3.5), (3.6) and (3.7) it is necessary to know the bearings configuration of the machine. However, according to Benbouzid [101] like most induction machines have the same bearings configuration (six and twelve balls), the expressions (3.5) and (3.6) can be approximated by,

$$\begin{cases} f_{b,o} = 0.4 n f_r \\ f_{b,i} = 0.6 n f_r \end{cases} \tag{3.8}$$

The *MCSA* method is only applied to machines that operate under steady state condition, because the results of the current spectrum and the amplitude value of the harmonics are dependent of the machine slip [102]. Therefore, it is desirable that the machine operate under full load conditions. The effect of time-varying load torques was investigated by Schoen and Habetler [103]. The authors support the idea that these effects are undesirable for rotor faults detection.

According to Gazzana *et al.* [102] the frequency of the current harmonics in the spectrum changes with the motor load. It was also verified that for values below 40% of the motor nominal load there is no change in the amplitude values of the current harmonics. The same authors [102] recommended carrying out various tests to the machine but with different values of slip to be sure that the sideband component in the spectrum corresponds to a broken rotor bar. If the amplitude of these sideband harmonics in the spectrum is 50dB smaller than the fundamental frequency the rotor should be considered healthy.

There also another problem that was reported by Riera-Guasp *et al.* [65], that for the case of bars broken at intervals of $\pi/2$ electrical radians, the current analysis is unable to detect the broken rotor bar, because the frequency components of the expression (3.1) does not exist.

3.4.2.6 Instantaneous Power Analysis

In this method the supply currents and voltages of the machine are acquired and multiplied between them in order to obtain the total instantaneous power. This method consists in making a spectral analysis of the instantaneous power signal to search for amplitude changes in the alternate component of the total instantaneous power. In an ideal situation with a machine supplied by a symmetric voltage source, the sum of the instant power absorbed by the motor is a constant term thanks to the cancellation of the alternate components of the power in each phase [104]. The constant term correspond to the total active power absorbed by the machine.

Benbouzid [101] argues that the amount of information carried by the instantaneous power signal is higher compared with the information carried by the current signal. By itself, this factor is an advantage compared with the methods based only on the measurement of the motor currents.

However, in real situations an electrical machine presents small unbalances that are related to unbalanced voltage sources, mechanical asymmetries and noise associated with the sensors used for signal acquisition. These unbalances will cause variations in the signal that represent the sum of the three instant powers absorbed by the motor. In the case of a fault situation, using the spectral analysis of the power signal it is possible to verify the appearance of a constant component and an alternate component with a frequency equals to twice the frequency of the supply voltage [105]. The fault related harmonics appear at the following frequencies:

$$f_b = 2ksf_1 \tag{3.9}$$

Thus, setting a threshold value for the amplitude of the alternate component is possible to detect the presence of faults in the machine. The fact of having to establish a threshold value for the amplitude of the alternate component limits the use of this method, since each machine is a different case. Legowski [42] investigated the effect of time varying torque and concluded that as happened in the MCSA, the amplitude value of the harmonics are dependent of the machine slip.

The closed loop control techniques, such as vector control or direct torque control (*DTC*) also limits the use of this method because these techniques tend to compensate the unbalances caused by the faults [106, 107].

3.4.2.7 Air-Gap Torque Analysis

This method is very similar to the analysis of total instantaneous power, but in this case it is used the electromagnetic/air-gap torque to detect the presence of faults in the machine. Therefore, it is also necessary the measurement of input voltages and currents to estimate the

electromagnetic torque and then proceed to a spectral analysis. In [108] is stated that the air-gap torque represents the combined effect of all the flux linkages and currents in stator and rotor. Therefore, the electromagnetic torque signal has more information when compared with the current and power signals.

According to Hsu [108] the air-gap torque can be estimated based on the mathematical expressions of the supply currents and voltages of the machine. Through these mathematic equations it is easily shown that an asymmetry in the supply voltage or in the stator windings causes an unbalance in the supply currents.

Thus, the spectral analysis of the electromagnetic torque will show an amplitude change in the alternate component that is directly related to the asymmetries in the machine. All asymmetries in the machine both in the stator or rotor cause a general increase in the alternate component.

Bikfalvi and Imecs [105] describes the Vienna Monitoring Method (*VMM*) as one of the most used and successful air-gap torque methods. *VMM* is a model-based technique that calculates the air-gap using two different model structures for the same machine. The models are used to evaluate the space phasors (current and voltage) and the rotor position. In the case of a healthy machine the final result for the space phasors and the air-gap torque is the same in both models. Therefore, the difference between the outputs of the models is zero. For an induction motor with asymmetries the double slip frequencies are sensed by the two models, but in different ways. So the difference between the model torques will contain the double slip frequency oscillations, that are proportional to the load torque. Kral *et al.* [109] show that the *VMM* is independent from inertia and transient regimes. The same authors state that even small rotor faults can be detected due the high sensivity of *VMM*.

For the same reasons of the total instantaneous power analysis, this air-gap torque analysis is not very effective. The measurement of the electromagnetic torque is not economically viable due to its complexity, so in this case the followed approach is the spectral analysis of electromagnetic torque through the estimation of electrical quantities (current and voltage) that is used [105].

3.4.2.8 Artificial Intelligence Techniques

The diagnostic techniques that make use of artificial intelligence (*AI*) methods are a way to make the fault diagnosis system less dependent of the presence of human specialists [110]. The great advantage of this technique, besides the possibility of the system becomes almost automatic, is the ability to store large amounts of information that can later be compared with the information

being processed in that instant, allowing the detection of faults based on the parameters previously collected [106]. Another advantage of using *AI* techniques is that these techniques do not need a detail knowledge of the system behavior when compared with other methods such as mathematical modeling [110].

There are a number of techniques based on artificial intelligence that are used for diagnosis, which includes expert systems [111], neural networks [112], fuzzy logic [113], neuro-fuzzy systems [114, 115] among others. The expert systems are one of the most widely [116] used *AI* techniques for detecting faults in induction motors. For example, if this type of technique is associated with the *MCSA*, the inference engine of the system can have a set of rules that associates each fault of the machine to a frequency of the current spectrum. Then using a database that contains the history of the machine it is performed a diagnostic that concludes if the machine has a malfunction.

Another type of technique also widely used to diagnose faults in motors are the neural networks. In the past, neural networks were also used to estimate torque and motor control [117, 118]. Li *et al.* [119] use neural networks for detect and diagnose bearing faults based on the extracted bearing vibration measurements. The vibrations features are obtained from the frequency domain using the Fast Fourier Transform (*FFT).* The tests were conducted with simulated and vibration measurements. The obtained results indicate that neural networks can be used for diagnosis various types of bearings faults through appropriate measurement and interpretation of motor bearing vibration signals.

Filippetti *et al.* [112] show a neural network approach for rotor fault diagnosis. A neural network was trained using the collected data obtained from experimental tests in a healthy machine. For the faulted machines the data was obtained by simulation. The proposed neural network was able to distinguish between "healthy" and "faulty" machines.

Jack and Nandi [120] used a neural network helped by a genetic algorithm to make the operation of faults classification faster and also to increase the accuracy of the faults classification. In this study, the input features of the neural network are estimated vibrations signals based on vibration data taken from performed experimental tests. The final results show that the genetic algorithm was able to select a subset of six input features from a large set of input features with an accuracy classification of about 99%.

However, despite the several advantages enumerated, the need of a training phase is a limitation to the widespread use of neural networks, since it requires a large amount of data collected that is related to the different situations of machine’s operation mode, for example, various load levels, different frequency in the voltage source among others.

3.5 Synthesis

In this section will be made a brief synthesis of the *FDD* approaches discussed in this chapter. The Table 3.2 is adapted from [121] and presents several characteristics of the *FDD* methods presented in the previous section.

FDD Approach	Measurement Device	Measurement Frequency	Non-Intrusive	Potential Information	Required Computational Capacity	On-line/Off-line	Possible means of analysis
Current	Hall effect Current transformer (CT)	Continuous	Yes	Average	Low	On	RMS trending, Time-domain analysis, Spectral analysis, Statistical methods
Voltage	Voltage transformer (VT)	Continuous	Yes	Average	Low	On	RMS trending, Time-domain analysis, Spectral analysis, Statistical methods
Partial Discharges	Capacitors	Continuous	No	Average	Low	On	RMS trending, Time-domain analysis, Spectral analysis, Statistical methods
Flux	Search coil / Hall effect transducer	Sporadic(Hourly, monthly)	Yes	Very High	Low	On	RMS trending, Time-domain analysis, Spectral analysis, Statistical methods
Vibration	Accelerometer	Sporadic(Hourly, monthly)	No	High	Low	On	RMS trending, Time-domain analysis, Spectral analysis, Statistical methods
Acoustic	Microphone	Sporadic(Hourly, monthly)	Yes	High	Low	On	RMS trending, Time-domain analysis, Spectral analysis, Statistical methods
Temperature	Thermocouple / Infra-red camera	Continuous / Sporadic	Yes / No	Average / High	Low	On	RMS trending, Time-domain analysis, Spectral analysis, Statistical methods Visual Interpretation
Instantaneous Power Air-gap torque	Instrumentation Transformers (CT's and VT'S)	Continuous	Yes	Very High	Low	On	Time-domain analysis, Frequency domain analysis, Statistical methods
AI Techniques	Various types of sensors/transducers	Continuous	Yes	Average	High	On	Neural Networks, Data-based models, Observer-based approaches

Table 3.2- Comparison between FDD methods

Chapter 4

TPU: Hardware and Software Description

This chapter presents a major description of the Terminal Protection Unit (*TPU*) x220 used in this work. Initially is made an introduction to the equipment, why it was developed and what is his objective. In the final sections it is made description of the hardware and software architecture.

4.1 Introduction

The Terminal Protection Unit (*TPU*) *x220* belongs to the range of digital compact relays produced by *EFACEC*. This multifunctional relay is a robust and cost-effective solution for protection and control of *HV / MV* systems, such as lines, transformers, generators and motors. Usually *TPU x220* is used in the protection of power system aerial lines or underground cables. It is also used in transformer applications, as backup protection for main transformer differential protection. In the *TPU x220* are incorporated functions such as:

- Protection Functions – Phase Overcurrent, Underfrequency, Thermal Overload, Phase Overvoltage;
- Control and Supervision Functions – Circuit Breaker Failure, Synchronism and Voltage Check, Broken Conductor Check;
- Monitoring and Recording Functions – Disturbance Recorder, Fault Locator, Three-Phase Measurements.

This relay can be used standalone, without communication with other equipments or system integrated, taking advantage of its multiple communication protocols options. In the Figure 4.1 are presented the various products from *TPU x220* line.

Figure 4.1 – List of *TPU x220* line products

A key aspect is the fact that all the features of *TPU x220* are compatible with the latest international standards and allow the use of multiple communication standards. The *TPU x220* is

fully programmable in various languages, due to a built-in logic engine that allows further application flexibility, alternatives for customization of protection and control schemes and implementation of *PLC* logic defined by the user.

The local interface (Figure 4.2) includes an *LCD* and a 20x4 alphanumeric keyboard that allows the access to the relay status. There are also 8 programmable *LED*'s and 4 programmable function keys that indicate the operating status of the relay.

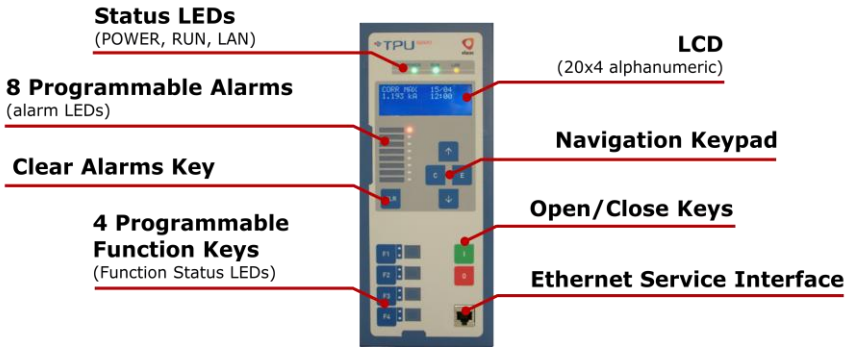

Figure 4.2 – Illustration of the *TPU* front panel [122]

For remote interface (Table 4.1), the relay provides an optional embedded web server (available in the front or rear Ethernet ports), where all the local operations are available. Thus, the interaction with the device does not require external software tools or the presence of technical experts near the equipment.

Interfaces	
Communications	RS 232/RS 485 (Cooper)
	RS 232 / RS 485 (Cooper or optical fiber)
	10/100 BaseTx or 10/100 BaseFx
Time Synchronization	Input *IRIG*- B
	Client *SNTP*
Alternative Communication Protocols	*IEC* 61850 *Server* and *GOOSE*
	IEC 60870-5-104 (*TCP/IP*)
	IEC 60870-5-103 (Serial)
	DNP 3.0 (Serial)
	IEC 60870-5-101 (Serial)

Table 4.1 – Various types of remote interfaces

4.2 Hardware Architecture

The general hardware architecture is presented in Figure 4.3. The presented modules will be explained in the following sections.

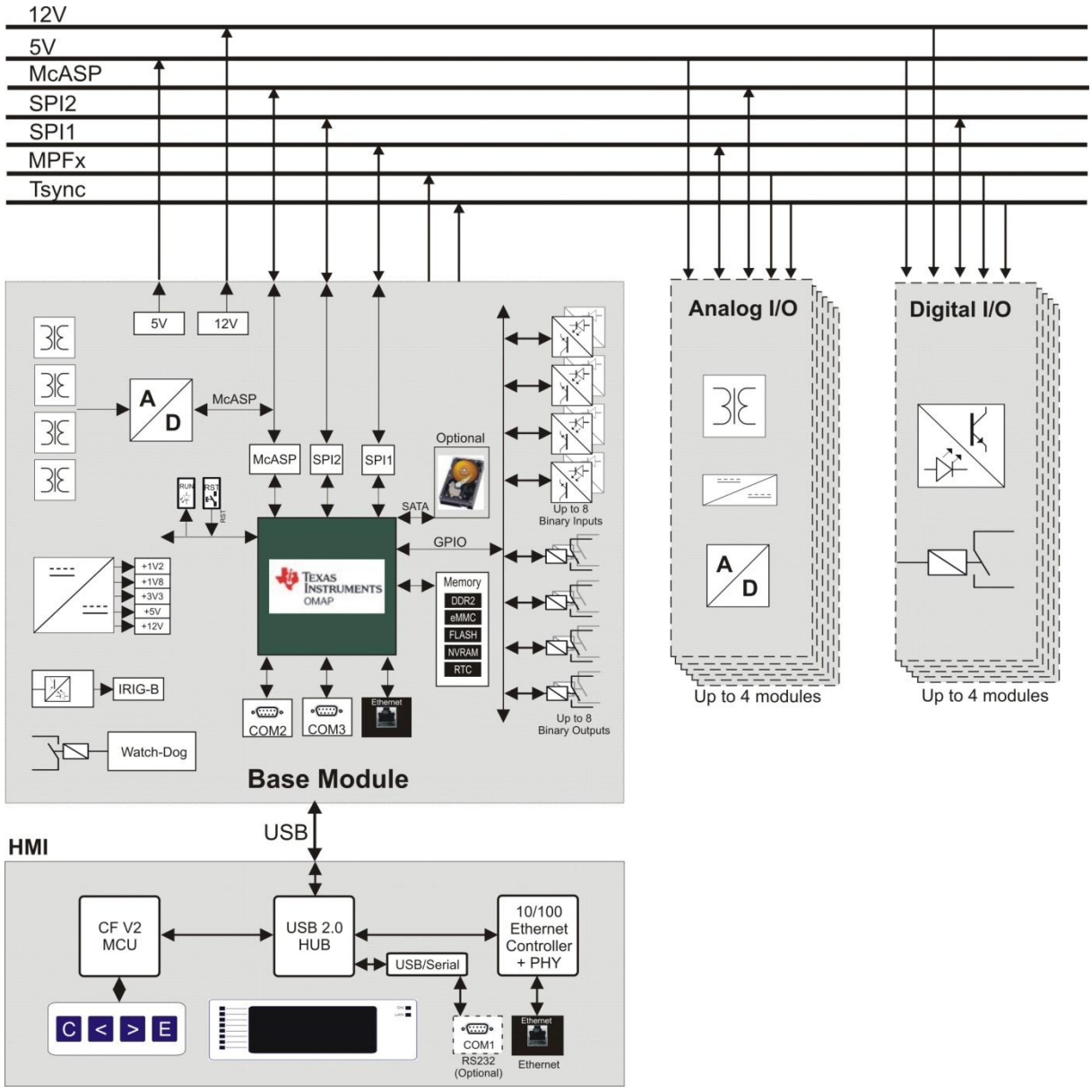

Figure 4.3 – Hardware Architecture of the *TPU x220* products [123]

The hardware architecture is composed by a mandatory basic module, called *base module*. This *base module* and the *HMI* module are the base of all *TPU* units. Sometimes some applications require more *I/O* in addition to those available in the *base module*. This hardware architecture can be divided in the following sub-modules (Figure 4.3):

- Processing and communications module;

- Power supply module;
- Digital I/O module;
- Analog I/O module;

The communication between the digital *I/O* modules and the *base module* is made through SPI_2 bus. In the case of the local digital *I/O* (digital *I/O* located in the *base module*) the data is acquired via main processor *GPIOs*. *DC* analog *I/O* modules and the *base module* communicate through SPI_1 bus and the communication between *ac* analog modules and the *base module* is made through the McASP bus.

4.2.1 Processing and communications module

The processing unit is based on a 32 bit Texas Instruments *OMAP-L138* Low Power Applications Processor. Thus, it is possible to have a low-cost and high peripheral integration solution based on a single processing device.

The *OMAP-L138* Applications Processor is composed by two primary *CPU* cores: an *ARM RISC CPU* for general-purpose processing, communication and systems control. A *DSP* to handle analog processing tasks (protection, measurements, etc.). The *OMAP-L138* Applications Processor consists of the following primary components:

- 32 bit *ARM926EJ RISC CPU* core and associated memories;
- *DSP* (TMS320C674x) and associated memories;
- *I/O* peripherals;
- *DMA* subsystem and *SDRAM EMIF* interface.

4.2.2 Power supply module

The power supply is a switched-mode power supply, with a *flyback* topology and an output power of up to 40 *W*. This power supply provides 2 output voltages: 5 V_{dc} for powering the electronic components and 12 V_{dc} for powering the relay-based binary outputs.

4.2.3 Digital *I/O*

The digital *I/O* included in the base module consists in 4 digital inputs, as well as 4 digital outputs by relay. There is a fifth output, used for the *Watchdog* function that indicates the functioning state of the unit. The digital inputs and outputs are both floating and insulated to ensure the security of the unit.

4.2.4 *A.C.* Analog *I/O*

This module provides at least four *ac* analog inputs (voltage and/or currents) through the use of instrumentation transformers. The Voltage Transformers (*VT*'s) operate in the scale of 100*V*, 110*V* 115*V* and 120*V*, and the Current Transformers (*CT*'s) use the scale of 1*A* or 5*A*. The specific operating values for the *VT*'s and the *CT*'s depend on the final application of the product. The configuration of the current and voltage inputs scales can be changed by a jumper.

4.3 Software Architecture

The software architecture is divided in 2 main frameworks: *Syrius* and *Cerberus*, where *Syrius* is the master framework and *Cerberus* is the slave framework. As stated before the processing unit is a Texas Instruments *OMAP-L138* with two *CPU* cores. The *Syrius* framework uses the *ARM CPU* core and the *DSP CPU* is used by the *Cerberus* framework.

The *Syrius* framework is responsible for the resource management of the various hardware and software components of the *TPU x220*. The *HMI*, digital *I/O*, settings, reports, and historical record of events are resources that are under the responsibility of *Syrius*. The only feature that is not under the responsibility of *Syrius* is the analog *I/O* (*CT*'s and *VT*'s) due to the large amount of data collected by these *I/O* that put in risk the stability of the processing unit.

The core of the *Syrius* framework is the Real-Time Database (*RTDB*). In this database are registered all the settings and events that can occur in the *TPU x220*. Any change in these settings or events must be reported to the *RTDB*. It can be said that the *Syrius* is an on event framework, *Syrius* only updates its states when occurs a change in the variables registered in the *RTDB*.

Contrary to *Syrius*, the *Cerberus* Framework is responsible for the acquisition, filtration and estimation (all these processes are done by software) of the data collected by the analog *I/O*. The data acquisition is maintained by the interrupt service routine (*ISR*) triggered by the hardware that performs the sampling. Besides that, *Cerberus* is the framework that stores all the application functions and algorithms of *TPU x220*.

Although *Syrius* and *Cerberus* are two different frameworks, it is necessary the existence of communication between them, because the function settings of the algorithms stored in *Cerberus* are in the *Syrius* side. It is also important to note that there are functions and algorithms that operate on inputs and outputs (responsibility of *Syrius*), which reinforces the need for communication between *Cerberus* and the *Syrius*. In the communication process between the two frameworks is used a zone of shared memory, where each framework places the information that the other framework needs. In the Figure 4.4 is shown the software architecture described above.

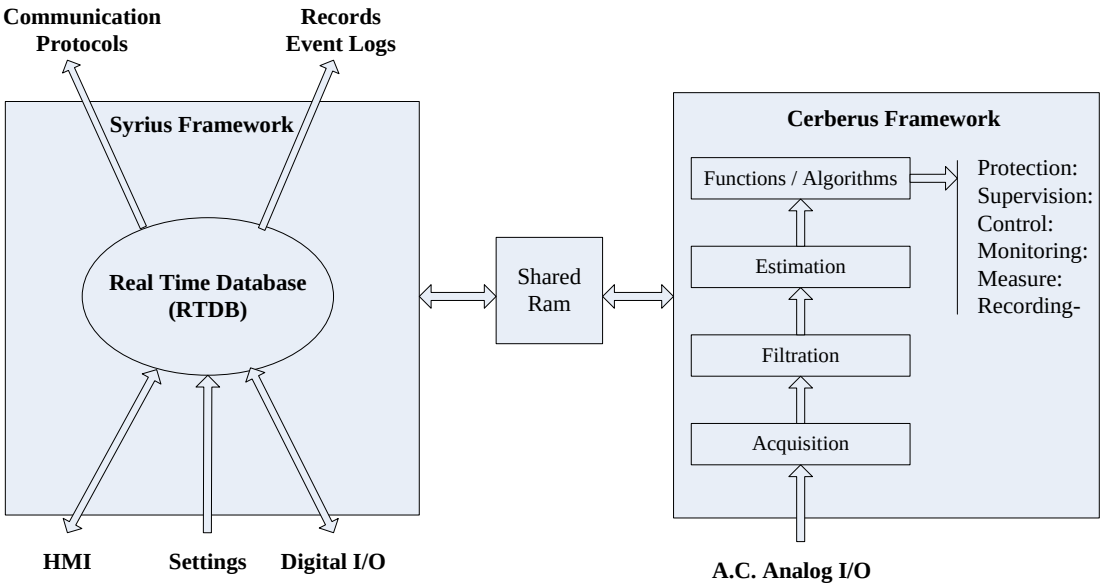

Figure 4.4 – Software architecture of the *TPU x220* products

In *Cerberus* there is an application framework (Figure 4.5), where each application function is considered a task. To integrate an application in the application framework of *Cerberus*, there are a set of rules in the framework that must be respected. First, each application launched in *Cerberus* should be associated with a hexadecimal word that identifies the application internally.

Second, all applications have three key items, the index, priority, and multiplicity. The index indicates the position of the application in the list of all existing functions in the *TPU x220*. The multiplicity indicates how many instances of an application can be linked to another application. The priority indicates the frequency of execution of each application on the device, according to the importance of the task. The priorities are divided into four categories:

- P1 - 1/16 to 1/8 of the cycle;
- P2 - 1/4 cycle;
- P3 - half cycle;
- P4 - a cycle period. Used for execution periods (t) that does not need to be less than 50 *ms*.

For example *CT*'s supervision and differential protections have a P1 priority due to their high importance. On the other side, three-phase measurements, disturbance recorder and incident reports have a low importance in comparison with differential protection, therefore they have a P4 priority.

Third, each application has a set of configurations, where are defined the analog and digital inputs that will be used, the settings that an application need to be executed and the final

results (outputs) that an application should return. This information is introduced in the *Syrius* Framework using the *XML* language. However, in the *Cerberus* side the applications must have defined the same settings inserted in *Syrius*.

Finally, as the programming language used for the development of the *TPU x220* applications is an object oriented language (*OOL*), each application is defined as a class. Therefore, the applications must contain a constructor, a destructor, an initiator and an executioner. The digital inputs, analog inputs and outputs defined in the *XML* files inserted in the *Syrius* Framework should also be initialized and configured for each application.

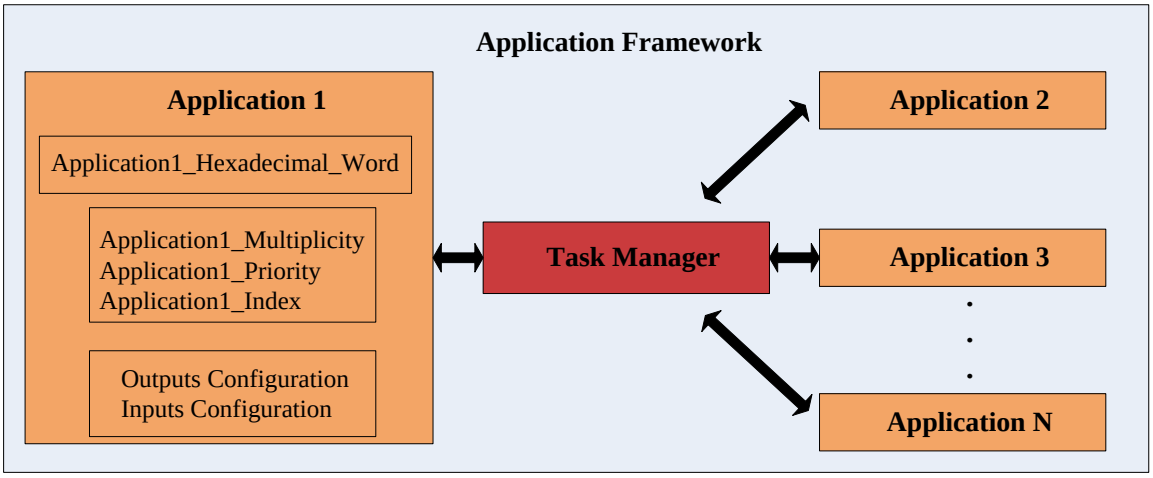

Figure 4.5 – Basic architecture of the Cerberus application framework

Chapter 5

MMoDiS : A *PCA* based Fault Detection and Diagnosis System

This chapter explains the whole architecture of *MMoDiS* since the high-level representations up to the description of the routines. Firstly it is described the faults detection and diagnosis method used, the *PCA*. Secondly, *MMoDiS* is presented as an on-line condition monitoring systems and are also discussed his operational requirements. Thirdly, it is described the conceptual model of the system, that basically is the idea that supports the developed solution. Finally, it is explained the architectural diagram of the system and finally the description of the existing routines inside the system.

5.1 Principal Component Analysis *(PCA)*

Principal Component Analysis is a non-parametric statistical method used to reduce the number of original variables, which are correlated, in a set of new uncorrelated variables referred as Principal Components (*PC*). The first public descriptions of this method were given in 1901 by Pearson [124] and latter developed in 1933 by Hotelling [125].

The application of *PCA* as a variable reduction technique for *FDD* purposes has been studied by several academic and industrial researchers [126-129]. For most applications, the data variability can be captured in two or three dimensions, and the visualization can be done on a single plot.

This concept of reducing the number of variables is useful in energy systems, particularly three-phase systems, such as three-phase induction machines. In fact, this method was already use for fault detection purposes. In [30] Cardoso and Saraiva discussed the subject of on-line detection of air-gap in three-phase induction motors. The experimental results shows that is possible to detect the presence of air-gap eccentricities in three-phase induction motors, through a computer-aided monitoring system that computes the αβ-vector transformation.

As stated before *PCA* is used in *FDD* systems to extract relevant information from huge data sets. The number of principal components is less than or equal to the number of original

variables and each principal component is calculated as a linear combination of the original variables.

PCA can be obtained through several ways, such as eigenvalue decomposition of a matrix or single value decomposition (*SVD*) of a matrix [130]. In the case of eigenvalue decomposition it consists in the representation of matrix in terms of its eigenvalues and eigenvectors. Through the definition of eigenvectors, this technique is able to obtain the main directions of the data sample on a space-vector. It also possible to measure the weight of the sampled data spread through the main directions defined by the eigenvectors. These metric values are defined as eigenvalues [33].

Let $X \in \Re^{n \times m}$ represents a data matrix, where n denotes the number of measurements and m denotes the number of physical variables. The $X^T \in \Re^{m \times n}$ represents the transposed matrix of X, where m and n have the same meaning as in the X matrix. From the product of the two matrixes X and X^T is obtained a square matrix $E \in \Re^{n \times n}$ called correlation matrix.

$$E = X^T \times X \tag{5.1}$$

After establishing the correlation matrix the eigenvectors and the respective eigenvalues, of E are calculated. There are several ways to define eigenvectors and eigenvalues, the most common approach defines an eigenvector of the matrix E as a vector that satisfies the following equation:

$$E \times u = \lambda \times u, \tag{5.2}$$

When rewritten, the equation becomes:

$$(E - \lambda I)u = 0, \tag{5.3}$$

Where λ is a scalar called the eigenvalue associated to the eigenvector u.

Concerning to some researches that use this technique, Cardoso *et al.* [31] also discussed the application of on-line detection of rotor cage in three-phase induction machines. The experimental results show that by observing the relative thickness of the motor current αβ-vector transformation is possible to detect the existence of broken rotor bars.

Önel and Benbouzid [72] studied the problem of bearings fault detection in induction motors when are used current space patterns. The obtained results indicate that both αβ-vector transformation and Concordia transform in the presence of bearing faults present changes in their shapes.

Pires *et al.* [33] proposed an on-line fault detection system based on the eigenvalue decomposition. The αβ-vector approach is used and the results show that is possible to detect rotor and stator faults with this approach. However, it is mentioned that this method requires expert technicians in order to distinguish a normal operation condition from a potential fault mode.

Martins *et al.* [32] developed a system based on the use of image processing techniques of the 3-D stator current space patterns. The authors argue that the use of pattern recognition techniques brings significant improvements in the field of fault detection in induction machines. Unfortunately, any unbalance in the power supply system as well as the existence of residual asymmetries in the machine may lead to variations in the stator currents, which can limit the use of this diagnostic method.

Martins *et al.* [34] investigated the effect of closed-loop drives in *PCA*. The authors conclude for closed-loop architectures, the observation of the input line is not a good approach because the fault influence is imperceptible. However, the fault influence appears in the supply voltage and the obtained results show that it is possible to use this method for *FDD* purposes.

In three-phase energy systems without neutral connection it is usual to use the αβ-vector transformation to reduce the number of original variables. This transformation converts the three-phase currents or voltages into an equivalent two-phase system. So the αβ-vector components are given by:

$$\begin{cases} i_\alpha = \sqrt{\frac{2}{3}} i_a - \frac{1}{\sqrt{6}} i_b - \frac{1}{\sqrt{6}} i_c \\ i_\beta = \frac{1}{\sqrt{2}} i_b - \frac{1}{\sqrt{2}} i_c \end{cases} \tag{5.4}$$

In ideal conditions, the three-phase currents lead to a αβ-vector with the following components:

$$\begin{cases} i_\alpha = \sqrt{\frac{6}{2}} i_M \sin(\omega t) \\ i_\beta = \sqrt{\frac{6}{2}} i_M \sin\left(\omega t - \frac{\pi}{2}\right) \end{cases} \tag{5.5}$$

Under normal conditions and with a balanced and constant frequency power supply, a pure sinusoidal signal makes a circular pattern centered at the origin of the $\alpha\beta$ coordinates. In Figure 5.1 there is the representation of a healthy motor input current in the $\alpha\beta$-vector pattern.

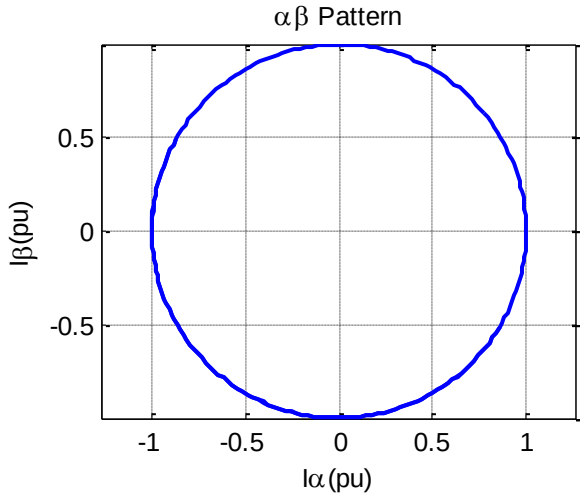

Figure 5.1 - Healthy motor input current *αβ* –vector pattern

However under abnormal conditions and considering a constant frequency power supply the previous conditions are no longer valid and the *αβ*-vector pattern loses its circular shape. For a situation where occurs a stator winding fault the input current *αβ*-vector pattern becomes an ellipse because there is an amplitude variation in the current of the winding that is in a fault situation. The patterns related to a stator winding fault are presented in the Figure 5.2.

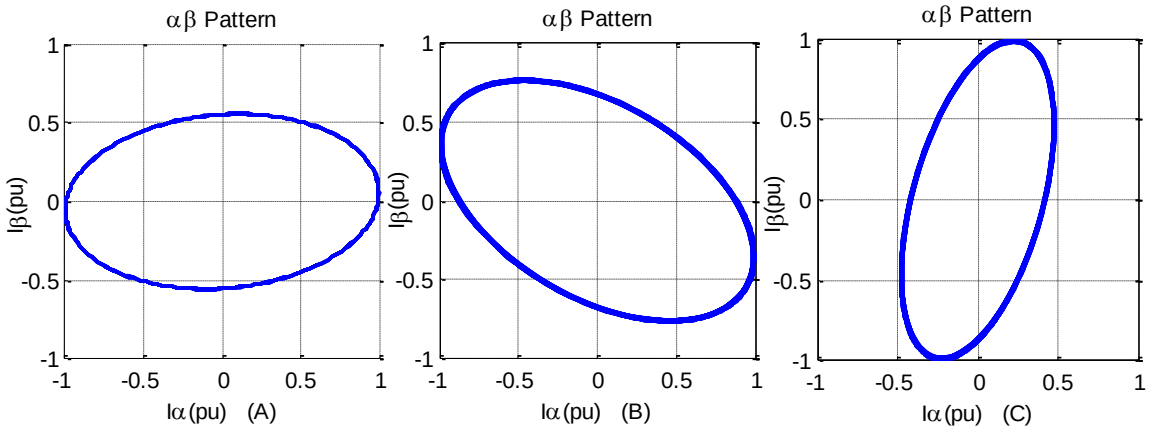

Figure 5.2 – Stator fault input current *αβ*-vector patterns. (A) stator fault in phase A (B) stator fault in phase B (C) stator fault in phase C

When the motor presents a rotor fault situation the *αβ*-vector pattern presents a circular shape but the eigenvalues are not constant. It is possible to observe (Figure 5.3) the appearance of a thick ring and the thickness of the ring increases with the severity of the fault. Cardoso *et al.* [31] concluded that the severity of the fault is proportional to the number of the rotor bars, but there is a moment where severity of the factor decreases as the number of broken bars increases.

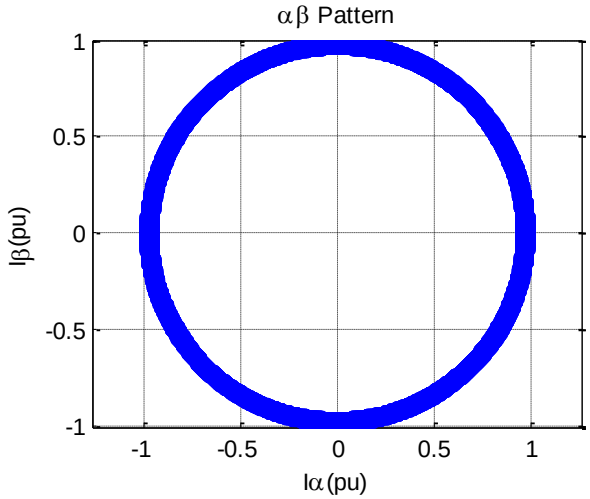

Figure 5.3 – Rotor fault input current *αβ*-vector pattern

5.2 *MMoDiS* as an On-line Condition Monitoring System

The *MMoDiS* is an on-line system for detection and diagnosis of electrical faults in three-phase induction machines that informs the user of the machine state. The *FDD* method used in *MMoDiS* is based on *PCA* (Section 5.1). According to the Isermann [76] *PCA* is classified as a multivariate data analysis fault detection method. The hardware and data acquisition used for monitoring and diagnosis the machine is based on the *TPU x220* developed by *EFACEC*.

The possibility of having knowledge of the machine state in real-time, allows the reduction or even the elimination of unexpected downtimes. As a result, the integrity of the machine is ensured, thereby reducing the replacement and maintenance costs.

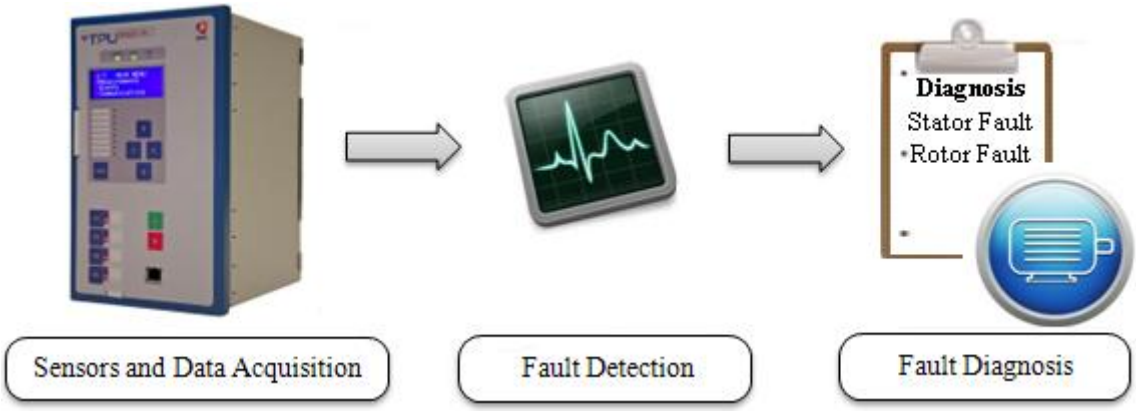

Figure 5.4 – Global vision of *MMoDiS*

As can be seen in Figure 5.4 the architecture chosen for the condition monitoring system is that proposed by Han and Song [83]. From the acquired data, *MMoDiS* can only act in one way

that is prediction. This prediction consists in a continuously and real-time evaluation of the machine state and then inform the user.

Obviously *MMoDiS* could integrate other features, but the focus of this dissertation is only the detection and diagnosis of electrical faults, and it is this aspect that this document will focus.

5.2.1 Pre-Operational Requirements

In order to proceed to a proper monitoring and diagnosis, *MMoDiS* must meet certain requirements, without them its objectives could not be fulfilled. Firstly, *MMoDiS* was designed only for three-phase induction machines. No tests were conducted in other types of machines, so there is no guarantee that the obtained results are reliable.

Secondly, the machine must be powered by a three-phase voltage source, should not be used current sources, once the system was developed for voltage controlled machines.

The machine must operate in a nominal regime or near the nominal regime , with a torque greater than 85% of the nominal torque. The machine should never run without any mechanical load. This factor is due to the need of increasing the reliability of the results provided by *MMoDiS*.

The machine must allow the connection of a *TPU x220* with current transformers (*CT*'s). This is a fundamental requirement, since *MMoDiS* depends on the machine's currents to carry out the monitoring and diagnosis.

Finally, any microprocessor is limited in terms of memory and processing power, the processor of the *TPU x220* is no exception. Therefore it is necessary to ensure a simple and efficient algorithm to avoid unnecessary use of resources (memory and processing power) and because there are other tasks running in parallel with the developed algorithm.

5.3 Functional Vision

Any system can interact with external entities, such as devices, people and other systems through the features it offers. On the other hand, the functionalities can be shared by several entities, with dependencies between the functionalities.

According to [131] the existence of a high-level representation or a model of the system is fundamental and have the objective of documenting the architectural structure and the features of the system. There are various types of models and high-level representations. In software

development one of the first models to be used is the conceptual model. This model is defined as a high-level representation of the system that presents the idea or concept that supports the solution developed and allows his organization into smaller pieces. Therefore, a conceptual model is a powerful tool because it is possible to visualize and document the system as it is or we want it to be.

To represent *MMoDiS* in the standard language of computer systems development, the system modeling was done using the language Unified Modeling Language (*UML*). In this type of modelation the use case diagram represents all the functionalities that a system offers to the user.

In the use case diagram, external entities such as people, devices, systems, are all referred as actors. An actor is someone or something that is external to the system, but that is going to interact with the system. This is the starting point for the development of *MMoDiS*, since it represents in a clear and objective way all the use cases of the developed infrastructure. In *MMoDiS* were defined two types of interactions, the user and the administrator. In the Table 5.1 is described which is the role of each actor in the developed system.

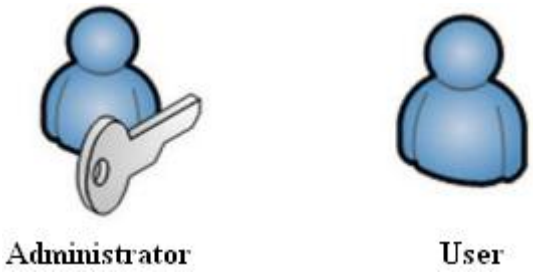

Figure 5.5 – Types of actor that exists in the developed system

Actor	Profile
User	Only has access to the outputs given by the system.
Administrator	Have access to everything that the User have and also have the possibility of changing the system settings.

Table 5.1 – Specification of the actor profiles

In the case of *MMoDiS* any actor has a set of features. However, there is a set of features, shown in Figure 5.6 that are common to all actors.

Figure 5.6 – Use Case diagram of the User profile

The features offered by the User Profile are the following:

- Start Warning - provides access to consult and change the situation of the machine start. In a starting situation there is a *LED* located in the front panel of the *TPU* that indicates this operation;
- Trash Warning - indicates if the currents acquired by the *CT*'s are inside the limits of the motor nominal current. If the obtained currents have a value less than 50% of the motor nominal current, the algorithm stops and waits for the currents to return to values inside the imposed limits;
- Calibration – allows the user the possibility to calibrate the algorithm for the motor that is in operation. In this feature the calculated eigenvectors and eigenvalues are stored as reference values;
- Motor Faults - shows to the user if the stator/rotor of the machine is in a fault situation. In the case of fault, this information is presented to the user using a *LED* located in the front panel of the *TPU*;
- Severity Factors - allows the user to see the severity of the stator/rotor fault. This information is presented to the user on the *LCD* of the *TPU* in the form of percentage;

- Eigenvalues – allows the user to see in real-time the values of the eigenvalues computed by the algorithm;
- Eigenvectors – through this option is possible to observe in real-time the eigenvectors computed by the algorithm;
- Phase Fault - indicates the stator phase that is in a fault situation. If there is no fault in the stator windings, this item presents the value 0.

The actor Administrator besides the features described in the Figure 5.1 have access to the functionalities presented in Figure 5.7.

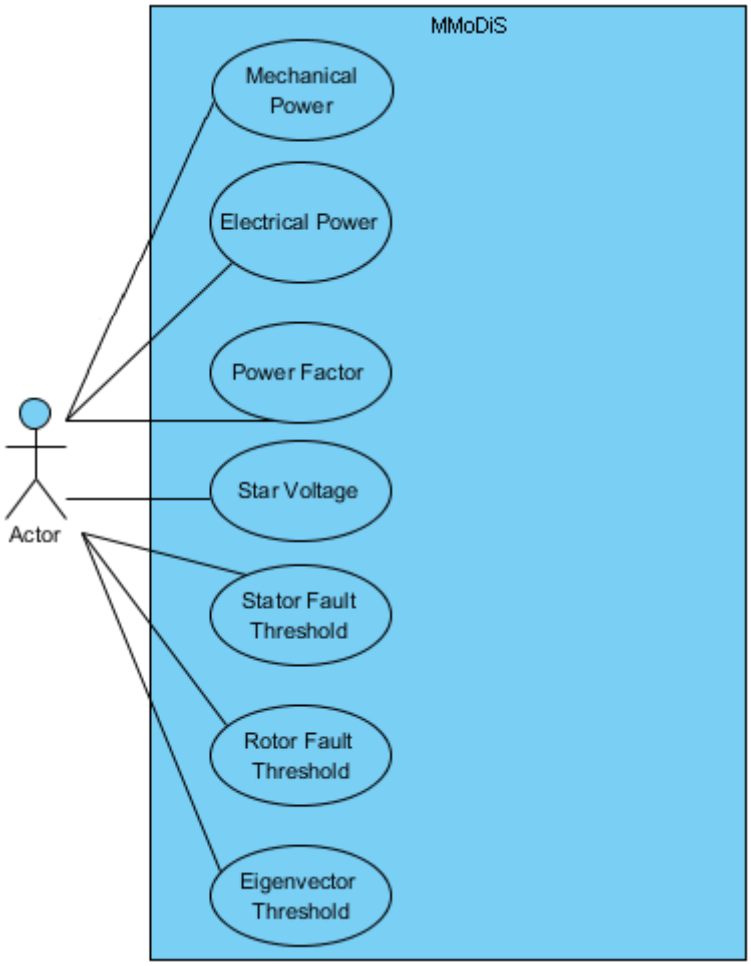

Figure 5.7 – Use Case diagram of the Administrator profile

Detailing each feature:

- Mechanical Power (P_M) - allows the administrator to change the mechanical power of the machine. This parameter can be used to calculate the nominal current of the machine if is not given the electrical power. The value must be given in *Hp*;

- Electrical Power (P_E) – allows the administrator to change the electrical power of the machine. This parameter is used to calculate the nominal current of the machine. The value must be given in *kW*;
- Power Factor - power factor of the machine that will be subjected to detection and diagnosis tests. This value is used to calculate the nominal current of the machine. The given value must be between 0,5 and 0,95;
- Star Voltage (*U*) – voltage value between the neutral and the phase. This value is used to calculate the nominal current. The given values must be between 110 *V* and 230 *V*;
- Stator Fault Threshold - Severity factor value from which the algorithm detects the existence of a fault in the stator. This value is given in percentage with values between 0 and 0,13;
- Rotor Fault Threshold - Severity factor value from which the algorithm detects the existence of a fault in the rotor. This value is given in percentage with values between 0 and 0,07;
- Eigenvector Threshold - This threshold is used to distinguish the faults in the stator phases.

5.4 Architectural Diagram

The aim is *MMoDiS* be a modular system, because in the future if the system is changed and improved, it is only necessary to add the other modules to the existing ones. Therefore the architecture of the system was organized in three modules: Data Acquisition, Fault Detection, Fault Diagnosis and Interface. This architecture is shown in Figure 5.8.

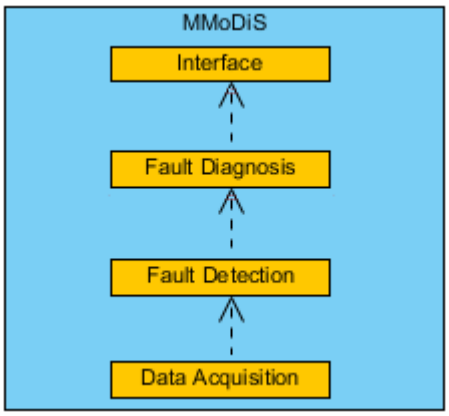

Figure 5.8 – Architectural Diagram of *MMoDiS*

The first level, Data Acquisition, is responsible for reading and processing the obtained data from the sensors, more precisely the acquisition of current samples through the current transformers (*CT*'s).

The second level, Fault Detection, uses the data collected from the data acquisition module. It is in this level that the data is analyzed to verify if there is any change that indicates the presence of a fault. There are a set of determinant conditions obtained by the αβ-vector transformation that indicate the presence of a fault.

At the third level, Fault Diagnosis, if a fault is detected this module is informed. This module has the ability to detect which is the source of the fault, from the information provided by the Fault Detection module. This module should be necessarily separated from Fault Detection, because compared with the Fault Detection module, this module requires a larger time interval to evaluate the information obtained. It is in this module that is detected the location of fault, if the fault occurs in the stator side or in the rotor side and then it is obtained magnitude of the fault.

Finally, the interface module allows to the user the visualization of the options provided by *MMoDiS*. The options available were characterized previously in the conceptual model.

5.5 Used Technologies

Taking into account the main features and specifications of a condition monitoring system (*CMS*) mentioned in Chapter 3, for the implementation of *MMoDiS* there are several technologies in the market. However, as *MMoDiS* will be developed based on the *TPU S220*, were used the existing technologies in that equipment. Therefore, *MMoDiS* is part of *Cerberus* Framework, which is one of the existing frameworks in the *TPU x220* products.

The development of *MMoDiS* was made using C++ programming language. The fact of using a low level programming language such as C++, provides temporal efficiency in the algorithm routines related to data acquisition from sensors, because it does not require the use of *DLL's* that other high-level languages, such as Java and *C#* need. The software used for programming the system was the Code Composer Studio (*CCS*) from Texas Instruments (*TI*). Code Composer Studio is an integrated development environment (*IDE*) used to develop applications for Texas Instruments embedded processors. In the Figure 5.9 are presented the used technologies and the relationship between those technologies.

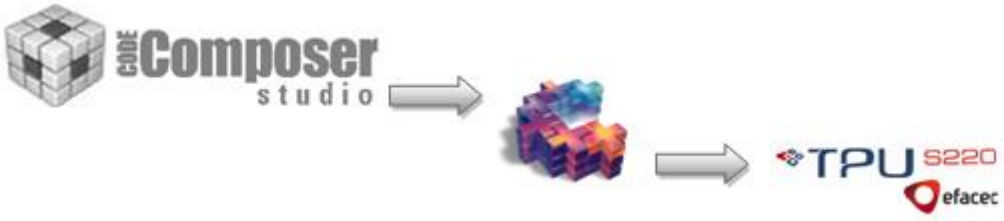

Figure 5.9 – Used Technologies in the implementation of *MMoDiS*

5.6 Routines Description

This section has the objective of explaining the implemented algorithm. The description of the algorithm routines will be made through activity diagrams. The construction of activity diagrams was made using the *UML* language. In the Figure 5.10 is presented an activity diagram that represents the basic workflow of *MMoDiS*.

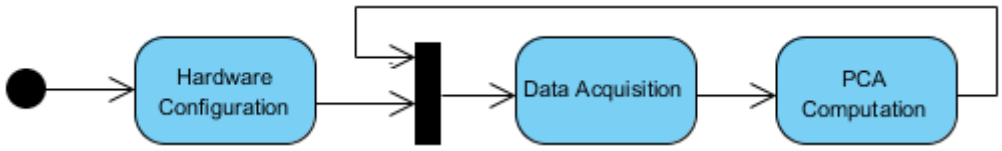

Figure 5.10 – Activity diagram related to the workflow of *MMoDiS*

As can be seen in Figure 5.10, the first block to be executed is the hardware configuration (Figure 5.11), which sets all the hardware used by the application. In this block are included the settings of the digital inputs used, the used analog inputs and outputs of the application. In the case of *MMoDiS* are used two digital inputs, one for the startup of the machine and the other for calibration purposes. Regarding to the analog inputs, are used three *CT*'s that corresponds to a current group, used to acquire the three-phase supply currents of the induction machine.

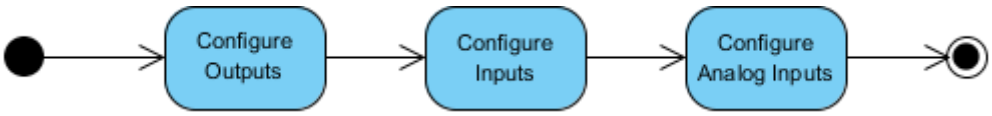

Figure 5.11 – Activity diagram of the hardware configuration block

The Figure 5.12 corresponds to the Data Acquisition block. This block is fundamental, because is in this block that are acquired the currents of the machine that are used to detect and diagnose the fault situations. Initially it is checked if the machine is in a start condition, in the case of a start situation the algorithm will wait until the machine operation mode is changed from start to nominal operation. To change the operating conditions in the machine it is necessary to press the Function Key F2 located in the front panel of the *TPU S220*. The user is informed of the machine operation mode through a *LED* located in the front panel of the *TPU*. The checks made after the current readings are conducted in order to prevent that the algorithm indicates to the user incorrect information about the state of the machine.

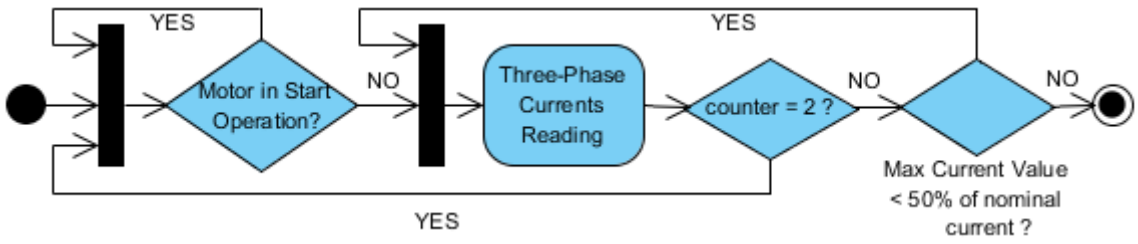

Figure 5.12 – Activity diagram of the Data Acquisition module

After the start situation when the machine is operating under nominal conditions, the machine supply currents are acquired. The currents are acquired using the *CT*'s of the *TPU*. The activity diagram of Figure 5.13 represents how the currents are acquired in the implemented algorithm.

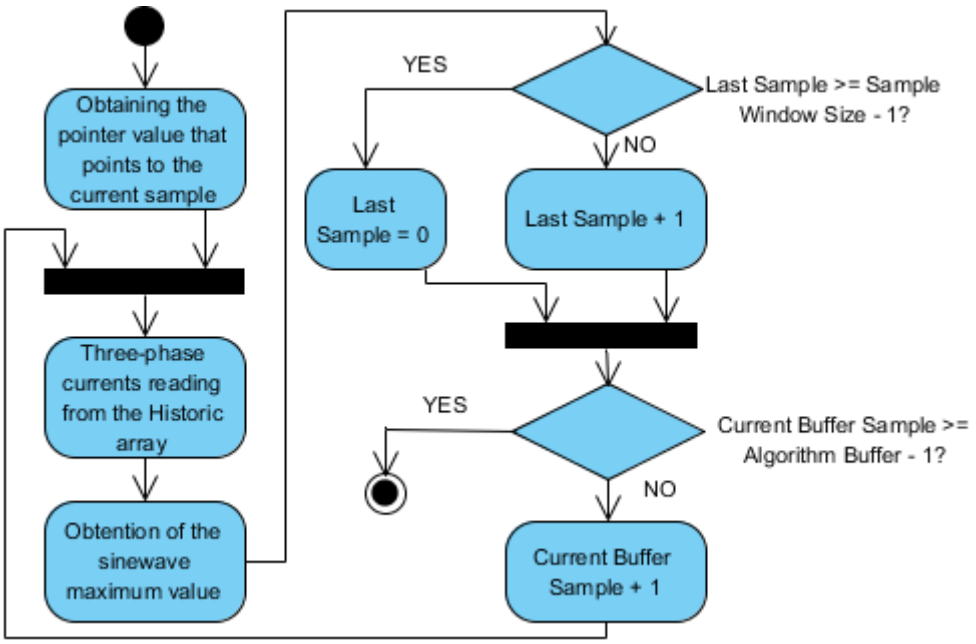

Figure 5.13 – Activity diagram of the three-phase current reading module

Initially in the data acquisition module it is necessary to obtain the current data sample from the historic array. This array is a buffer of 80 positions where are placed the samples filtered and read by the analog-digital converter (*ADC*).

After the location of the current data sample, the samples from historic array are copied to a structure in the application. As the samples are copied to the structure, the pointer to the historic array is incremented. When is reached the maximum length of the historic array the pointer returns to the initial position, the first sample (Figure 5.14).

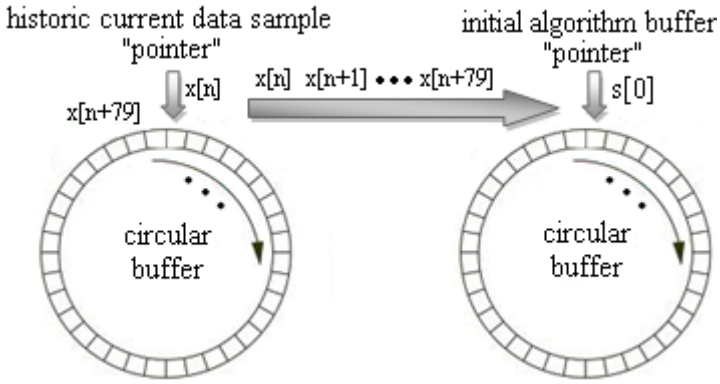

Figure 5.14 – Data acquisition process

The application structure has a buffer of 300 samples and as the array is filled, the current position is incremented. When the array length is reached, the read cycle is interrupted and the module of fault detection and fault diagnosis is executed. In the Figure 5.16 is represented the activity diagram of the *PCA* module.

The fault detection and diagnosis module (Figure 5.16) consists in a sliding window (Figure 5.15) with a predefined size of 20 positions. This sliding window has the objective to scroll all the 300 positions of the array that contains the current samples acquired in the data acquisition module. After the sliding window scroll all the positions of the data acquisition array, the algorithm returns to the data acquisition module.

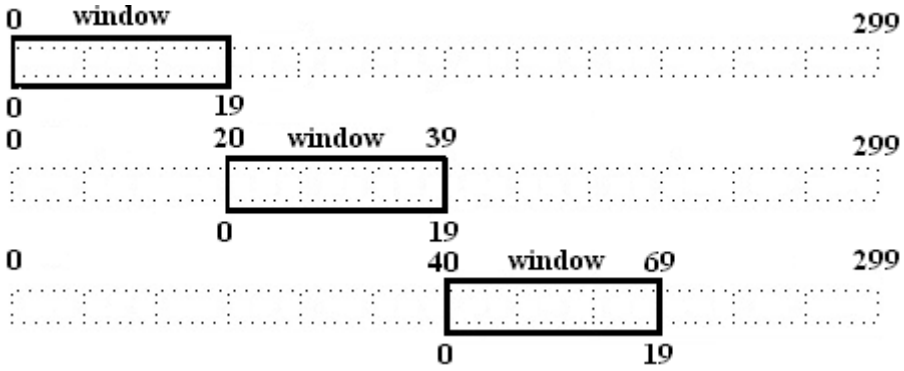

Figure 5.15 – Sliding window used in the algorithm

In each iteration the sliding window acquires 20 samples of the three-phase supply currents and executes a code equivalent to the activity diagram shown in Figure 5.16. Regarding to the *αβ*-vector transformation, this block is computed according to the equation 5.4 presented in the Section 5.1.

Since the covariance matrix (E) is a 2x2 square matrix, the eigenvalues are obtained through the calculation of the matrix determinant. For a 2x2 square matrix the determinant can be calculated with a quadratic equation solver. The expression to obtain the eigenvalues is the following:

$$\mathbf{E} = \begin{bmatrix} a & b \\ c & d \end{bmatrix}$$

$$\mathbf{det}(s * I - E) = 0 \Leftrightarrow \mathbf{det}\left(\begin{bmatrix} s & 0 \\ 0 & s \end{bmatrix} - \begin{bmatrix} a & b \\ c & d \end{bmatrix}\right) = 0 \Leftrightarrow \mathbf{det}\left(\begin{bmatrix} s-a & -b \\ -c & s-d \end{bmatrix}\right) = 0$$

$$s^2 - s(d + a) + (a * d + c * d) = 0 \qquad (5.6)$$

The eigenvectors are obtained from the expression 5.3 defined in Section 5.1. The severity factor of stator faults is obtained through the following expression:

$$SF = 1 - \frac{\lambda_{min}}{\lambda_{max}} \qquad (5.7)$$

If the expression 5.7 returns a value below 12%, the machine is considered healthy and both eigenvalues will return the same value. In the case, the value returned by the expression 5.7 has a value greater than 12% is considered that the machine is in a fault condition. The fault severity factor is given by the expression 5.7 and is presented in the *HMI* of the *TPU*.

For the detection of faults in the rotor, the respective eigenvalues are not constant. In this situation the eigenvalues present a sinusoidal behavior. Therefore, the eigenvalue with the highest value is stored in a buffer of 50 positions. After 50 iterations is obtained the maximum and minimum values of this buffer and if the expression 5.7 returns a severity factor below 6% the machine is considered healthy, otherwise it is considered that the machine has broken rotor bars. The severity factor is given by the expression 5.7 and is presented in the *HMI* of the *TPU*.

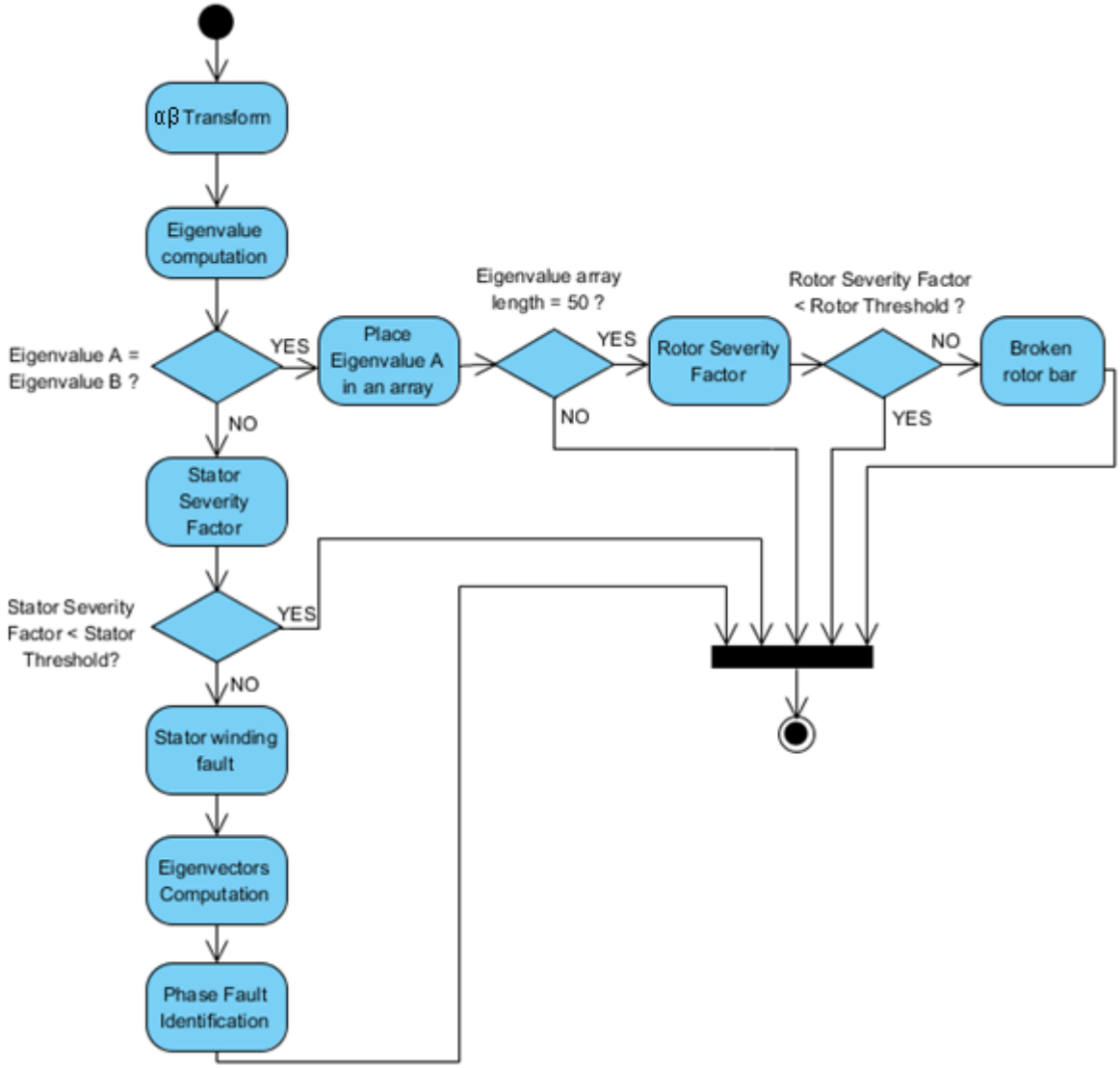

Figure 5.16 – Activity diagram of *PCA* module

Chapter 6

Results

In this chapter will be shown an example of *MMoDiS* in operation, as well as several tests made to the proposed solution. First is described the experimental setup used, and finally it is shown the simulation and experimental results obtained.

6.1 Experimental Set Up

The experimental set up of this research is depicted in Figure 6.1 and Figure 6.2. In the Figure 6.1 is represented the schematic diagram of the set up and in the Figure 6.2 is shown the real experimental apparatus. A series of tests were conducted on three squirrel-cage induction motor with a mechanical power (P_{mec}) of 2 *Hp*, 230/400 *V* nominal voltage (V_{nom}), a rated speed (N) of 3000 *rpm*, all with same parameters. One motor was considered a healthy motor and tested. The other two motors were tested with stator short-circuits and broken rotor bars faults. The nameplate data of the tested motors is given in the Figure 6.3.

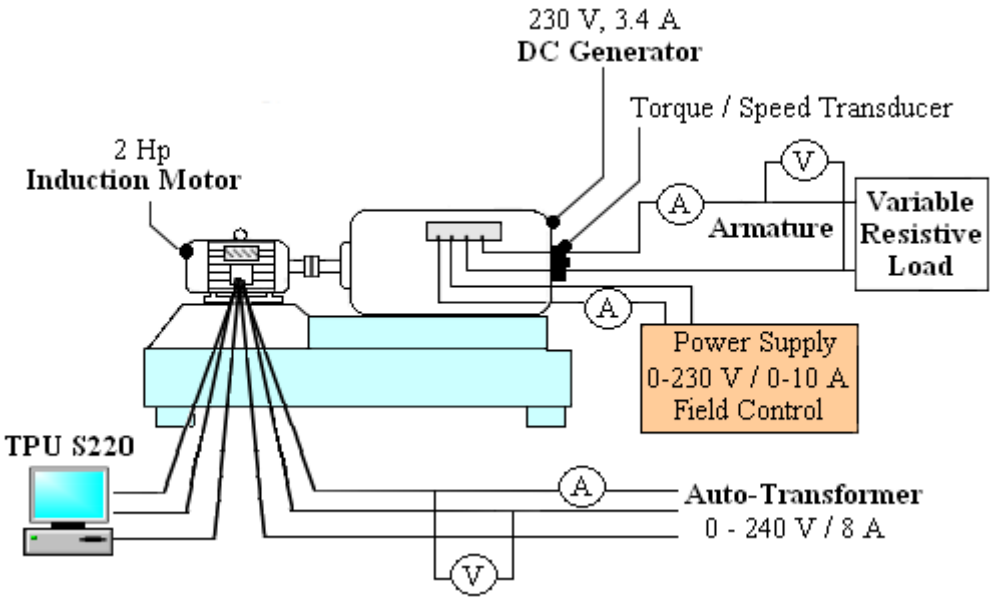

Figure 6.1 – Schematic diagram of the experimental set up used

The power supply used was a three-phase auto-transformer with an apparent power (S) of 4 *kVA* and 0-400 V_{rms} (line-to-line), from *De Lorenzo*. The mechanical load was applied to the induction motor by connecting the shaft to a *dc* generator of 0.75 *kW* rated power (P_{el}), 230 *V* of

nominal voltage (V_{nom}), rated current (I_{nom}) of 3.4 A. The output of the *dc* generator was connected to a variable resistive load. In order to allow tests to be performed at different load levels, the *dc* excitation current and the load resistor were both adjustable.

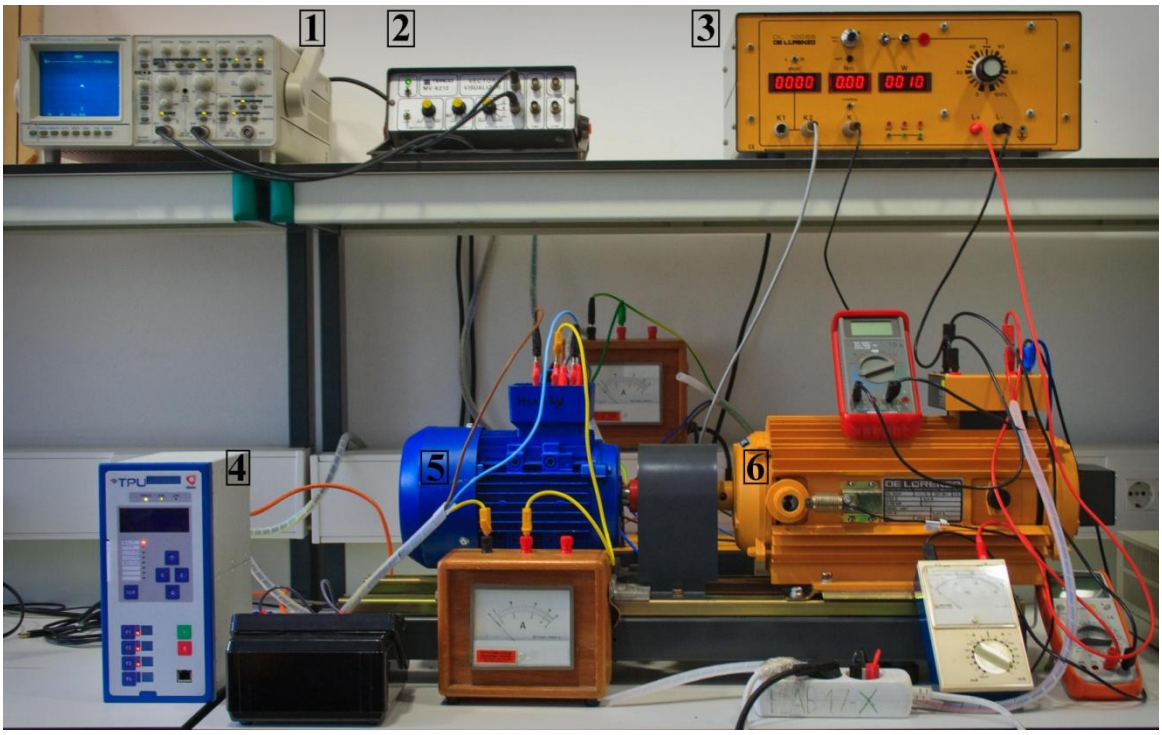

Figure 6.2 – Experimental apparatus used in this work

Legend:

1. Oscilloscope;
2. Vector visualizer;
3. Current source and measurements module;
4. *TPU S220*;
5. Induction machine;
6. *DC* machine.

Figure 6.3 – Nameplate data of the induction machine (left) and *dc* machine (right)

For speed and torque measurements (Figure 6.4) were coupled to the shaft of the *dc* Generator torque and speed transducers both from *De Lorenzo*. These transducers were connected to a *De Lorenzo* module that measures the torque and the mechanical power. The electrical measurements in the induction motor were carried out using an *ac* voltmeter and ammeter connected to the stator. In the *dc* generator was used an ammeter in the excitation circuit (rotor) to measure the current that produces the electromagnetic field. In the armature side (stator) were used a voltmeter and an ammeter.

Figure 6.4 – Equipment used for torque and speed measurements

The data acquisition, signal conditioning and data processing are performed by the *TPU S220* developed by *EFACEC*. For the laboratory tests, a broken rotor bar fault was introduced by drilling a hole into a bar, the hole diameter is slightly larger than the bar width as can be seen in the example shown in the Figure 6.5.

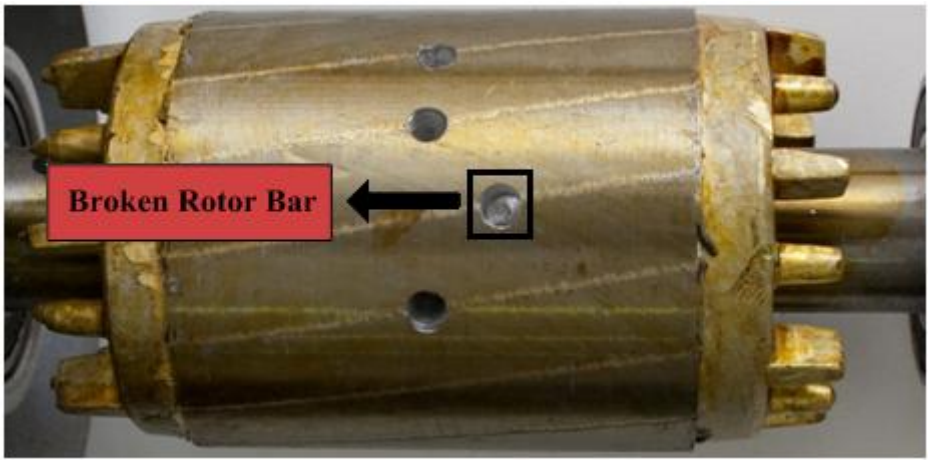

Figure 6.5 – Example of a broken rotor bar fault applied artificially

In the case of short-circuits in the stator windings they were applied by introducing an external variable resistor in series with the windings of each phase (Figure 6.6).

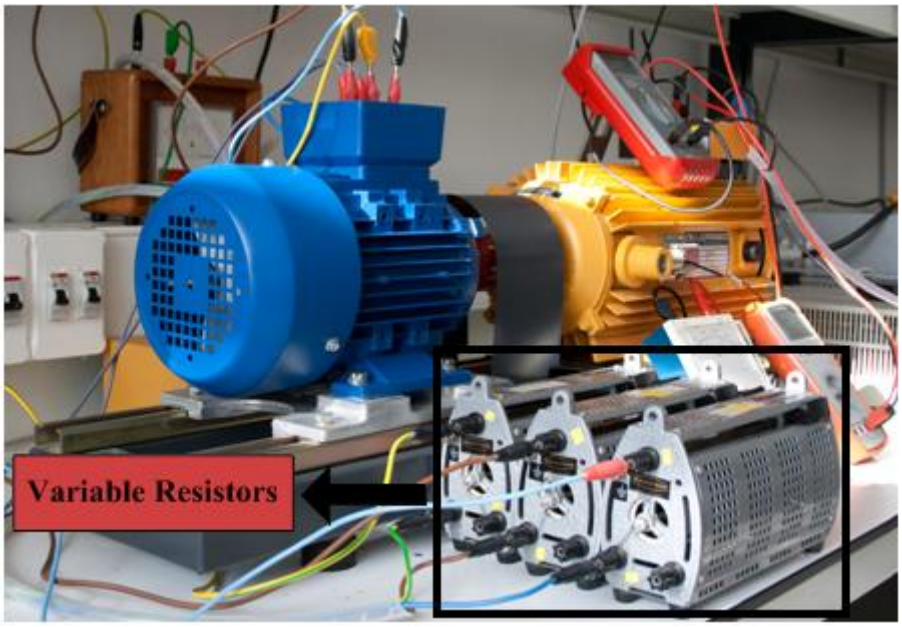

Figure 6.6 – Example of the application of a stator fault

In the Table 6.1 is provided a summary of the carried tests in the motors. From the performed tests the experimental data collected is related to the stator currents. The tests were conducted first in full load, then in half load conditions and no-load conditions. The connection used in the stator windings was a triangle (wye) connection.

Tests	Description
#1	Stator Faults (in all phases) – with severity factors below 50%
#2	Stator Faults (in all phases) – with severity factors above 50%
#3	One broken rotor bar
#4	Three broken rotor bars
#5	More than four broken rotor bars

Table 6.1 – Summary of the conducted tests

The main purpose of the experimental data collected from the tests described in the table 6.1 is the comparison between the experimental results and the simulation results.

6.2 Simulation Results

Using the current samples taken from an induction machine mathematical model, were carried out the tests described in Table 6.1, under conditions equivalent to a three-phase sinusoidal voltage. The model used for simulation is described in [132, 133] and presents similar

characteristics to the induction machine used in the experimental tests. Each period of the collected data is composed by 20 samples. All simulations were performed using *MATLAB* software.

6.2.1 Healthy Motor

In the conducted simulations to a healthy machine mathematical model, were applied various levels torque, more precisely the nominal torque (4.7 Nm), half the nominal torque (2.35 Nm) and no load. The start-up condition was discarded since it is not considered by the algorithm. The temporal evolution of the motor stator currents is represented in the Figure 6.7 (A). The Figure 6.7 (B) presents the $\alpha\beta$-vector transformation with a circular shape, which indicates a healthy condition. In the Figure 6.7 (B) is also represented with green and red colors the eigenvectors.

From the spectrogram that corresponds to the steady state current (Figure 6.7 (C)), it is possible to observe only the fundamental component in the 50 Hz. The non-observation of other harmonic components in the spectrogram relates that the power supply is almost ideal.

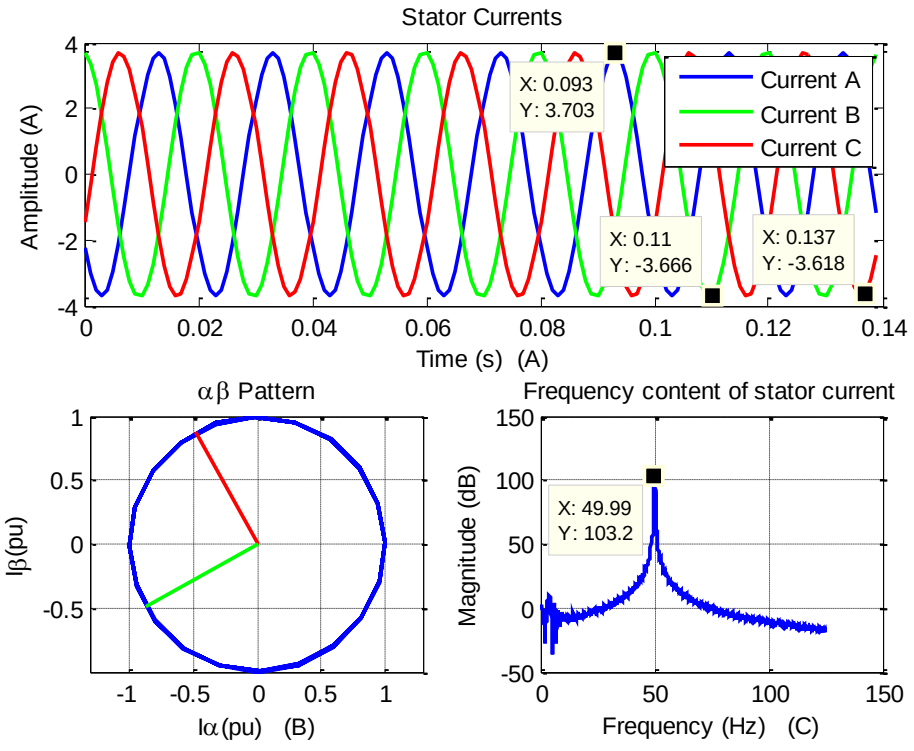

Figure 6.7 – (A) Stator currents of the induction machine in nominal operation (B) Simulated $\alpha\beta$-vector Transformation (C) Current A spectrum

From the figure 6.7 (A) it is possible to observe that all the stator currents have the same amplitude values and the $\alpha\beta$-vector pattern presents a circular shape. The eigenvalues obtained for this situation were the following:

$$\lambda_{min} = 205{,}28 \quad \lambda_{max} = 205{,}67$$

Therefore the fault severity factor is,

$$SF = \left(1 - \frac{\lambda_{min}}{\lambda_{max}}\right) = \left(1 - \frac{205{,}28}{205{,}67}\right) = 0{,}19\ \%$$

In the situation where the torque applied corresponds to 50% of the nominal torque, the obtained results are presented in Figure 6.8. As in the previous case all the stator currents have the same amplitude values. However, there is a decrease of maximum amplitude values that occurs due to decrease in the resistant torque applied in the shaft of the machine. The *αβ*-vector transformation also presents a circular shape and the magnitude of the current spectrum has a value close to the nominal value, there is only a variation of 5 dB.

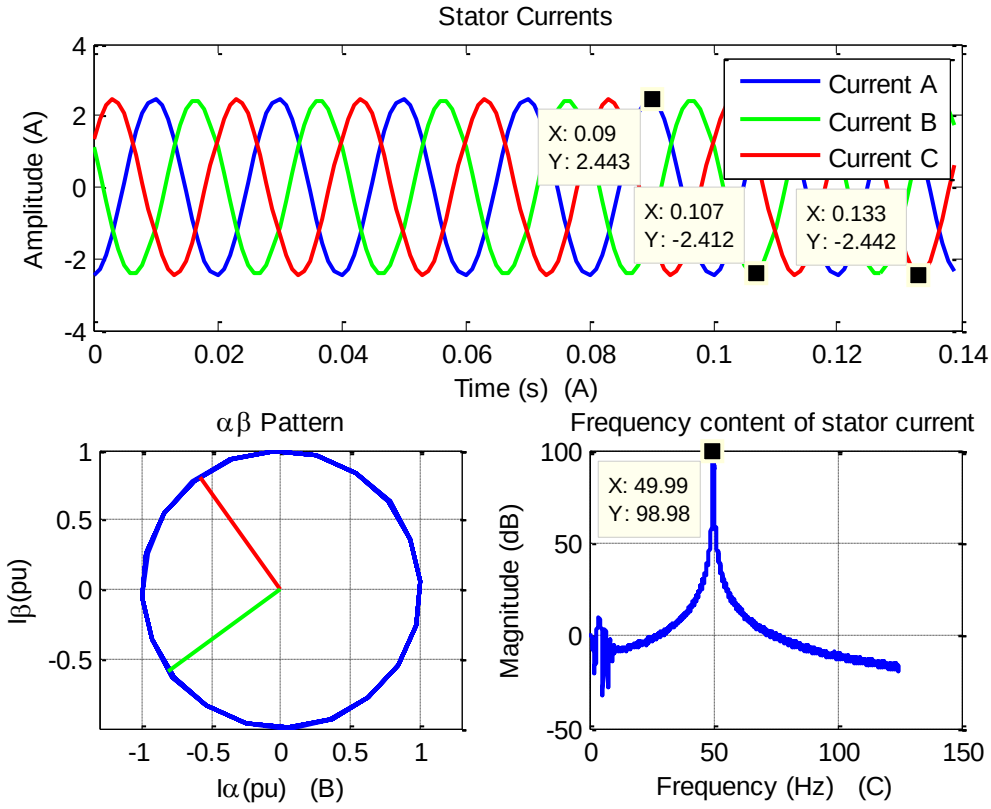

Figure 6.8 – (A) Stator currents of the induction machine with an applied torque of 50% of the nominal torque (B) Simulated *αβ*-vector Transformation (C) Current A spectrum

The eigenvalues obtained for this situation were the following:

$$\lambda_{min} = 89{,}72 \quad \lambda_{max} = 89{,}78$$

Therefore the severity factor is,

$$SF = \left(1 - \frac{\lambda_{min}}{\lambda_{max}}\right) = \left(1 - \frac{89{,}72}{89{,}78}\right) = 0{,}06683\ \%$$

In a situation where there is no torque applied to the machine (Figure 6.9) the results obtained are similar to the two previous cases, there is only a decrease in the maximum value of the stator currents which is expected since the stator current is related with the machine torque.

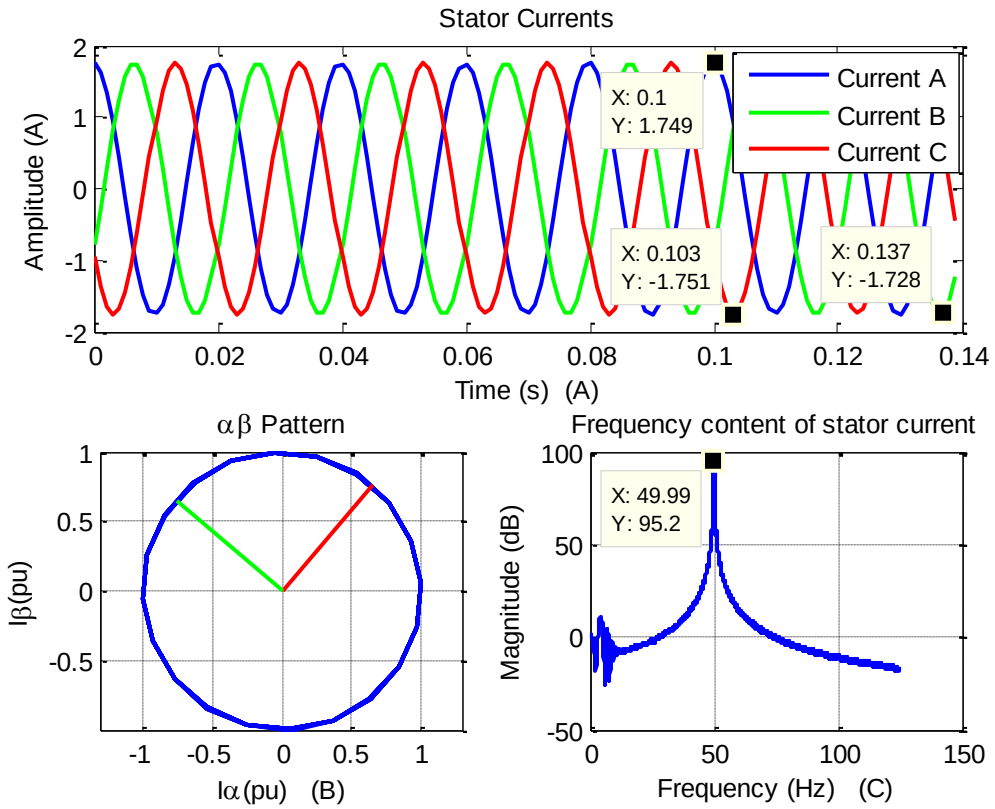

Figure 6.9 – (A) Stator currents of the induction machine with an applied torque of 0% compared with the nominal torque (B) Simulated $\alpha\beta$-vector Transformation (C) Current A spectrum

The eigenvalues obtained for this situation were the following:

$$\lambda_{min} = 46{,}11 \qquad \lambda_{max} = 46{,}14$$

Therefore the severity factor is,

$$SF = \left(1 - \frac{\lambda_{min}}{\lambda_{max}}\right) = \left(1 - \frac{89{,}72}{89{,}78}\right) * 100 = 0{,}06502\%$$

6.2.2 Stator Faults

In this section will be discussed the stator faults applied to the mathematical model of the induction machine. In the case of a healthy induction machine all the 3 stator phases should have an equal value for their impedance. However, in an unbalance of a stator phase there is a decrease in the impedance value which causes an increase in the current of the affected phase.

In the mathematical model used, the impedance of each stator phase consists in a resistor in series with a coil. To cause unbalances in the stator phases, there are factors that when multiplied by the phase total impedance allow to use only a part of that value. For example, in a phase where the resistive part (R) of the impedance is 4 ohm (Ω) and the inductive part (L) is 0.5 Henry (H). The impedance phasor is given by:

$$Z_{total} = 10{,}0125 \angle 0.05° \, \Omega$$

For example if a multiplicative factor (K) is added to Z_{total} and is equal to 0.8 the total impedance will be $|Z_{total}| = 0.8 * 10{,}0125 = 8{,}01 \, \Omega$ instead of being $Z_{total} = 10{,}0125 \angle 0.05° \, \Omega$.

6.2.2.1. Stator Fault in Phase A

Firstly, were applied short circuits in the phase A of the machine for different fault severity factors, more precisely severity factors of 60% and 30%. To this end, in the case of a severity factor of 60% (Figure 6.10), was applied to the mathematical model a multiplicative factor of 0.82 in the impedance of the phase A, which indicates that 18% of the windings were short-circuited. For the severity factor of 30% (Figure 6.12), a multiplicative factor of 0,93 was applied, which means 7% of the windings in short-circuit.

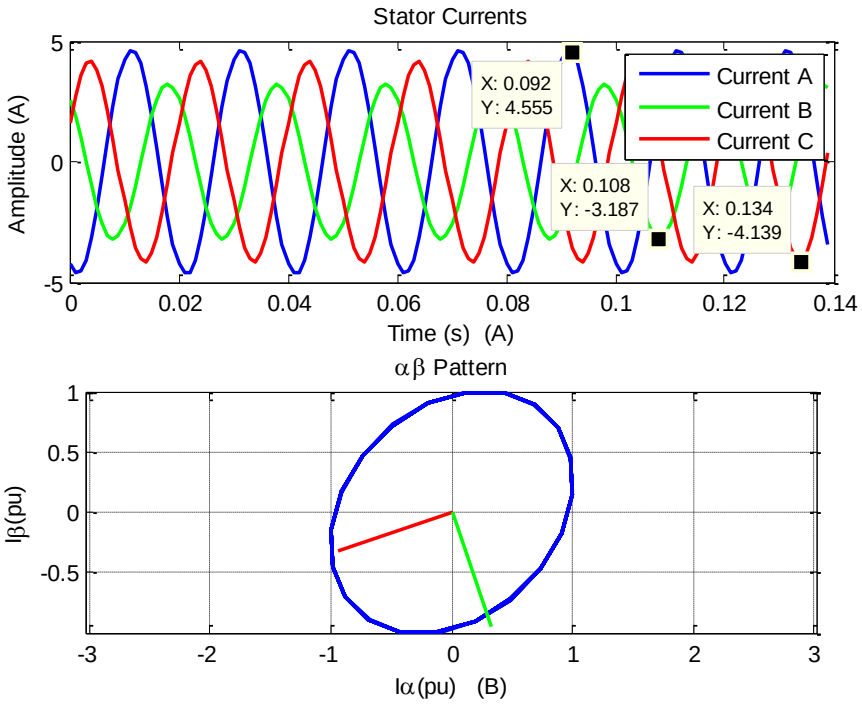

Figure 6.10 - (A) Stator currents of the induction machine in nominal operation with 18% of the phase A stator windings short-circuited (B) Simulated *αβ*-vector Transformation

The Figure 6.10 (A) shows the temporal evolution of the stator currents in a nominal operation (4.7 Nm) with 18% of the phase A stator windings short-circuited. In this situation all the stator currents present different values for the maximum amplitude values, where the current A presents the highest value. The $\alpha\beta$-vector pattern (Figure 6.10 (B)) no longer presents a circular shape and exhibit an elliptical shape. The Fault Severity Factor (*SF*) was computed as follows:

$$\mathrm{SF} = \left(1 - \frac{\lambda_{\min}}{\lambda_{\max}}\right)$$

,where $\lambda_{\min}$ represents the eigenvalue with the smallest value and $\lambda_{\max}$ represents the eigenvalue with highest value in a 20 sample window. So for a 20 sample window of the Figure 6.9 (A), the results obtained were the following:

$$\lambda_{min} = 145{,}76 \quad \lambda_{max} = 344{,}74$$

Therefore the severity factor is,

$$\mathrm{SF} = 1 - \frac{\lambda_{\min}}{\lambda_{\max}} = \left(1 - \frac{145.76}{344{,}74}\right) * 100 = 57{,}7\%$$

Through the application of expression 5.1 are obtained the eigenvectors, that indicate what is the phase of the machine where the short-circuit occurred.

$$\mathrm{V} = \begin{bmatrix} 0{,}323 & -0{,}946 \\ -0{,}946 & -0{,}323 \end{bmatrix}$$

In the figure 6.11 is shown the variation of the eigenvalues after 15 computation cycles which corresponds to 300 samples. The graphic shows that the variation of the eigenvalues is minimal, which indicates that a stator fault does not affect the eigenvalues as time passes.

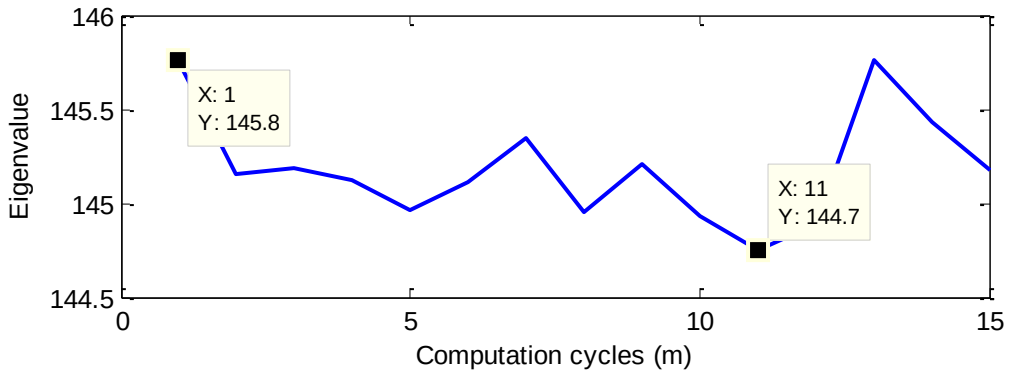

Figure 6.11 – Variation of eigenvalues over the computing cycles

The Figure 6.12 represents the obtained results for a fault severity factor of 30%. In the Figure 6.12 (A) it is possible to see that as the severity of the fault decreases, the difference

between the maximum amplitude values of the stator currents tends to decrease, since the motor is approaching to a healthy situation. From the Figure 6.12 (B) it is also possible to observe that with the decrease of the severity factor the $\alpha\beta$-vector pattern tends to gain the circular shape.

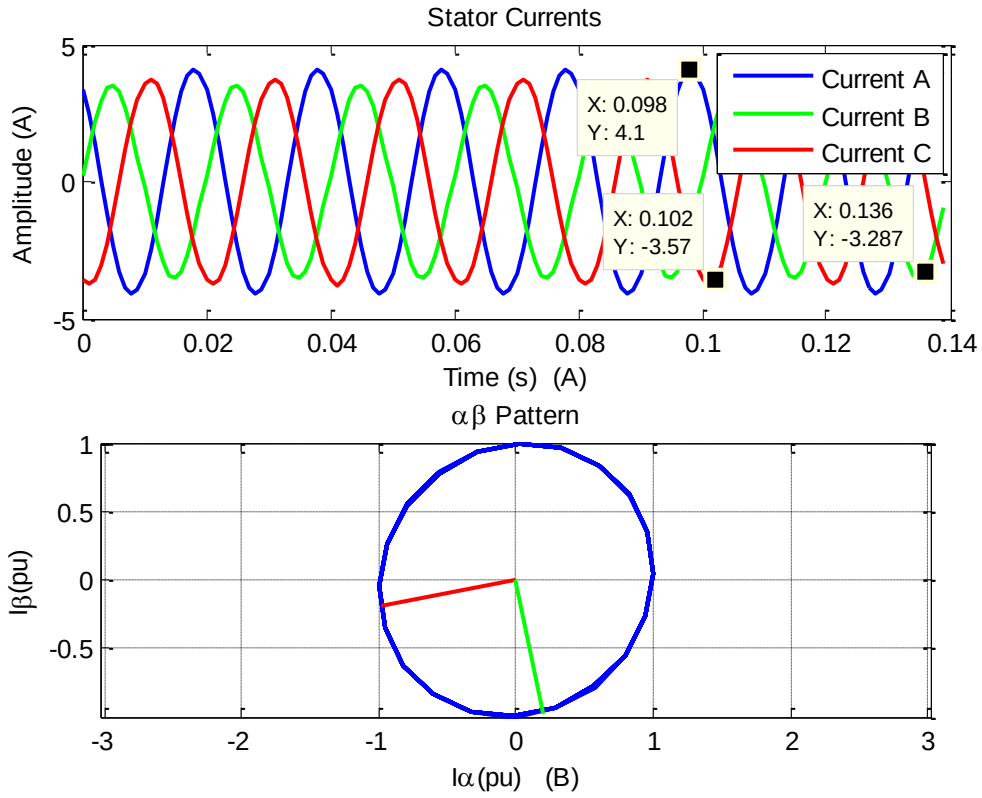

Figure 6.12 - (A) Stator currents of the induction machine in nominal operation with 7% of the phase A stator windings short-circuited (B) Simulated $\alpha\beta$-vector Transformation

The eigenvalues obtained for this situation were the following:

$$\lambda_{min} = 177{,}6 \qquad \lambda_{max} = 255{,}3$$

Therefore the severity factor is,

$$SF = \left(1 - \frac{\lambda_{min}}{\lambda_{max}}\right) = \left(1 - \frac{177{,}6}{255{,}3}\right) * 100 = 30{,}4\%$$

The eigenvectors obtained were the following:

$$V = \begin{bmatrix} -0{,}290 & -0{,}956 \\ -0{,}956 & 0{,}290 \end{bmatrix}$$

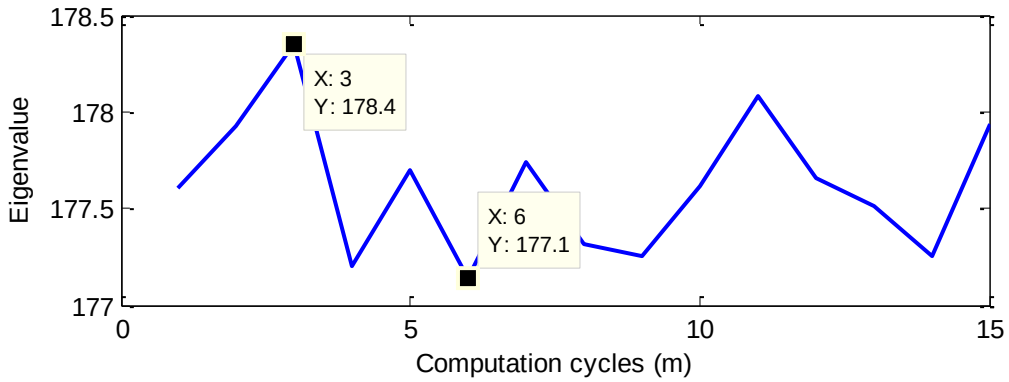

Figure 6.13 – Variation of eigenvalues over the computing cycles

For this situation of fault severity factor of 30 % it is to conclude that the variation of the eigenvalues along the computing cycles is approximately zero, as happened for the fault severity factor of 60%. Therefore, in a stator fault situation the variation of the severity of the fault does not affect the eigenvalues.

In the Figure 6.14 is presented the fault severity factor in function of the machine load level. These simulations results shows that, the defined severity factor change significantly with the motor load level, as can be concluded from the results presented in Figure 6.14.

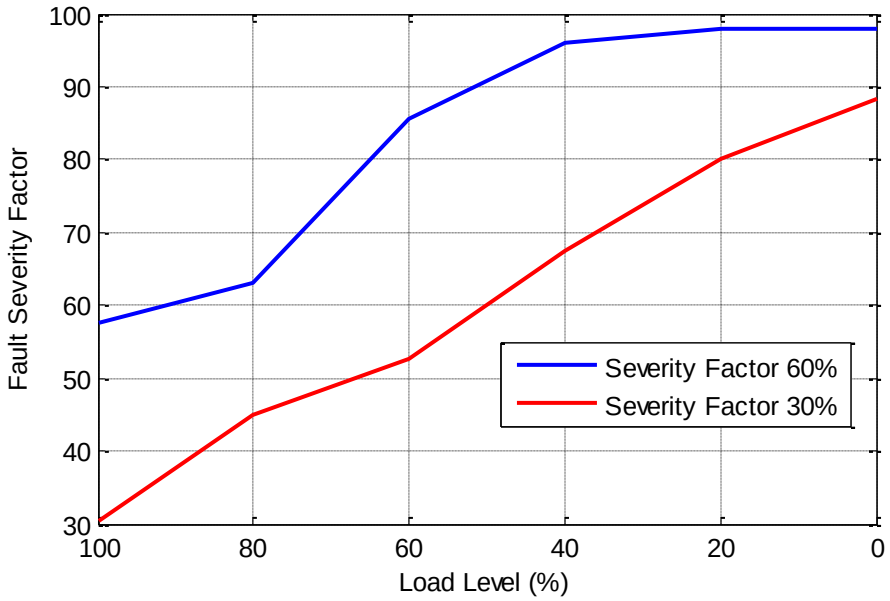

Figure 6.14- Evolution of the fault severity factor with the motor load level for the case of a motor with 7% (red) and 14% (blue) of the stator windings short-circuited

The results obtained for different fault severity factors also demonstrate that the rotor speed after the start-up situation is not affected by the faults applied in the stator (Figure 6.15). During the evolution of the rotor speed (Figure 6.15), the time interval that the machine takes to reach the rated speed is the only visible change. As the fault severity factor increases, the machine

will take more time to reach the rated speed. However, this situation does not affect the performance of the algorithm since the start-up situation is discarded.

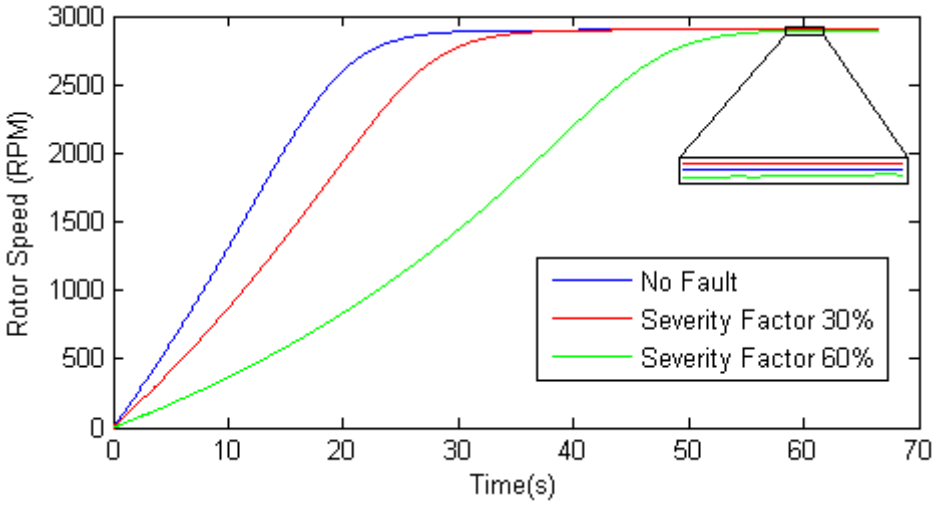

Figure 6.15 – Evolution of the rated speed in 3 different situations: healthy condition and two fault situations

6.2.2.2. Stator Fault in Phase B

For the stator faults applied to the phase B of the machine, the multiplicative factors used were the same used for the faults in phase A, K = 0,82 for a fault severity factor (SF) of 60% and K = 0.93 for a SF = 30 %.

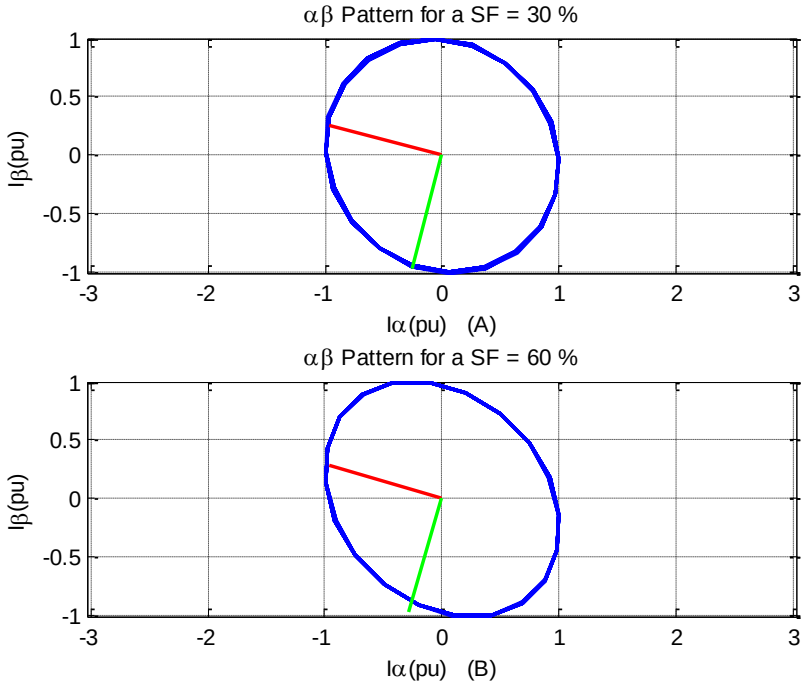

Figure 6.16 – *αβ*-vector Transformation for different fault severity factors applied to the phase B

The results obtained for the $\alpha\beta$-vector transformation presented in Figure 6.16 indicate that for this situation the $\alpha\beta$-vector transformation tends to lose its circular shape and gain an elliptical shape as the severity factor (*SF*) increases. This phenomenon also occurred before in the fault applied to the phase A. However, in this situation for a fault applied in phase B the orientation of the ellipse is different and is given by the eigenvectors.

The results from Figure 6.17 also indicate that for stator faults applied to the phase B the fault severity factor changes with the motor load level. Comparing these results with those obtained for the stator faults in the phase A of the machine (Figure 6.14), in this situation results show minor variations.

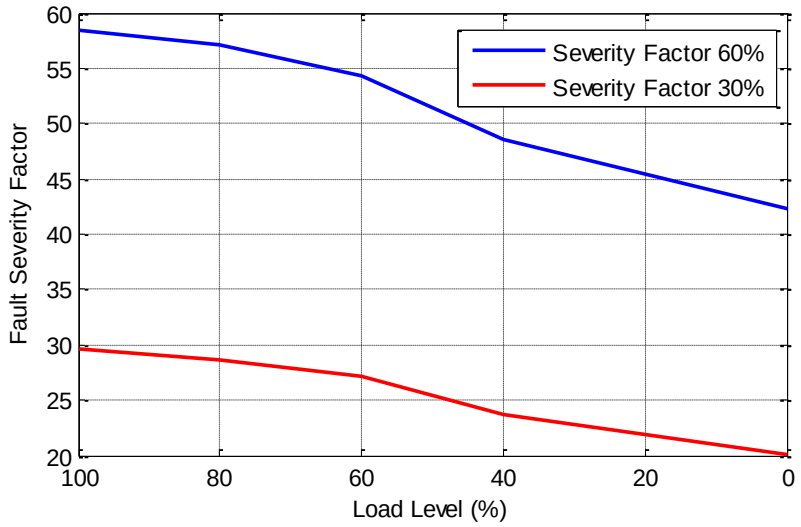

Figure 6.17 - Evolution of the fault severity factor with the motor load level for the case of a motor with 7% (red) and 14% (blue) of the stator windings short-circuited

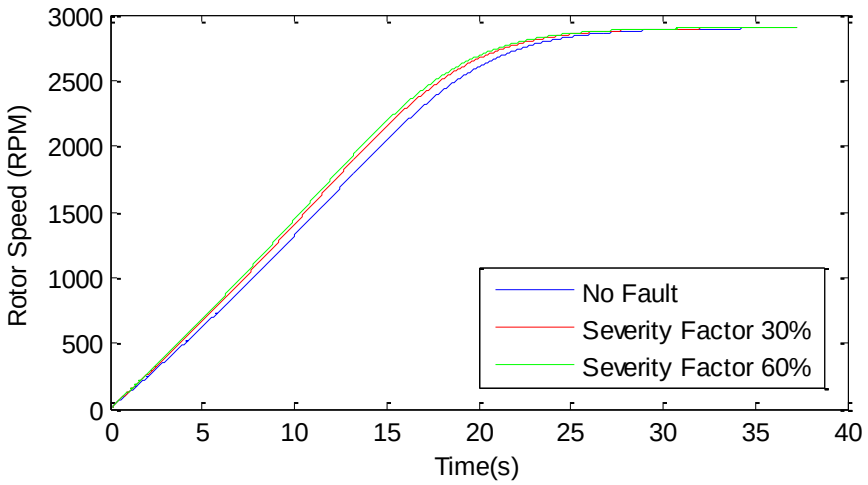

Figure 6.18 - Evolution of the rated speed in 3 different situations: healthy condition and two fault situations in the phase B

As stated before (Section 6.2.2.1) the rated speed of the machine in a stator fault situation is not affected as can be seen from the Figure 6.18. Contrary to what happened in the fault applied in the phase A of the machine (Figure 6.15), in this case the start-up of the machine is not affected by the applied fault.

6.2.2.3. Stator Fault in Phase C

For the stator faults applied to the phase C of the machine, the multiplicative factors used were the same used for the faults in phase A, K = 0,82 for a fault severity factor (SF) of 60% and K = 0.93 for a SF = 30 %.

The results obtained from Figure 6.19 demonstrate that the *αβ*-vector transformation in this situation also tends to lose its circular shape and gain an elliptical shape as the fault severity factor increases. This also occurred before in the faults applied to the phase A and phase B of the machine. However, for a stator fault applied to the phase C the orientation of the ellipse is different from the other presented cases (Section 6.2.2.1 and 6.2.2.3).

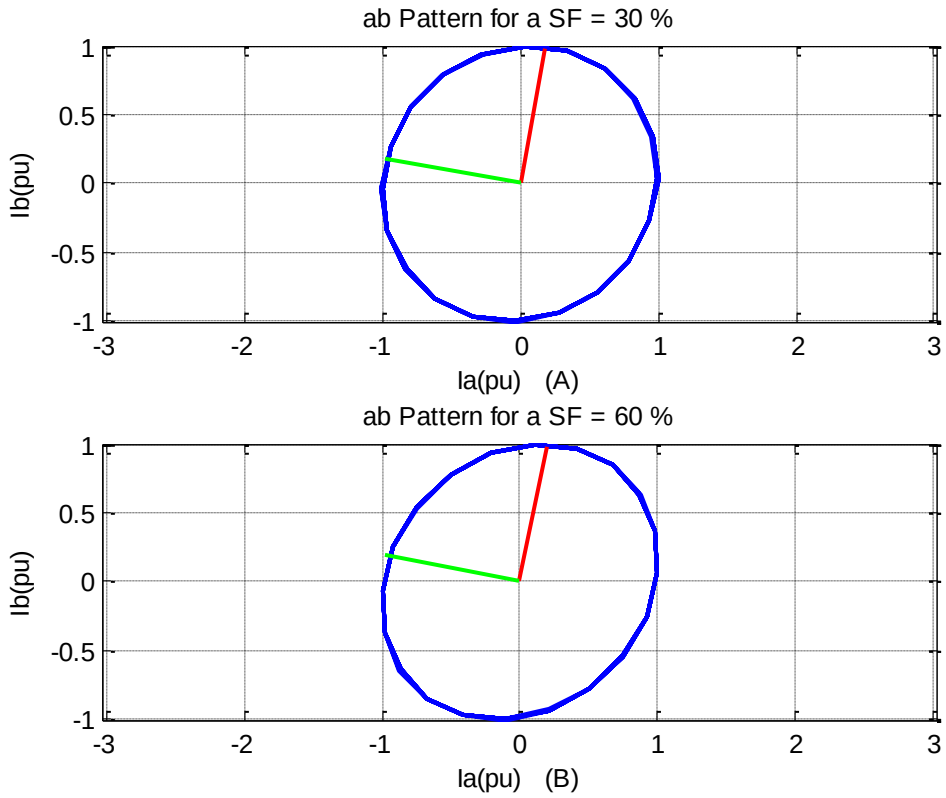

Figure 6.19 – *αβ*-vector Transformation for different fault severity factors applied to the phase C

The simulation results obtained and presented in the Figure 6.20 (A) have similar results to those that have been presented in Figure 6.17. The severity factor of the stator faults applied to the phase C changes with the motor load level.

For the Figure 6.20 (B) the results are also similar to those represented in the Figure 6.18. After the start-up condition in a permanent regime the rotor speed is not affected by the stator faults.

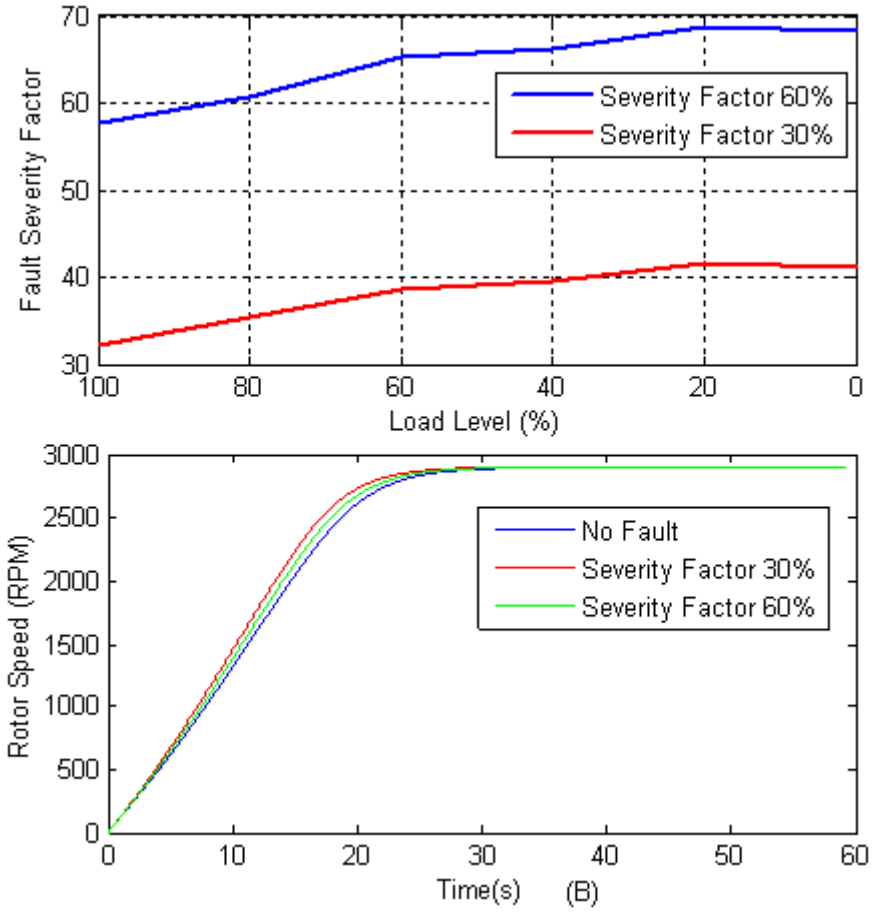

Figure 6.20 – (A) Evolution of the fault severity factor with the motor load level for the case of a motor with 7% (red) and 14% (blue) of the stator windings short-circuited (B) rated speed in 3 different situations: healthy condition and two fault situations in the phase C

6.2.3 Rotor Faults

As the mathematical model of the induction machine used have a wound rotor, the application of faults in the rotor is made in the same manner as in the stator. The impedance of each phase of the machine is multiplied by a multiplicative factor. In the simulation results presented in the Figure 6.21 and Figure 6.22 the multiplicative factors used were K = 0,7 and K = 0.5, respectively.

The temporal evolution of the stator currents presented in the Figure 6.21 (A) and 6.22 (A) shows that a rotor faults causes a variation in the maximum amplitude value of the currents as time passes. From the Figure 6.21 (B) and 6.22 (B) it is also possible to observe that the $\alpha\beta$-vector pattern does not lose the circular shape, but occurs the appearance of a thick ring.

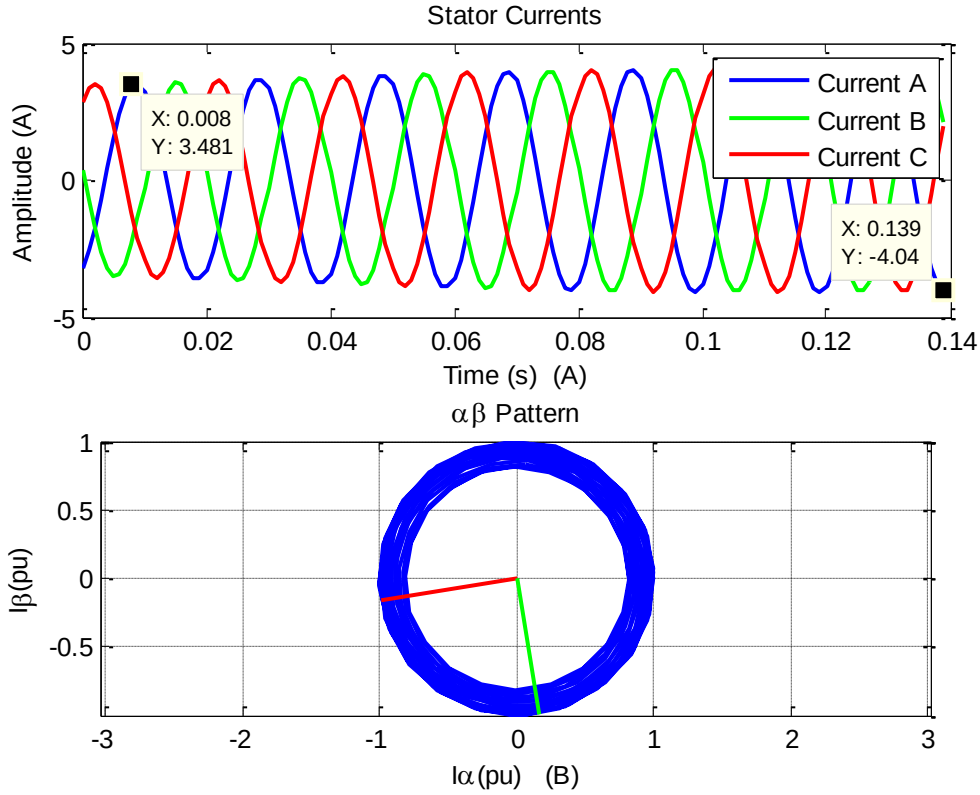

Figure 6.21 - (A) Stator currents of the induction machine in nominal operation with 30% of the phase A rotor windings short-circuited (B) Simulated *αβ*-vector Transformation

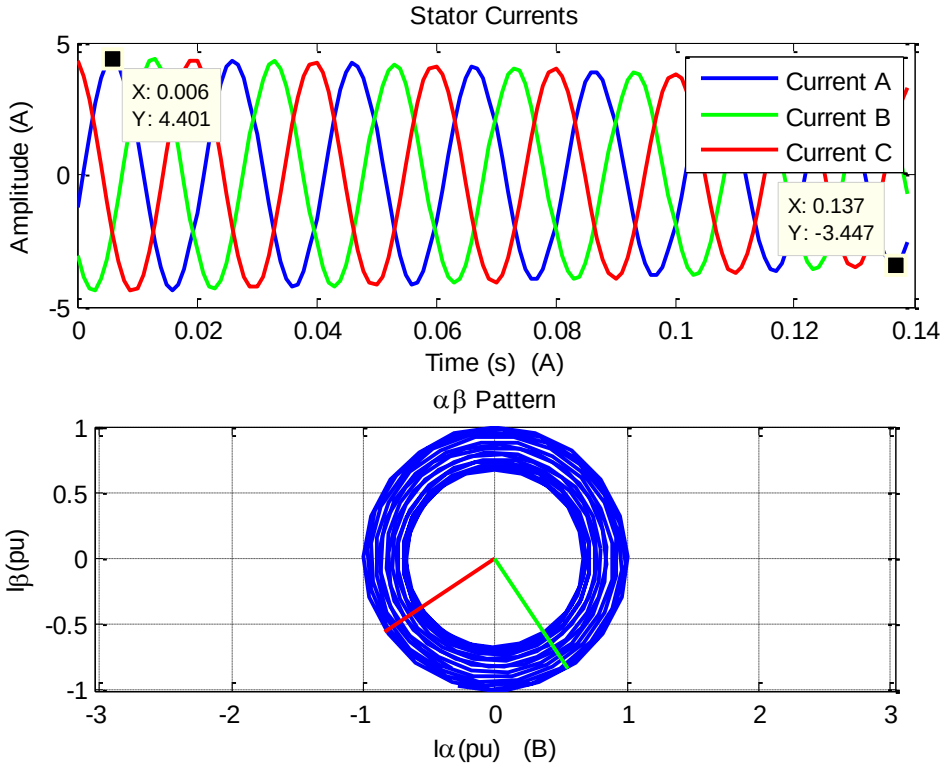

Figure 6.22 - (A) Stator currents of the induction machine in nominal operation with 50% of the phase A rotor windings short-circuited (B) Simulated *αβ*-vector Transformation

The appearance of a thick ring in a rotor fault situation can be detected through the variation of eigenvalues (Figure 6.23). In this situation the eigenvalues present a sinusoidal behavior, due to induced frequency components that appear in the stator current frequency.

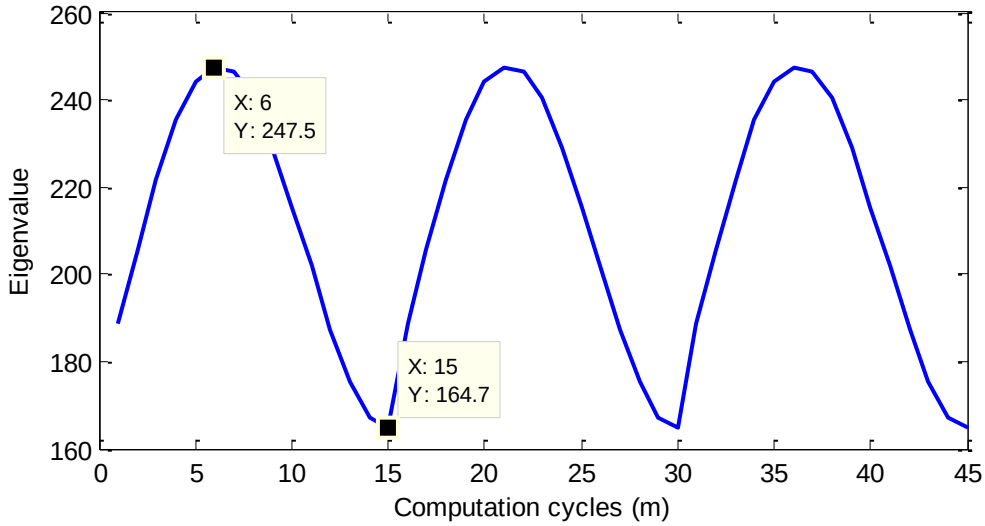

Figure 6.23 – Variation of the eigenvalues in function of computation cycles

As occurred in the stator fault simulations, for rotor fault situations the simulations results (Figure 6.24) shows that, the severity factor change significantly with the motor load level

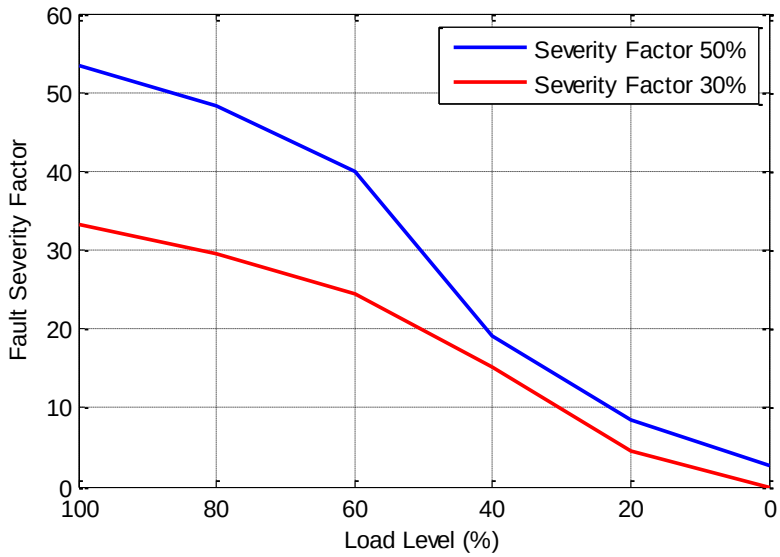

Figure 6.24 - Evolution of the fault severity factor with the motor load level for the case of a motor with 30% (red) and 50% (blue) of the phase A rotor windings short-circuited

The temporal evolution of the rotor speed is shown in the Figure 6.25. In a rotor fault situation the rated speed of the machine present small oscillations and there is a small error between the rated speed of a healthy machine and a faulty machine. This effect does not happen in the stator fault situations and can indicate the presence of rotor problems.

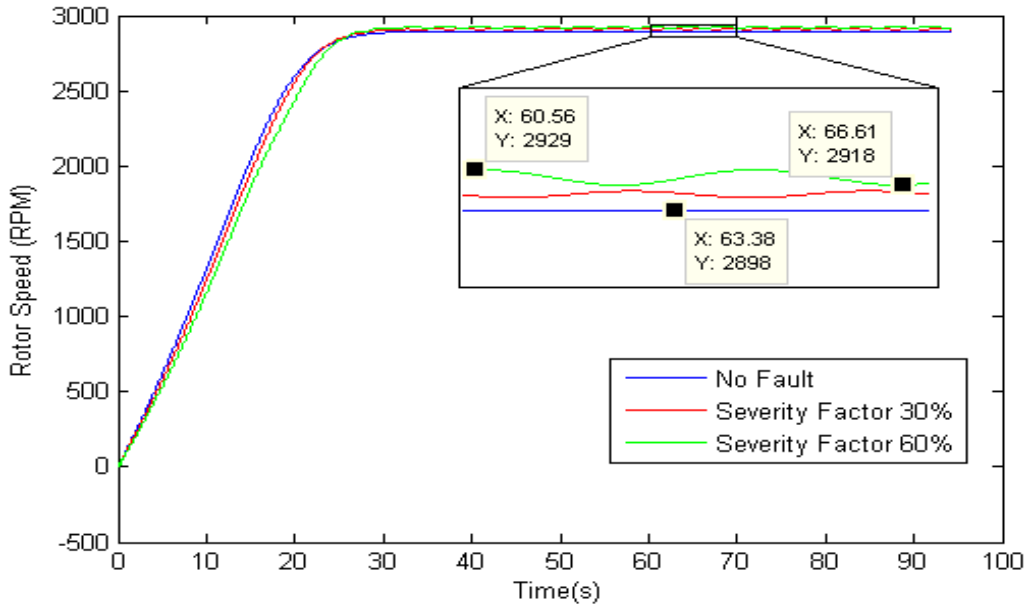

Figure 6.25 – Temporal evolution of the machine rated speed in 3 different situations.

6.3 Experimental Results

The motor was initially tested in a healthy situation, with the stator windings and its cage intact, in order to verify the current $\alpha\beta$-vector transformation reference pattern. In the conducted tests were applied various levels torque, in order to verify the robustness of the algorithm at different load levels. The start-up condition was discarded since it is not considered by the algorithm.

6.3.1 Healthy Motor

The temporal evolution of the motor stator currents is represented in the Figure 6.26 (A). The $\alpha\beta$-vector pattern presented in the Figure 6.26 (B) does not present a circular shape, because the supply voltage is distorted and the field distribution is not perfectly sinusoidal. However the machine was considered in a healthy condition.

The spectral analysis to the steady state current is shown in the Figure 6.26 (C). The obtained results show that the fundamental component is in the 50 Hz. The observation of other harmonic components in the current spectrum relates that the power supply is non-ideal. The stator currents have other harmonic components in the 250 Hz, 350 Hz and 400 Hz.

These harmonics contributes to shape of the $\alpha\beta$-vector pattern. In this case the machine is in a healthy condition but in some cycles the algorithm indicates that the machine has a stator fault. It was necessary to establish a threshold value for the fault severity factor (as stated in the

Chapter 5), from which the machine is in a fault situation. The value use for the threshold was 12%.

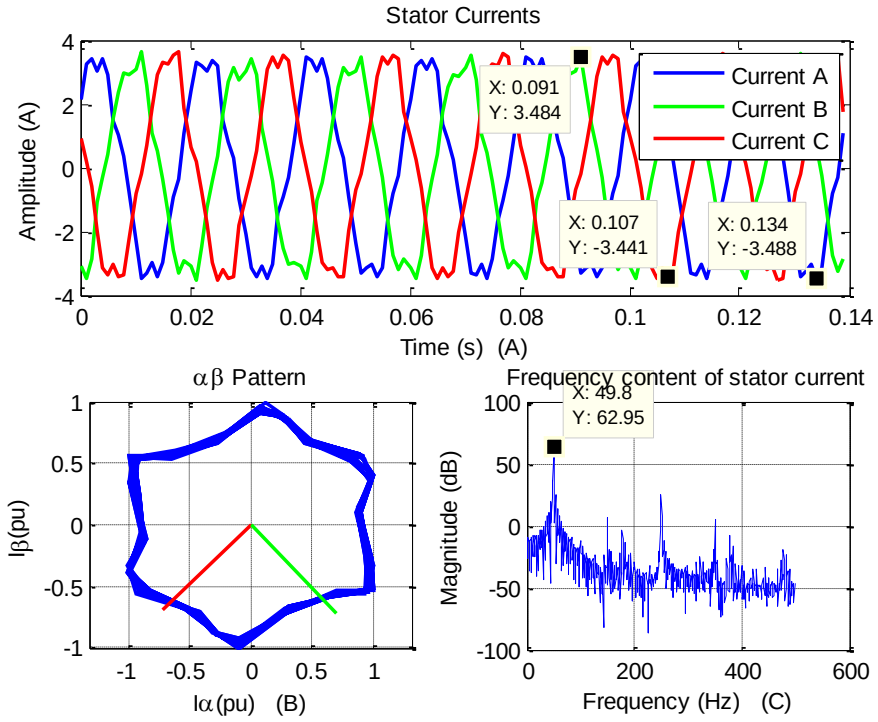

Figure 6.26 - (A) Stator currents of the machine in nominal operation (B) Experimental *αβ*-vector Transformation (C) Current A spectrum

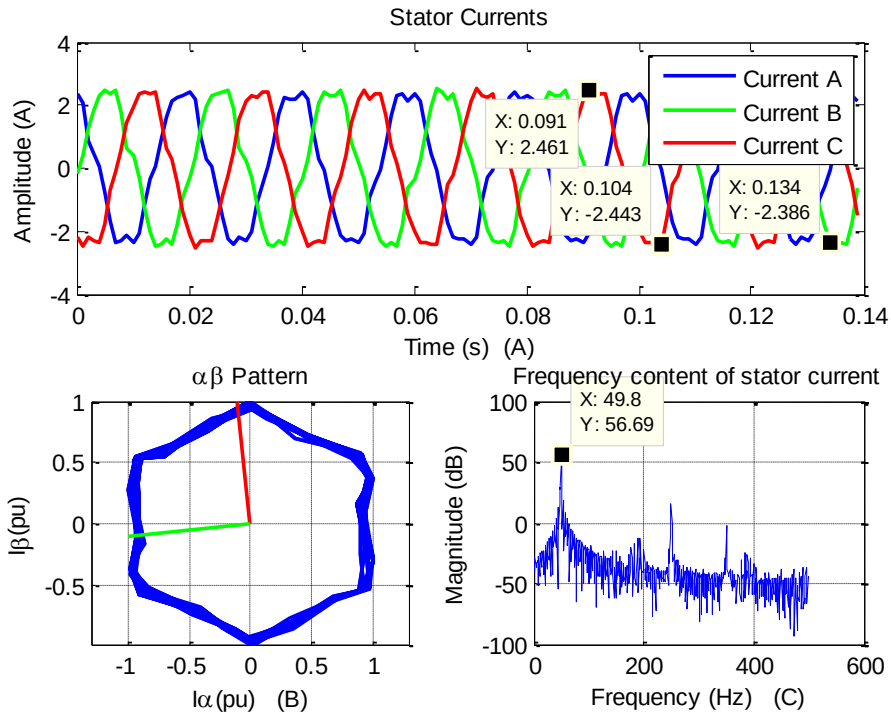

Figure 6.27 - (A) Stator currents of the machine with 50% of the nominal torque (B) Experimental *αβ*-vector Transformation (C) Current A spectrum

So for a 20 sample window of the Figure 6.26 (nominal torque), the results obtained for the fault severity factor were the following:

$$\lambda_{min} = 172{,}97 \quad \lambda_{max} = 192{,}58$$

Therefore the severity factor is,

$$SF = 1 - \frac{\lambda_{min}}{\lambda_{max}} = \left(1 - \frac{172.97}{192{,}58}\right) * 100 = 10{,}23\%$$

For the case of the machine with 50% of the nominal torque, the results obtained were the following:

$$\lambda_{min} = 88{,}5 \qquad \lambda_{max} = 99{,}7$$

$$SF = 1 - \frac{\lambda_{min}}{\lambda_{max}} = \left(1 - \frac{88.5}{99{,}7}\right) * 100 = 11{,}23\%$$

6.3.2 Stator Faults

The conducted tests were similar to tests performed in the simulations (Section 6.2), more precisely to a fault severity factor of 30% and 60%. To this end, were used three variable resistors with 11.2 Ω/ 5A (Figure 6.28) in series with the impedance of each phase of the machine (Z = 4.8 Ω).

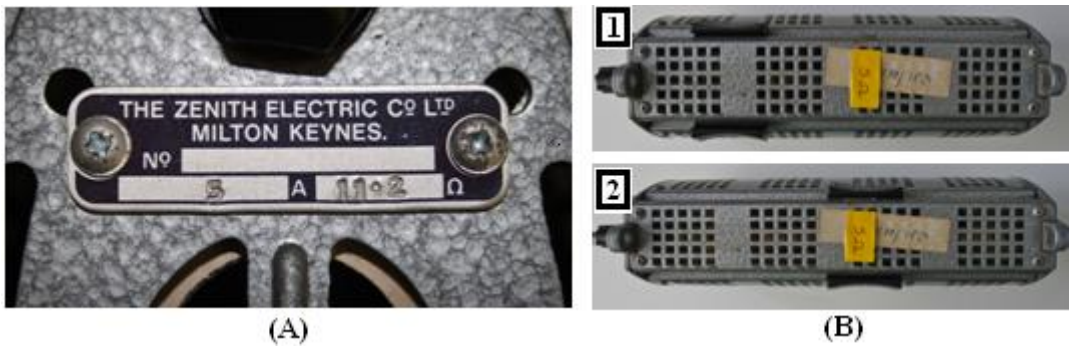

Figure 6.28 – Illustration of the variable resistors used. (A) Parameters of the resistor (B-1) Impedance for the SF = 60% (B-2) Impedance for the SF = 30%

In the case of a fault severity factor of 30% the resistance value is 6.8 Ω (Figure 6.28 B-2) for a severity factor of 60% the value of the resistance is 1.2 Ω (Figure 6.28 B-1).

6.3.2.1. Stator Fault in Phase A

The temporal evolution of the stator currents presented in the Figure 6.29 (A) and 6.30 (A). The *αβ* pattern (Figure 6.29 (B)) no longer presents a circular shape and exhibit an elliptical shape as was observed in the Figure 6.10 (B) (SF = 30%) and Figure 6.12 (B) (SF = 60%).

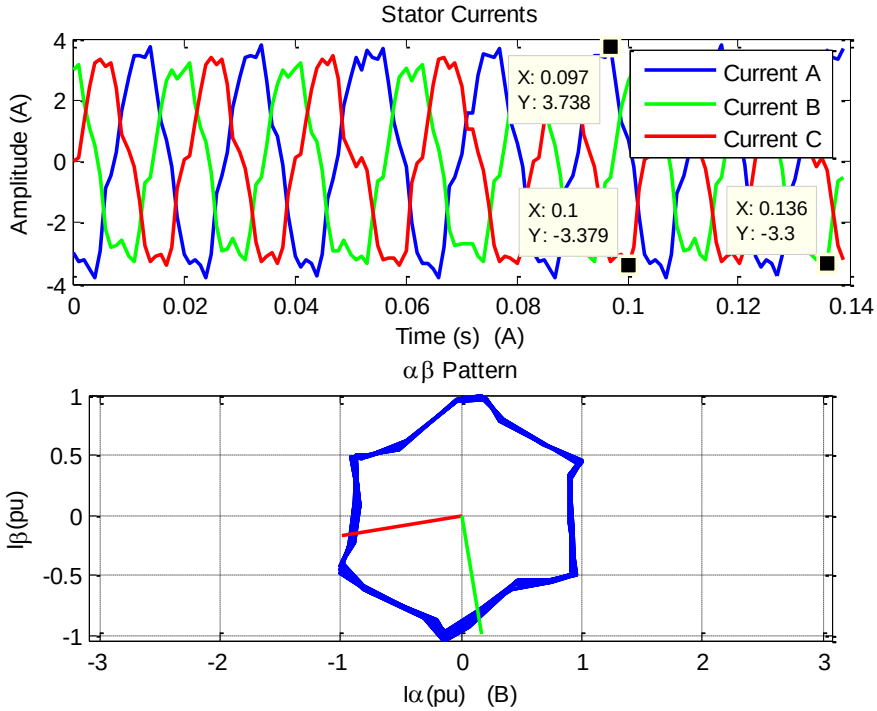

Figure 6.29 – Experimental results obtained for a stator fault situation in nominal operation with a SF = 30 % in the phase A (A) Stator currents of the machine (B) Experimental *αβ*-vector Transformation

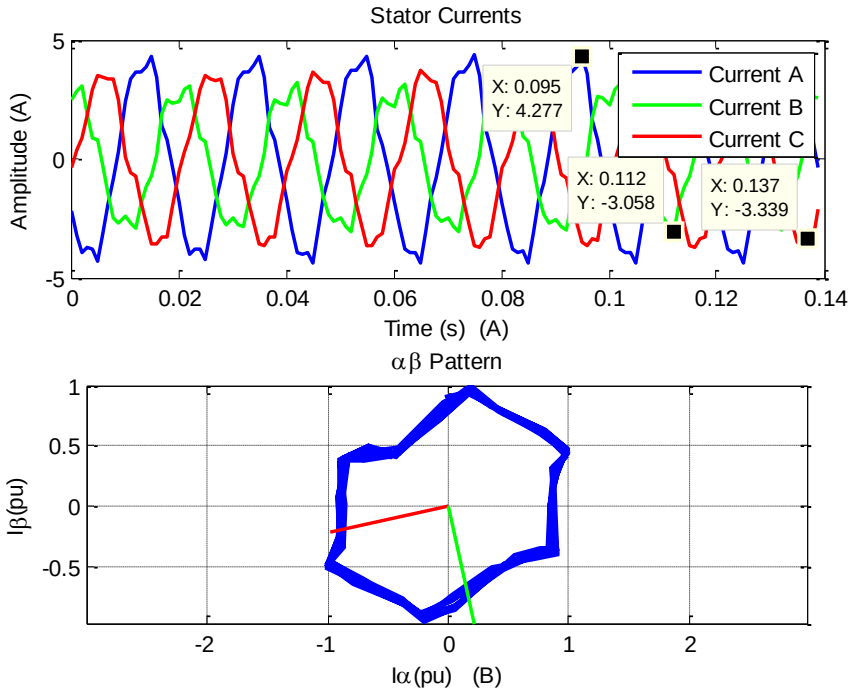

Figure 6.30 – Experimental results obtained for a stator fault situation in nominal operation with a SF = 60 % in the phase A (A) Stator currents of the machine (B) Experimental *αβ*-vector Transformation

The results from Figure 6.31 also indicate that for stator faults, the fault severity factor is independent from the motor load level. Comparing these results with the simulation results, it is

observed that the results do not match. However, experimental results are desirable since it allows the application of the algorithm to variable speed drives.

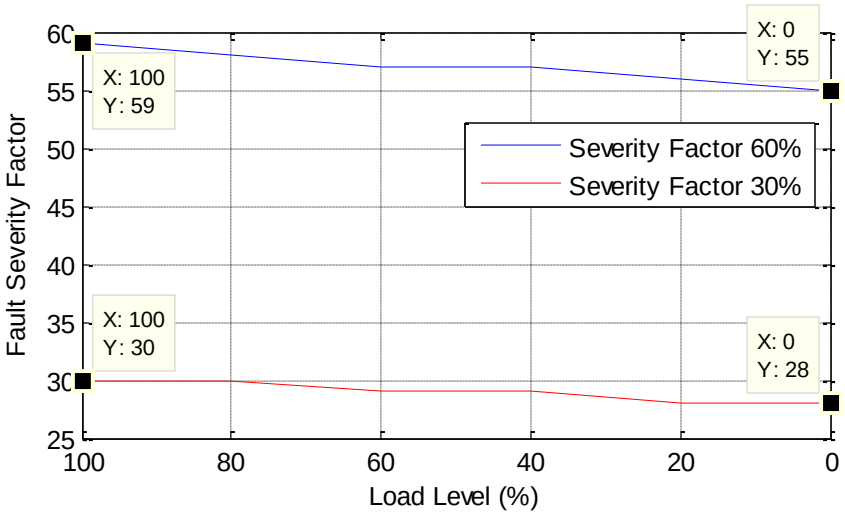

Figure 6.31 - Evolution of the fault severity factor with the motor load level. The blue line is for a SF = 60% and the red line for a SF = 30%

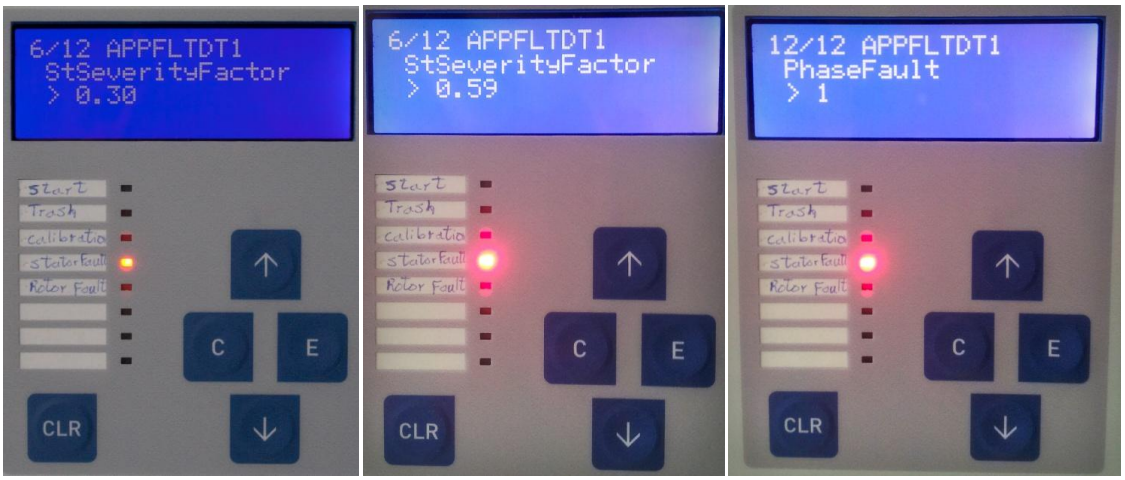

Figure 6.32 – *HMI* of the *TPU* with the indication of a stator fault in the phase 1 (A)

6.3.2.2. Stator Fault in Phase B

The results presented in Figure 6.33 (A) and Figure 6.34 (A) demonstrates that the highest amplitude value is in the current B, which can indicate the presence of a short circuit in that phase of the machine. The $\alpha\beta$-vector transformation (Figure 6.33 (B) and Figure 6.34 (B)) in this situation loosed its circular shape and gain an elliptical shape as the fault severity factor increases. This also occurred before in the faults applied to the phase A of the machine. However, for a stator fault applied to the phase B the orientation of the ellipse is different from the other presented cases.

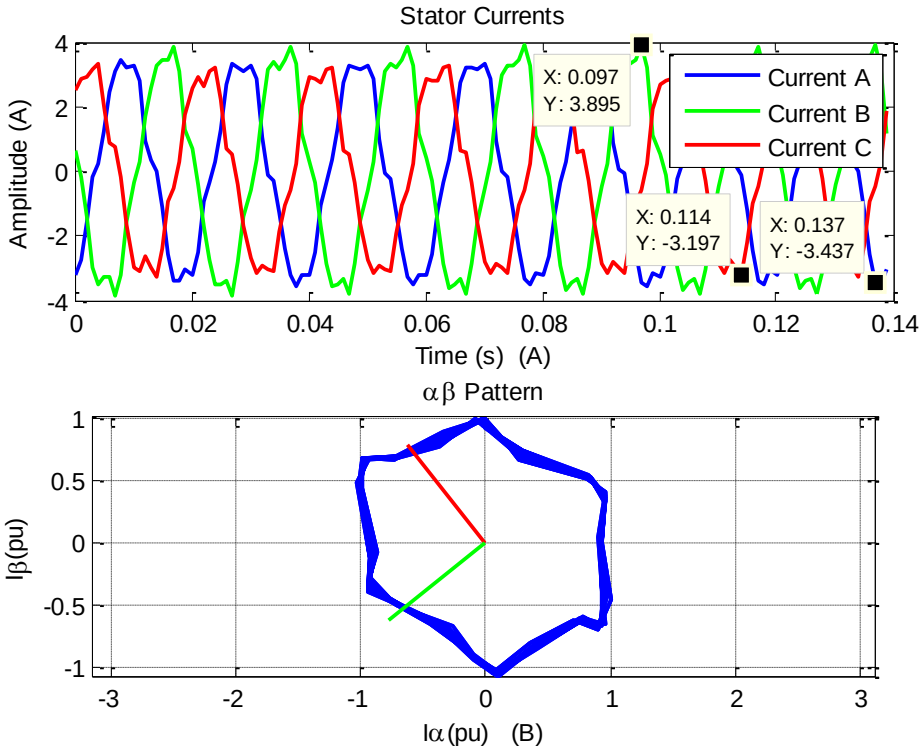

Figure 6.33 – Experimental results obtained for a stator fault situation in nominal operation with a SF = 30 % in the phase B (A) Stator currents of the machine (B) Experimental *αβ*-vector Transformation

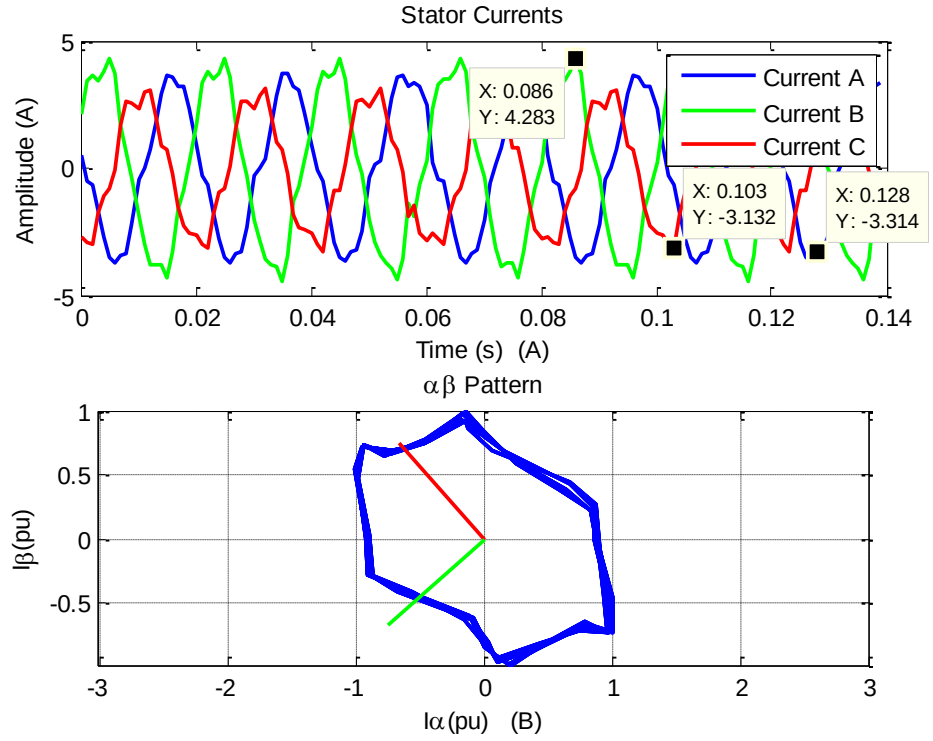

Figure 6.34 – Experimental results obtained for a stator fault situation in nominal operation with a SF = 60 % in the phase B (A) Stator currents of the machine (B) Experimental *αβ*-vector Transformation

Figure 6.35 – *HMI* of the *TPU* with the indication of a stator fault in the phase 2 (B)

6.3.2.3. Stator Fault in Phase C

For the stator faults applied to the phase C of the machine, the results obtained for the temporal evolution the stator currents (Figure 6.36 (A) and Figure 6.37 (A)) and the *αβ*-vector pattern (Figure 6.36 (B) and Figure 6.37 (B)) are similar. When compared with results obtained for the other fault situation (Section 6.3.2.1 and 6.3.2.2) only change is the orientation of the *αβ*-vector pattern that is given by the eigenvectors, that indicate the phase of the machine where the short-circuit occurred.

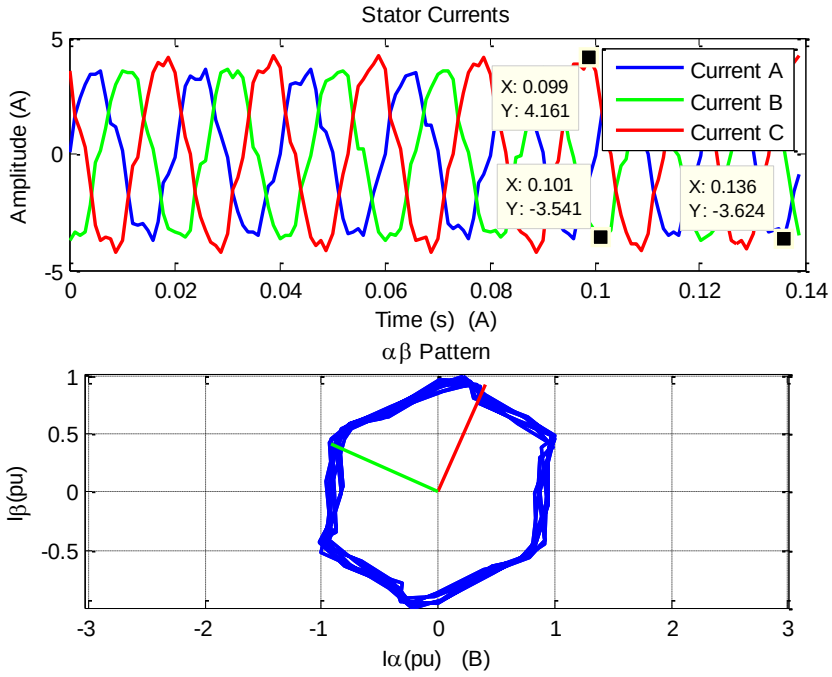

Figure 6.36 – Experimental results obtained for a stator fault situation in nominal operation with a SF = 30 % in the phase C (A) Stator currents of the machine (B) Experimental *αβ*-vector pattern

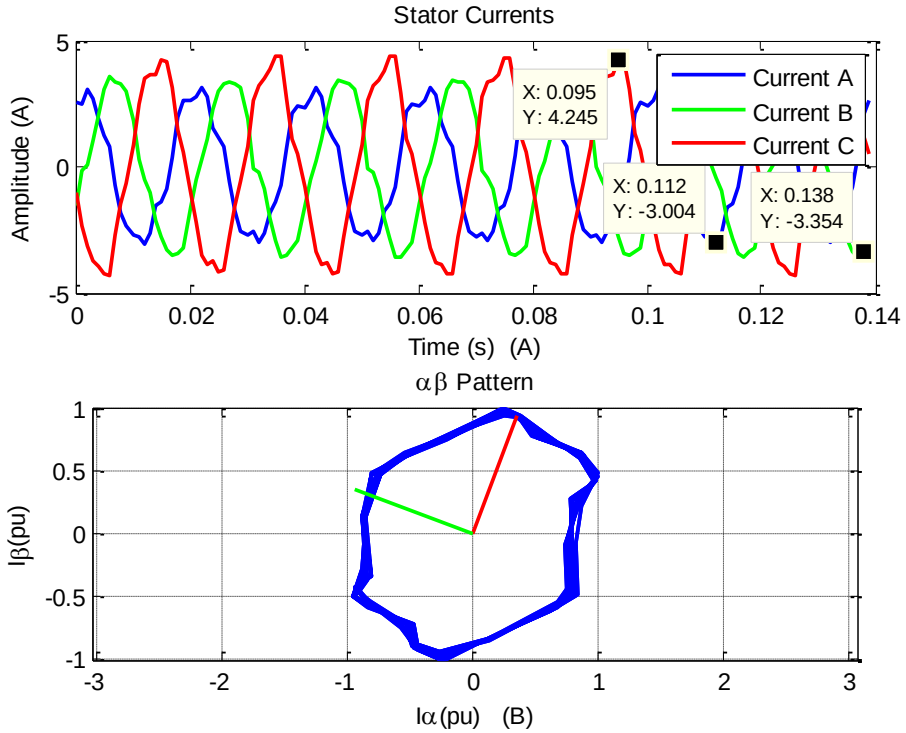

Figure 6.37 – Experimental results obtained for a stator fault situation in nominal operation with a SF = 60 % in the phase C (A) Stator currents of the machine (B) Experimental *αβ*-vector Transformation

Figure 6.38 – *HMI* of the *TPU* with the indication of a stator fault in the phase 3 (C)

The variation of the eigenvalues in terms of computation cycles of the algorithm in cases of stator faults is shown in Figure 6.39. Through this Figure it can be seen that the variation of the eigenvalues in this situation is minimal, both for minor faults (Figure 6.39 (A)) and major faults (Figure 6.39 (B)). The difference between the minimum value and the maximum value in both faults is approximately 1%.

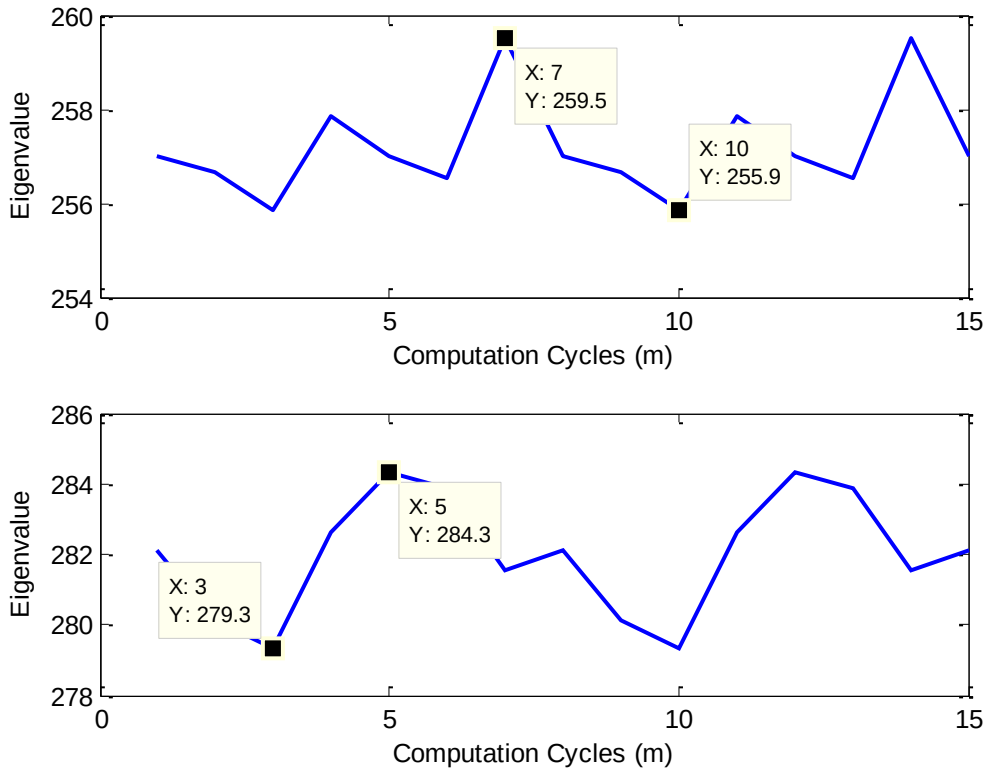

Figure 6.39 - Variation of the eigenvalues over the computation cycles in a stator fault situation (A) Stator fault with a SF = 30% (B) Stator fault with a SF = 60%

In the Table 6.2 are presented the matrixes with the eigenvectors obtained in the simulation and experimental results for stator fault situations with a severity factor (*SF*) equal to 60%. Despite having different lengths, the simulated and experimental eigenvectors present the same directions in all fault situations. In this situation the direction of the eigenvector is more important than the length of the vector, because through the direction of the eigenvector is possible to identify the phase that is in a fault situation.

	Phase A	**Phase B**	**Phase C**
Simulation	$V = \begin{bmatrix} 0{,}323 & -0{,}946 \\ -0{,}946 & -0{,}323 \end{bmatrix}$	$V = \begin{bmatrix} -0{,}290 & -0{,}956 \\ -0{,}956 & 0{,}290 \end{bmatrix}$	$V = \begin{bmatrix} -0{,}981 & 0{,}193 \\ 0{,}193 & 0{,}981 \end{bmatrix}$
Experimental	$V = \begin{bmatrix} 0{,}2261 & -1 \\ -1 & -4{,}4178 \end{bmatrix}$	$V = \begin{bmatrix} -1 & -1 \\ -1{,}1162 & 0{,}89 \end{bmatrix}$	$V = \begin{bmatrix} -1 & 1 \\ 2{,}6921 & 0{,}371 \end{bmatrix}$

Table 6.2 – Comparison between the eigenvectors obtained in simulation and experimental tests

6.3.3 Rotor Faults

The conducted tests for rotor fault situation were different from tests carried out in simulation. The mathematical model of the machine used is a wound rotor induction machine and induction machine used for experimental tests is a squirrel-cage machine. In the experimental set up the rotor faults were applied by drilling a hole into the rotor bars, in order to broke the rotor bar and simulate a rotor fault situation.

The results obtained for one broken rotor bar (minor fault) and 6 broken rotor bars (major fault) are shown in the Figures 6.40 and 6.41. For the evolution of the stator currents in the time domain (Figure 6.40 (A) and Figure 6.41 (B)) it is possible to observe that the results are similar to the simulation results obtained in the Section 6.2.3 of this Chapter.

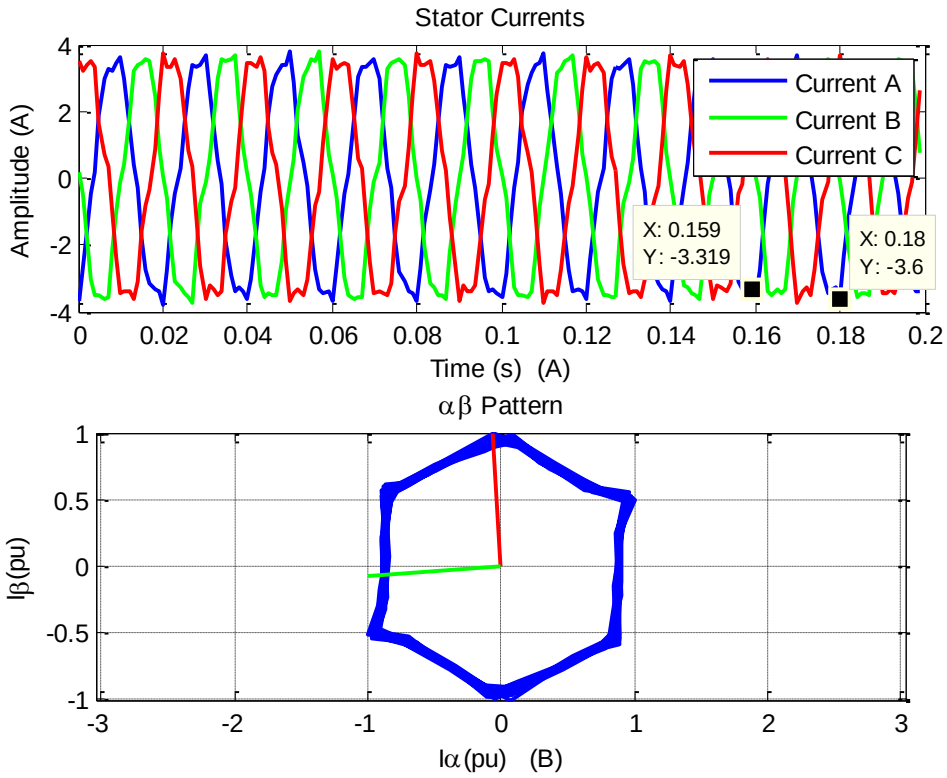

Figure 6.40 - Experimental results obtained for the machine with 1 broken rotor bar (A) Stator currents of the machine (B) Experimental $\alpha\beta$-vector Transformation

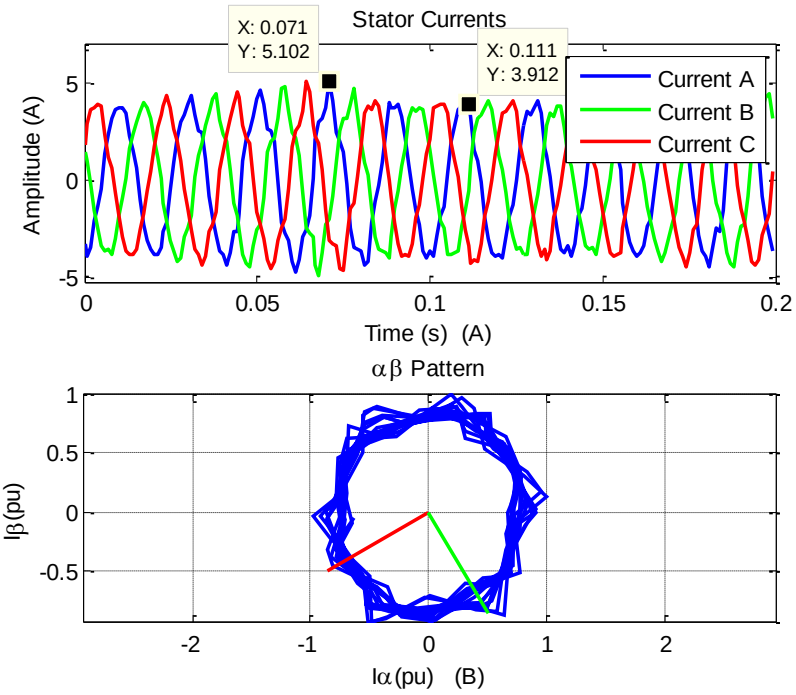

Figure 6.41 - Experimental results obtained for the machine with 6 broken rotor bars (A) Stator currents of the machine (B) Experimental $\alpha\beta$-vector Transformation

As happened in the simulations, the appearance of a thick ring (Figure 6.40 (B) and Figure 6.41 (B)) in a rotor fault situation can be detected through the variation of eigenvalues (Figure 6.42). In the experimental results the eigenvalues does not present a sinusoidal behavior, but show a periodic variation over time as can be seen in the Figure 6.42.

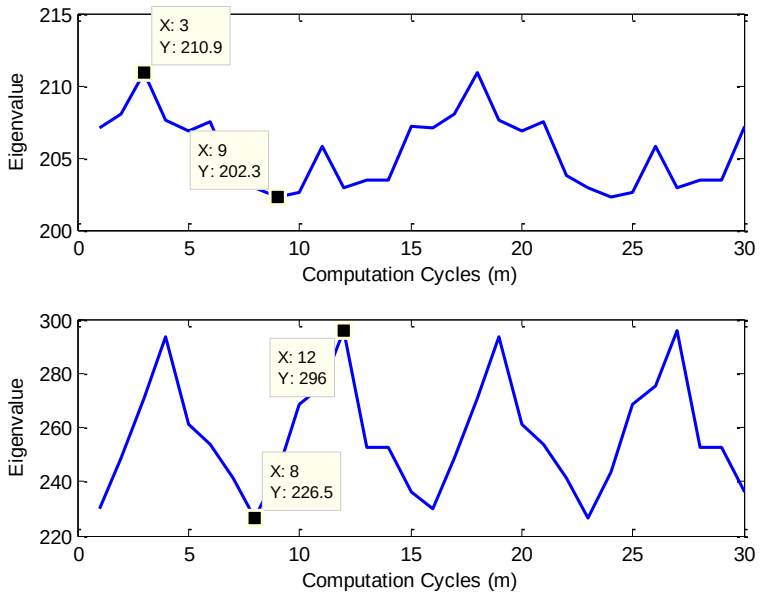

Figure 6.42 - Variation of the eigenvalues over the computation cycles in a rotor fault situation (A) 1 broken rotor bar (B) 6 broken rotor bars

The severity factors obtained for the rotor faults presented are the following:

$$SF_{1BB} = \left(1 - \frac{202,3}{210,9}\right) * 100 = 3.91\% \quad SF_{6BB} = \left(1 - \frac{226,5}{296}\right) * 100 = 23.4\%$$

Figure 6.43 – *HMI* of the *TPU* with the indication of a rotor fault

The results from Figure 6.44 indicate that for rotor faults, the fault severity factor changes with the motor load level. Unlike the stator faults, the detection of faults in the rotor is dependent on the torque applied to the machine. Comparing these results with the simulation results, it is observed that the results match. This phenomenon is not desirable since it requires the machine to work always in nominal regime. So it is not possible to apply the algorithm to variable speed drives.

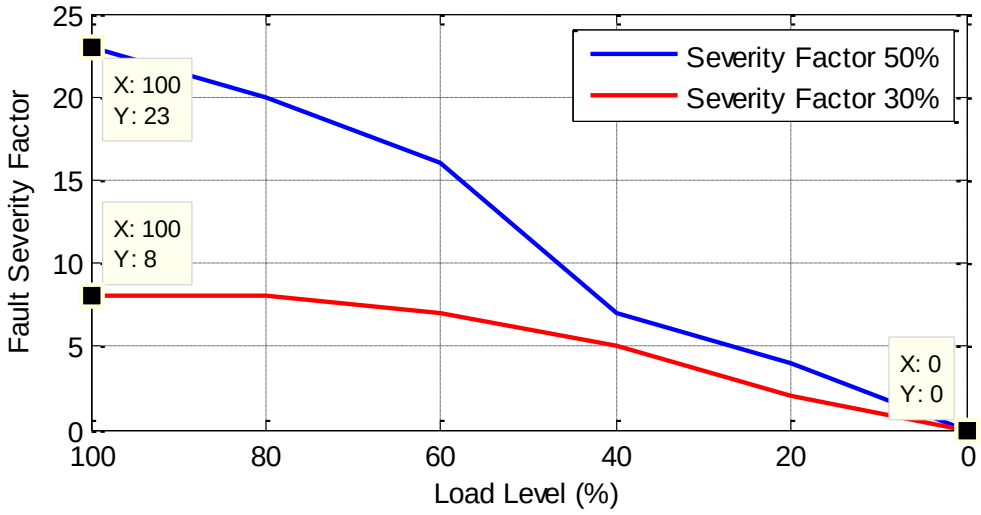

Figure 6.44 - Evolution of the fault severity factor with the motor load level. The blue line is for a rotor fault situation with 6 *BRB* and the red line for 2 *BRB*

In the Figure 6.45 it is possible to observe the evolution of the fault severity factor (in a rotor fault situation) as a function of the number of broken rotor bars. Initially it appears that the

severity factor grows proportionally with the number of broken bars, but from 6 broken rotor bars there is a decay in the severity factor. Therefore, the presented results indicate that a low value for the fault severity factor does not necessarily mean a low number of broken rotor bars.

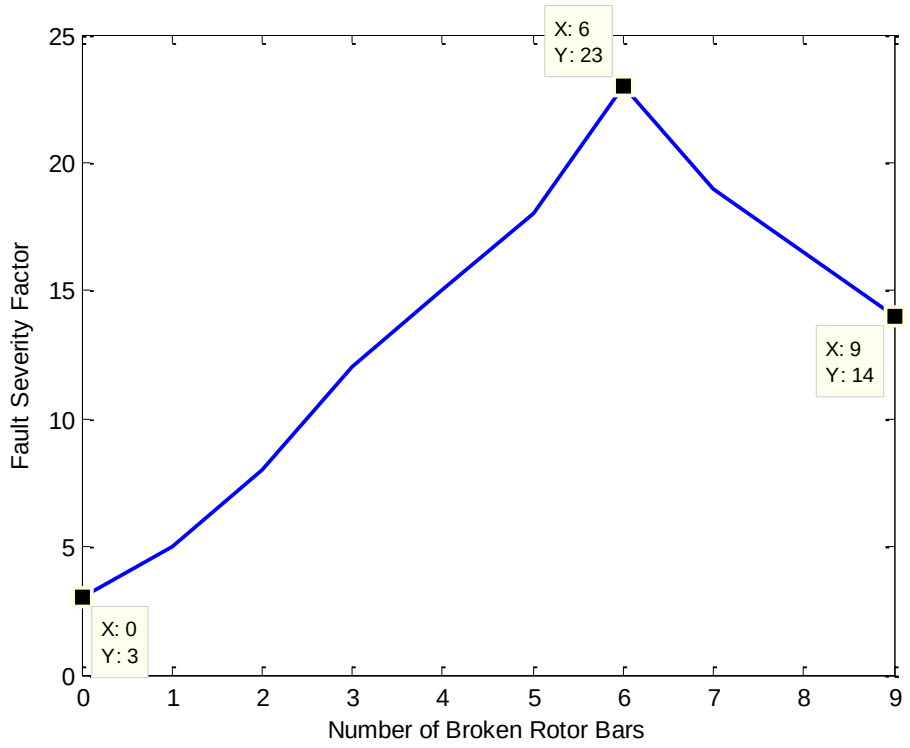

Figure 6.45 – Experimental results for fault severity factor as a function of the number of broken rotor bars

Chapter 7

Conclusions and Future Work

This chapter provides an overview of the work, reviews the contributions of this thesis and the possible future work.

7.1 Summary of the Thesis

The application of induction motors in sensitive areas, such as petrochemical industries and nuclear power plants has increased the need of condition monitoring systems (*CMS*). In addition, the increase of raw materials used to build electrical machines and the existing international crisis, means that it is increasingly necessary to maintain existing equipment in good operating conditions. Therefore the aim of this dissertation was the development of a commercial application for fault detection and diagnosis system in three-phase induction motors.

As was also presented and discussed throughout this work, electrical faults represent almost 50% of the reported faults. So the detection and diagnosis of electrical faults in induction motors such as, short-circuits in stator and broken rotor bars are the focus of this work. Apart from electrical faults this work addresses only induction motors fed by sinusoidal voltage sources.

One steady-state fault detection method, *PCA*, have been used to detect and diagnose the mentioned electrical faults. The proposed technique is based primarily on the verification of differences between the scalar values of the eigenvalues and in the verification of eigenvectors orientation. To this end it is necessary to reduce the number of variables, in this case this was made through the αβ-vector transform. By comparing the eigenvalues, it is possible to verify the presence of unbalances in the stator. The orientation of the eigenvectors indicates the phase that created the unbalance. In the case of broken rotor bars, this fault results in a sinusoidal variation of the scalar values of the eigenvalues.

A detailed literature review presents in the Chapter 2 the common types of faults in induction machines and their causes. In the Chapter 3 the various types of monitoring and fault diagnosis techniques are also reviewed.

The description of the device used for data acquisition, signal conditioning and processing of data is described in Chapter 4. Initially was presented the *x220* line of *TPU* developed by *EFACEC*, and then is exposed in detail the hardware and software architecture.

In the Chapter 5 is described the idea that supports the developed system, the conceptual model. Next is described the system architecture and finally are shown and described the routines executed by the system.

The work in Chapter 6 deals with the experimental validation of the proposed model in the Chapter 5, where are compared the simulation results with those obtained in the experimental test.

7.2 Conclusions

The advent of *FDD* systems for electrical machines has been an important research topic in the last century, as can be seen from the bibliography included in this work. The fact that there is a system that identifies and determines the type of fault and his severity changed the paradigm of the type of maintenance performed (*PM*) in the equipments. The trends in *FDD* moved from a corrective (*BM*) or planned maintenance that causes downtimes in case of faults, to a condition based maintenance (*CBM*) which keeps the machine in operation and allow us to have knowledge of the equipment status in real-time, which allows to have a maintenance schedule established.

Concerning to the developed work it is important to note that the presence of a digital signal processor (*DSP*) in the *TPU* as well as the presence of current sensors allows the possibility of integration of the diagnostic system into the hardware and software already developed for protection and control purposes. This means that the diagnostic technique can be incorporated into the system at little or no additional cost.

In this thesis is presented an on-line *FDD* system for three-phase induction machines. The practical feasibility of on-line monitoring through current space pattern analysis was demonstrated. The *FDD* method chosen is based on the application of *PCA* to the stator currents. From the stator currents the Principal Components of the αβ-vector transformation are analyzed and it is possible to detect electrical faults, such as short-circuits in the stator windings and broken rotor bars.

Regarding to stator faults, they cause a deformation in the current αβ-vector pattern, which leads to the appearance of an elliptic shape in the current αβ-vector pattern that increases with the seventy of the fault. These faults were detected using the respective eigenvalues of the

Principal Components. Furthermore, using the obtained eigenvectors, the algorithm can also identify the phase where the fault occurred.

For rotor fault detection it is known that by observing the relative thickness of the ring formed by the αβ-vector transformation it is possible to detect this kind of faults. It also known that in rotor fault situations the respective eigenvalues are not constant and present a sinusoidal behavior. To this end, analyzing the variation of the eigenvalues over the computation cycles it is possible to detect the existence of rotor faults.

From the results obtained in the Chapter 6 it can be concluded that the developed application detect the presence of short-circuits in the stator windings and the presence of broken rotor bars in three-phase induction machines. It is also possible to infer that the obtained results coincide with the results found in the literature.

For stator faults both experimental and simulation results show that the severity of these faults is proportional to the decrease in impedance of the phase which is in short circuit means that the severity factor is proportional to the number of turns in short circuit. From the experimental results it was also possible to verify that stator faults do not cause oscillations at rated engine speed. It was also verified that the variation of the eigenvalues is minimal, both for minor faults and major faults. For fault classification purposes it was proven that in stator fault situations the load of the machine does not influence the severity factor.

In rotor fault situations was observed that these faults cause an oscillation in the rated speed of the machine and the accuracy of the severity factor changes with the motor load. For motor loads below 50% of the rated torque the fault severity factor is lower when compared to the severity factors obtained for motor loads above 50% of the rated torque. Below 50% of the rated torque, the amplitude of the stator currents becomes very similar to the amplitudes in a healthy case. This phenomenon is a problem because the machine has to run always in nominal regime. However, despite the limitations of the algorithm the faults where predicted successfully. Thus, the developed work confirms the well-known difficulty of diagnose a fault when a motor is lightly loaded.

A determinant factor for the use of this *FDD* method is the manufacturing quality of the motor. This factor directly affects the field distribution in the machine and will increase the harmonic distortion in the currents if the field distribution is not approximately sinusoidal. The used supply voltage is also important to minimize the presence of harmonic distortion. The factors mentioned above are a problem, because it causes variations in the principal components of the *PCA.* Thus, the output produced by the algorithm can have a high level of uncertainty and can induce in error the user in relation to the machine's state.

7.3 Recommendations for future work

Condition-based maintenance is an area with significant growth potential, as a result of this work, there is some possibility of research and development. Thus, this work can be expanded further by implementing in the developed algorithm the detection of mechanical faults, such as bearing damages, air-gap eccentricities and shaft deflection that are the most common cause of faults in induction machines. The application of vibrations to the machine during the algorithm execution must be made in order to demonstrate the robustness and reliability of the developed algorithm.

The stator faults were applied through the addition of variable resistors in series with the stator windings. This setup can be considered as an approximation to the fault situation, because the resistances were used to create the unbalances in the phases of the stator. In the future should be short-circuited some stator windings and test the algorithm to observe his behavior.

In the case of motors controlled by current the algorithm does not work, because the algorithm uses the input currents to proceed to the detection and diagnosis. If the current is controlled there is no deviation from the rated values. It would be interesting to improve the algorithm with the objective of operating in motors controlled by current. Thus, the range of motors covered by this detection and diagnosis algorithm is greater.

There is a particular situation that was verified during the implementation of the algorithm. The fault severity factors change when the stator connections scheme is changed from triangle to delta. This effect is not desirable, the algorithm must keep the fault severity factors independently from the stator connection scheme. Besides that, induction motors usually work with a delta connection scheme, the triangle connection scheme is used only in the startup. This situation must be investigated in the future to improve the robustness and the reliability of the algorithm.

During the development of the algorithm, several problems have been found challenging and left unsolved at the present stage. First, the developed algorithm did not consider the signal problems. If a variable is unavailable, the developed algorithm will not work. In the future the incorporation of advanced techniques, such as estimation and state observation are alternatives that need to be developed.

Second, the proposed algorithm can only detect a single fault at a time, simultaneous multiple fault detection is not considered. Although the occurrence simultaneous multiple faults in electrical machines are rare, the algorithm should be able to detect and diagnose all the possibilities of fault occurrences.

Finally, the fact that there are several motors with various sizes and various values for the output power (P_{mec}) can cause changes in the threshold values set for stator and rotor faults. One possible improvement would be the development of an algorithm that automatically attributes values to the fault thresholds.

Bibliography

[1] J. Cusidó, L. Romeral, J. A. Ortega, J. A. Rosero and A. G. Espinosa, "Fault Detection in Induction Machines Using Power," *IEEE Trans. Ind. Appl.,* vol. 55, no. 2, pp. 633-643, Feb. 2008.

[2] I. Ahmed, R. Supangat, J. Grieger, N. Ertugrul and W. L. Soong, "A Baseline Study for On-Line Condition Monitoring of Induction Machines," *Australasian Universities Power Engineering Conference (AUPEC),* pp. 26-29, Sept. 2004.

[3] P. J. Tavner, L. Ran, J. Penman and H. Sedding, Condition monitoring of electrical machines, Herfordshire, England: Research Studies Press Lts, 1987.

[4] D.J.T. Siyambalapitiya and P. G. Mclaren, "Reliability Improvement and Economic Benefits of On-Line Monitoring Systems for Large Induction Machines," *IEEE Trans. Ind. Appl.,* vol. 26, no. 6, pp. 1018-1025, Nov./Dec. 1990.

[5] E. O. Lunn, "Induction Motors Under Unbalanced Conditions," *American Institute of Electrical Engineers, Transactions of the,* pp. 387-393, Apr. 1936.

[6] P. H. Trickey, "Die cast rotor testing by test stator method," *Trans. Amer. Inst. Elect. Engrs,* vol. 65, pp. 139-141, 1946.

[7] A. M. Armour and J. W. Walley, "A magneto-electric method for detecting defects in cast aluminium rotor windings for squirrel-cage motors," *Metropolitan-Vickers Gazette,* vol. 27, pp. 314-317, 1956.

[8] D. Teodorescu, "'A new method of finding casting defects in the bars of squirrel-cage rotors," *Vestn. Elektropromyl.,* vol. 7, pp. 52-54, 1963.

[9] J. F. Heidbreder, "Induction Motor Temperature Characteristics," *AIEE Trans. Power Apparatus Systems,* vol. 77, no. 3, pp. 800-804, 1958.

[10] M.E.H. Benbouzid, "Bibliography on Induction Motors Faults Detection and Diagnosis," *IEEE Trans. on Energy Conversion,* vol. 14, no. 4, pp. 1065-1074, 1999.

[11] J. Penman and S. A., "Broken Rotor bars: their effect on the transient performance of induction machines," *IEE Procs. Electric Power Applications,* vol. 143, no. 6, pp. 449-457, 1996.

[12] F. D. Smith and K. L. Hanson, "Rotor protection of large motors by use of direct temperature monitoring," *IEEE Trans. Ind. Appl.,* vol. 11, no. 4, pp. 340-343, 1975.

[13] S. A. Swann, "Effect of rotor eccentricity on the magnetic field in airgap of a nonsalient pole machine," *Proc. IEE,* vol. 110, no. 5, pp. 903-915, 1963.

[14] S. Williamson and A. C. Smith, "Steady-state analysis of 3-phase cage motors with rotor-bar and end-ring faults," *Proc. IEE,* vol. 129, no. 3, pp. 93-100, May 1982.

[15] K. J. Binns and M. Dye, "Identification of principal factors causing unbalanced magnetic pull in cage induction motors," *Proc. IEE,* vol. 120, no. 3, pp. 349-354, 1973.

[16] S. Williamson and K. Mirzoian, "Analysis of cage induction motors with stator windings faults," *IEEE Transactions on Power Apparatus and Systems,* vol. 104, no. 7, pp. 1838-1842, Jul. 1985.

[17] A. J. Ellison and S. J. Yang, "Effects of rotor eccentricity on acoustic noise from induction machines," *Proc. IEE,* vol. 118, no. 1, pp. 174-184, 1971.

[18] J. Penman, J. Hadwick and B. Barker, "Detection of faults in electrical machines by examination of the axially directed fluxes," *Proceedings of 3rd International Conference on Electrical machines,* pp. R/5-1-R/5-1 O, 1978.

[19] M. N. Dey, "Online protection of electrical machines by micro-computer analysis of axial leakage flux, Ph.D. Thesis," University of Aberdeen, UK, 1983.

[20] W. T. Thomson and I. D. Stewart, "On-line current monitoring for fault diagnosis in inverter fed induction motors," *3rd International Conference on Power Electronics and Variable-Speed Drives,* pp. 432-435, Jul. 1988.

[21] G. B. Kliman, J. Stein and R. D. Endicott, "Noninvasive detection of broken rotor bars in operating induction motors," *IEEE Transactions on Energy Conversion,* vol. 3, no. 4, pp. 873-879, Dec. 1988.

G. B. Kliman, R. A. Koegl, M. W. Schulz and S. E. Grabkowski.U.S. Patent

[22] 4761703, 1987.

[23] G. B. Kliman, R. A. Koegl, J. R. Krahn and W. J. Premerlani.U.S. Patent 6262550, 1999.

[24] M.-y. Chow, P. M. Mangum and S. O. Yee, "Neural Network Approach to Real-Time Condition Monitoring of Induction Motors," *IEEE Trans. Ind. Elect.,* vol. 38, no. 6, pp. 448-453, Dec. 1991.

[25] Zhang Chaohai, Mao Zongyuan and Zhou Qijie, "On-line Incipient Fault Detection of Induction motors Using Artificial Neural Networks," *Proc. IEEE Ind. Tech.,* pp. pp. 458-462, 1994.

[26] D. Matic, F. Kulic, V. Climente-Alarcon and R. Puche-Panadero, "Artificial Neural Networks Broken Rotor Bars Induction Motor Fault Detection," *10th Symposium on Neural Network Applications in Electrical Engineering (NEUREL),* pp. 49-53, 2010.

[27] Chang-Eob Kim, Yong-Bae Jung, Sang-Baeck Yoon and Dal-Ho Im, "The Fault Diagnosis of Rotor Bars in Squirrel Cage Induction Motors," *IEEE Trans. on Magnetics,* vol. 33, no. 2, pp. 2131-2134, Mar. 1997.

[28] A. Bentounsi and A. Nicolas, "On Line Diagnosis of Defaults on Squirrel Cage Motors Using FEM," *IEEE Trans. on Magnetics,* vol. 34, no. 5, pp. 3511-3514, Sept. 1998.

[29] C. J. Aileen, S. Nagarajan and S. R. Reddy, "Detection of Broken Bars in Three Phase Squirrel Cage Induction Motor using Finite Element Method," *2011 International Conference on Emerging Trends in Electrical and Computer Technology (ICETECT),* pp. 249-254, 2011.

[30] A.J.M. Cardoso and E. S. Saraiva, "Computer Aided Detection of Airgap Eccentricity in Operating Three-phase Induction Motors, by Park's Vector Approach," *IEEE Trans. Ind. Appl.,* pp. 897-901, 1993.

[31] A. J.Marques Cardoso, S. M.A. Cruz, J. F.S. Carvalho and E. S. Saraiva, "Rotor Cage Fault Diagnosis in Three-Phase Induction Motors, by Park's Vector Approach," *IEEE Ind. Appl. Conference,* vol. 1, pp.642-646, 1995.

[32] João F. Martins, Vitor F. Pires and Tito Amaral, "Induction motor fault detection and diagnosis using a current state space pattern recognition," *Pattern Recognition Letters,*

vol. 32, no. 2, pp. 321-328, 2011.

[33] V. F. Pires, J. F. Martins and A. J. Pires, "On-Line Diagnosis of Three-Phase Induction Motor Using an Eigenvalue αβ-vector approach," *International Symposium on Industrial Electronics*, vol. 2, pp. 863-866, 2005.

[34] J. F. Martins, V. F. Pires and A. J. Pires, "On-Line Diagnosis of Three-Phase Closed Loop Induction Motor Drives Using an Eigenvalue αβ-vector approach," *7th Internacional Conference on Power Electronics and Drive Systems*, pp. 689-693, Nov. 2007.

[35] J. F. Martins, V. F. Pires and A. J. Pires, "PCA-Based On-Line Diagnosis of Induction Motor Stator Fault Feed by PWM Inverter," *IEEE International Symposium on Industrial Electronics*, pp. 2401-2405, 2006.

[36] H. Nejjari and M. E.H. Benbouzid, "Application of Fuzzy Logic to Induction Motors Condition Monitoring," *IEEE Power Engineering Review*, pp. 52-54, 1999.

[37] V. Mini, S. Setty and S. Ushakumari, "Fault Detection and Diagnosis of an Induction Motor using Fuzzy Logic," *IEEE R8 International Conference on Computational Technologies in Electrical and Electronics Engineering (SIBIRCON)*, pp. 459-464, 2010.

[38] K.R.Cho, J. H. Lang and S. D. Umans, "Detection of Broken Rotor Bars in Induction Motors Using State and Parameter Estimation," *IEEE Trans. Ind. Appl.*, vol. 28, no. 3, pp. 702-709, May 1992.

[39] S. Kumar, J. Prakash and S. S. Kumar, "Detection of Broken Rotor Bars in Induction Motor Using Derivative Free Kalman Filters," *International Conference on Process Automation, Control and Computing (PACC)*, pp. 1-7, 2011.

[40] W. Bradley, J. Victory, M. Ebrahimi, A. Wood and C. Pestell, "Model-Based Diagnosis of Induction Motor Failure Modes," *IEEE Conference on Emerging Technologies and Factory Automation (ETFA)*, pp.1-4, 2010.

[41] S.M.A. Cruz and A. J.M. Cardoso, "Rotor Cage Fault Diagnosis in Three-Phase Induction Motors by the Total Instantaneous Power Spectral Analysis," *IEEE Ind. Appl. Conf.*, vol. 3, pp. 1929-1934, 1999.

S. F. Legowski, A. H.M. Sadrul Ula and A. M. Trzynadlowski, "Instantaneous

[42] Power as a Medium for the Signature Analysis of Induction Motors," *IEEE Trans. Ind. Appl.*, vol. 32, no. 4, pp. 904-909, 1996.

[43] R. S. Kumar, K. K. Ray and K. V. Kumar, "Fault Diagnosis of Industrial Drives Using MCSA Techniques," *International Conference on Control, Automation, Communication and Energy Conservation (INCACEC)*, pp. 1-7, 2009.

[44] W. T. Thomson, "On-line MCSA to Diagnose Shorted Turns in Low Voltage Stator Windings of 3-Phase Induction Motors prior to Failure," *IEEE International Electric Machines and Drives Conference (IEMDC)*, pp. 891-898, 2001.

[45] N. Mariun, M. R. Mehrjou, M. H. Marhaban and N. Misron, "An Experimental Study of Induction Motor Current Signature Analysis Techniques for Incipient Broken Rotor Bar Detection," *International Conference on Power Engineering, Energy and Electrical Drives (POWERENG)*, pp. 1-5, 2011.

[46] Cao Zhitong, Chen Hongping, He Guoguang and E. Ritchie, "Rotor Fault Diagnosis of Induction Motor based on Wavelet Reconstruction," *IEEE Proc. on Electrical Machines and Systems (ICEMS)*, pp. 374-377, 2001.

[47] A. Bouzida, O. Touhami, R. Ibtiouen, A. Belouchrani, M. Fadel and A. Rezzoug, "Fault Diagnosis in Industrial Induction Machines Through Discrete Wavelet Transform," *IEEE Trans. Ind. Appl.*, vol. 58, no. 9, pp. 4385-4395, Sept. 2011.

[48] M. Arkan, D. K. Perovic and P. Unsworth, "Online stator fault diagnosis in induction motors," *IEE Proc. Electr. Power Appl.*, vol. 146, no. 6, pp. 537-547, Nov. 2001.

[49] S.M.A. Cruz, A. J.M. Cardoso and H. A. Toliyat, "Diagnosis of Stator, Rotor and Airgap Eccentricity Faults in Three-Phase Induction Motors Based on the Multiple Reference Frames Theory," *Industry Applications Conference*, pp.1340-1346, 2003.

[50] Zhenxing Liu, Xiaolong Zhang, Xianggen Yin and Zhe Zhang, "Rotor Cage Fault Diagnosis in Induction Motors Based on Spectral Analysis of Current Hilbert Modulus," *IEEE Power Engineering Society General Meeting*, pp. 1-4, 2004.

[51] M. Pineda-Sanchez, M. Riera-Guasp, J. Roger-Folch, J. Antonino-Daviu, J. Perez-Cruz and R. Puche-Panadero, "Diagnosis of Induction Motor Faults in Time-Varying Conditions Using the Polynomial-Phase Transform of the Current," *IEEE Trans. Ind.*

Electr., vol. 58, no. 4, pp. 1428-1439, 2011.

[52] Ahan Li and Shi Li-ping, "Fault diagnosis of induction motor based on information entropy fusion," *International Conference on Advanced Computer Control (ICACC)*, pp. 48-51, 2010.

[53] M. Tsypkin, "Induction Motor Condition Monitoring: Vibration Analysis Technique - a Practical Implementation," *IEEE International Electric Machines & Drives Conference (IEMDC)*, pp. 406-411, 2011.

[54] Xin Wen, D. J. Brown and Qizheng Liao, "Online Motor Fault Diagnosis Using Hybrid Intelligence Techniques," *IEEE Symposium on Industrial Electronics and Applications (ISIEA)*, pp. 355-360, 2010.

[55] WEG, AC Electrical Motors Catalogue, Brazil: WEG Electromotors, Jun. 2005.

[56] S. Nandi and H. A. Toliyat, "Fault Diagnosis of Electrical Machines - A Review," *International Conference on Electric Machines and Drives (IEMD)*, pp. 219-221, 1999.

[57] Motor Reliability Working Group, "Report of Large Motor Reliability Survey of Industrial and Commercial Installations," *IEEE Trans. Ind. Appl.*, pp.853-872, 1985.

[58] EPRI, "Improved Motors for Utility Applications," *Publication EL-2678*, Vols. 1-2, pp. 1-478, 1982.

[59] H. Behbahanifard, H. Karshenas and A. Sadoughi, "Non-invasive On-line Detection of Winding Faults in Induction Motors – A Review," *International Conference on Condition Monitoring and Diagnosis*,pp.188-191, 2008.

[60] Andrea Stefani, "Induction Motor Diagnosis in Variable Speed Drives," Bologna, Italy, 2010.

[61] "Damages in the Stator Windings," [Online]. Available: http://marcusdasilva.blogspot.pt/2009/04/danos-em-enrolamentos-motores.html. [Accessed 26 August 2012].

[62] A. H. Bonnett and G. C. Soukup, "Cause and Analysis of Stator and Rotor Failures in Three-phase Squirrel-Cage Induction Motors," *IEEE Trans. Ind. Appl.*, vol. 28, no. 4,

pp. 921-937, 1992.

[63] M. Olyphant, "Corona and Treeing Breakdown of Insulation - Progress and Problems," *Insulation Magazine*, 1963.

[64] A. Mbaye, J. P. Bellomo, T. Lebey, J. M. Oraison and F. Peltier, "Electrical stresses applied to stator insulation in low voltage induction motors fed by PWM drives," *IEEE Procs. Electric Power Applications*, vol. 144, no. 3, pp. 191-198, 1997.

[65] M. Riera-Guasp, M. Cabanas, J. Antonino-Daviu, M. Pineda-Sanchez and C. Garcia, "Influence of Nonconsecutive Bar Breakages in Motor Current Signature Analysis for the Diagnosis of Rotor Faults in Induction Motors," *IEEE Trans. Energy Conv.*, vol. 25, no. 1, pp. 80-89, Mar. 2010.

[66] A. H. Bonnett and G. C. Soukup, "Rotor Failures in Squirrel Cage Induction Motors," *IEEE Trans. Ind. Appl.*, vol. 22, no. 6, pp. 1165-1173, Nov. 1986.

[67] D. G. Dorrell, W. T. Thomson and S. Roach, "Analysis of Airgap Flux, Current and Vibration Signals as a Function of the Combination of Static and Dynamic Airgap Eccentricity in 3-Phase Induction Motors," *IEEE Trans. Ind. Appl.*, vol. 33, no. 1, pp. 24-34, Jan. 1997.

[68] Cleber Gustavo Dias, "Proposta de um novo método para a detecção de barras rompidas em motores de indução com rotor em gaiola," São Paulo, Brasil, 2006.

[69] Ye Zhongming and Wu Bin, "A Review on Enduction Motor Online Fault Diagnosis," *IEEE Proc. Power Electronics and Motion Control Conference (IPEMC)*, vol. 3, pp. 1353-1358, 2000.

[70] S. Barker, "Avoiding premature bearing failure with inverter fed induction motors," *Power Engineering Journal*, vol. 4, no. 4, pp. 182-189, 2000.

[71] J. R. Stack, "Fault signature detection for rolling element bearings in electrical machines, PhD Thesis," Department of Electrical Engineering, Institution of Technology, Atlanta, 2002.

[72] I. Önel and M. El Hachemi Benbouzid, "Induction Motor Bearing Failure Detection and Diagnosis: Park and Concordia Transform Approaches Comparative Study," *IEEE Trans. Mechatronics, vol.13, no.2*, pp.257-262, 2008.

[73] P. Vas, Parameter estimation, condition monitoring, and diagnosis of electrical machines, UK: Oxford University Press, 1993.

[74] V. Venkatasubramanian, R. Rengaswamy and S. N. Kavuri, "Areview of process fault detection and diagnosis Part I: Quantitative model-based methods," *Computers and chemical engineering,* vol. 27, pp. 293-311, 2002.

[75] R. Isermann and B. P., "Trends in the Application of the Model-based Fault Detection and Diagnosis of Technical Processes," *Control Engineering Pratice,* vol. 5, no. 5, pp. 709-719, 1997.

[76] R. Isermann, Fault-Diagnosis Systems: An Introduction from Fault Detection to Fault Tolerance, Berlin: Springer, 2006.

[77] Samuel J. Biondo, Fundamentals of expert systems technology : principles and concepts, Norwood, N.J.: Ablex Pub. Corp., 1990.

[78] Albert H. C. Tsang, Andrew K.S. Jardine and Harvey Kolodny, "Measuring maintenance performance: a holistic approach," *International Journal of Operations & Production Management,* vol. 19, no. 7, pp. 691 - 715, 1999.

[79] D. C. Brauer and G. D. Brauer, "Reliability-Centered Maintenance," *IEEE Trans. Reliability,* vol. 36, no. 1, pp. 17-24, 1987.

[80] J. Moubray, Reliability-Centered Maintenance, US: Industrial Press Inc., 1997.

[81] E. Levrat, B. Iung and A. C. Marquez, "E-Maintenance: Principles, Review and Conceptual Framework," *Production Planning & Control: The Management of Operations,* vol. 19, no. 4, pp. 408-429, 2008.

[82] J. Lee, J. Ni, D. Djurdjanovic, H. Qiu and H. Liao, "Intelligent prognostics tools and e-maintenance," *Computers in Industry,* vol. 57, no. 6, pp. 476-489, 2006.

[83] Y. Han and Y. H. Song, "Condition Monitoring Techniques for Electrical Equipment—A Literature Survey," *IEEE Trans. Power Delivery,* vol. 18, no. 1, pp. 4-13, 2003.

W. T. Thomson, "A review of on-line condition monitoring techniques for three-phase squirrel-cage induction motors–past, present and future," *2nd IEEE International*

[84] *Symposium on Diagnostics for Electrical Machines, Power Electronics and Drives (SDEMPED),* pp. 3-17, 1999.

[85] Janos J. Gertler, Fault Detectiond and Diagnosis in Engineering Systems, Marcer Dekker Inc., 1 edition, 1998.

[86] M. L. Sin, W. L. Soong and N. Ertugrul, "Induction Machine On-Line Condition Monitoring and Fault Diagnosis - A Survey," *Australasian Universities Power Engineering Conference,* 2003.

[87] P. L. Timár, Noise and Vibration of Electrical Machines, US: Elsevier, 1989.

[88] ISO, "Mechanical vibration - Evaluation of machine vibration by measurements on non-rotating parts," *ISO 10816-3,*pp.1-18, 1998.

[89] M. W. Hawman and W. S. Galinaitis, "Acoustic emission monitoring of rolling element bearings," *IEEE Proceedings of Ultrasonics Symposium,* vol. 2, pp. 885-889, Oct. 1988.

[90] O. V. Thorsen and M. Dalva, "Condition monitoring methods, failure identification and analysis for high voltage motors in petrochemical industry," *IEEE Procs. Elect. Mach. Drives,* pp. 109 –113, 1997.

[91] M. S.N. Said and M. E.H. Benbouzid, "H-G diagram based rotor pa-rameters identi fication for induction motors thermal monitoring," *IEEE Trans. Energy Convers.,* vol. 15, no. 1, pp. 14 –18, Mar. 2002.

[92] "Thermal Vision - Mechanical Thermography," [Online]. Available: http://www.thermalvision.ie/thermography/mechanical/. [Accessed 27 08 2012].

[93] G. F. Skala, "The ion chamber detector as a monitor of thermally produced particulates," *Journal de Research Atmospherique,* 1966.

[94] C. C. Carson, S. C. Barton and F. S. Echeverria, "Immediate warning of local over-heating in electrical machines by the detection of pyrolysis products," *IEEE Trans. on Power Apparatus and Systems,* pp.533-542, 1973.

J. R. Cameron, W. T. Thomson and A. B. Dow, "Vibration and current monitoring for detecting air gap eccentricity in large induction motors," *IEEE Proc. Inst. Elect. Eng.,*

[95] vol. 133, no. 3, pp. 155-163, May 1986.

[96] P. J. Tavner, B. G. Gaydon and D. M. Ward, "Monitoring generators and large motors," *Proc. Inst. Elect. Eng. B,* vol. 133, no. 3, pp. 169–180, May 1986.

[97] V. Kokko, "Condition Monitoring of Squirrel-Cage Motors by Axial Magnetic Flux Measurements," Academic Dissertation, Faculty of Technology from University of Oulu, 2003.

[98] G. C. Stone, H. G. Sedding and M. J. Costello, "Application of partial discharge testing to motor and generator stator winding maintenance," *IEEE Trans. Ind. Appl.*, vol. 32, no. 2, pp. 459 –464, 1996.

[99] J. L. Kohler, J. Sottile and F. C. Trutt, "Alternatives for Assessing the Electrical Integrity of Induction Motors," *IEEE Trans. Ind. Appl.*, vol. 28, no. 5, pp. 1109-1117, Oct. 1992.

[100] S. Nandi and H. A. Toliyat, "Novel frequency-domain-based technique to detect stator interturn faults in induction machines using stator-induced voltages after switch-off," *IEEE Trans. Ind. Appl.*, vol. 38, no. 1, pp. 101-109, 2002.

[101] M.E.H. Benbouzid, "A Review of Induction Motors Signature Analysis as a Medium for Faults Detection," *IEEE Trans. Ind. Elect.*, vol. 47, no. 5, pp. 984-993, Oct.2000.

[102] Daniel da S. Gazzana, Luis Alberto Pereira and Denis Fernandes, "A System for Incipient Fault Detection and Fault Diagnosis Based on MCSA," *IEEE Transmission and Distribution Conference and Exposition,*pp.1-6, 2010.

[103] R. R. Schoen and T. G. Habetler, "Effects of time-varying loads on rotor fault detection in induction machines," *IEEE Trans. Ind. Appl.*, vol. 31, no. 4, pp. 900-906, Aug. 1995.

[104] A.M. Trzynadlowski, M. Ghassemzadeh and S. F. Legowski, "Diagnostics of Mechanical Abnormalities in Induction Motors Using Instantaneous Electric Power," *IEEE Trans. Energy Conversion*, vol. 14, no. 4, pp. 1417-1423, Dec.1999.

[105] P. Bikfalvi and M. Imecs, "Rotor Fault Detection in Induction Machines: Methods and Techniques - State-of-the-art," *IEEE International Conference on Automation, Quality*

and Testing, Robotics, vol. 1, pp.199-204, 2006.

[106] A. Bellini, F. Filippetti, G. Franceschini and C. Tassoni, "Closed loop influence on induction machine asymmetries effects," *IEEE International Symposium on Diagnostics for Electrical Machines, Power Electronics and Drives,* pp.43-50, 1999.

[107] A. Bellini, F. Filippetti, G. Franceschini and C. Tassoni, "Closed loop control impact on the diagnosis of induction motors faults," *IEEE Industry Applications Society Annual Meeting,* pp.1913-1921, 1999.

[108] J. S. Hsu, "Monitoring of Defects in Induction Motors Through Air-Gap Torque Observation," *IEEE Trans. Ind. Appl.,* vol. 31, no. 5, pp. 1016-1021, 1995.

[109] C. Kral, F. Pirker and G. Pascoli, "Influence of inertia on general effects of faulty rotor bars and the Vienna monitoring method," *IEEE Symposium on Diagnostics of Electrical Machines, Power Electronics and Drives, SDEMPED,* pp. 447-452, 2001.

[110] F. Filippetti, G. Franceschini, C. Tassoni and P. Vas, "Recent Developments of Induction Motor Drives Fault Diagnosis Using AI Techniques," *IEEE Trans. Ind. Elect.,* vol. 45, no. 5, pp. 1966-1973, 1998.

[111] F. Filippetti, M. Martelli, G. Franceschini and T. C., "Development of Expert System Knowledge Base to On-line Diagnosis of Rotor Electrical Faults of Induction Motors," *IEEE Ind. Appl. Society Annual Meeting,* pp.92-99, 1992.

[112] F. Filippetti, G. Franceschini and C. Tassoni, "Neural networks aided on-line diagnostics of induction motor rotor faults," *IEEE Trans. Ind. Applicat.,* vol. 31, no. 4, pp. 892-899, 1995.

[113] I. Lasurt, A. F. Stronach and J. Penman, "A fuzzy logic approach to the interpretation of higher order spectra applied to fault diagnosis in electrical machines," *19th International Conference of the North American Fuzzy Information Processing Society,* pp. 158-162, 2000.

[114] W. N. Sharpe, Mo-Yuen Chow, S. Briggs and L. Windingland, "A methodology using fuzzy logic to optimize feedforward artificial neural network configurations," *IEEE Trans., System, Man and Cybernetics,* vol. 24, no. 5, pp. 760-768, 1994.

P. V. Goode and Mo-Yuen Chow, "A hybrid fuzzy/neural system used to extract

[115] heuristic knowledge from a fault detection problem," *IEEE World Congress on Computational Intelligence Proceedings of the Third IEEE Conference on Fuzzy Systems*, vol. 3, pp. 1731-1736, 1994.

[116] D. Leith, N. Deans and L. Stewart, "Condition monitoring of electrical machine using real time expert systems," *Proc. Int. Conf. Electrical Machines*, vol. 3, pp. 297-302, 1988.

[117] L. Ben-Brahim and R. Kurosawa, "Identification of Induction Motor Speed using Neural Networks," *Conference Record of the Power Conversion Conference*, pp.689-694, 1993.

[118] R. M. Bharadwaj, A. G. Parlos and H. A. Toliyat, "Adaptive Neural Network-Based State Filter for Induction Motor Speed Estimation," *The 25th Annual Conference of the IEEE Industrial Electronics Society*, pp.1283-1288, 1999.

[119] B. Li, M. -Y. Chow, Y. Tipsuwan and J. C. Hung, "Neural-Network-Based Motor Rolling Bearing Fault Diagnosis," *IEEE Trans. Ind. Electr.*, vol. 47, no. 5, pp. 1060, 2000.

[120] L. B. Jack and A. K. Nandi, "Genetic algorithms for feature selection in machine condition monitoring with vibration signals," *IEEE Procs. - Vision, Imagem and Signal Processing*, pp.205-212, 2000.

[121] B. S. Payne, S. M. Husband and A. D. Ball, "Development of condition monitoring techniques for a transverse flux motor," *Internacional Conference (Conf. Publ. No. 487) on Power Electronics, Machines and Drives*, vol. 5, pp. 139-144, 2002.

[122] EFACEC, "Folheto de IEDs Série 220 (Protecção e Controlo)," Lisbon, Portugal, 2011.

[123] EFACEC, "Drago Architecture - Design," Lisbon, Portugal, 2010.

[124] K. Pearson, "On Lines and Planes of Closest Fit to Systems of Points in Space," *Philosophical Magazine*, pp. 559-572, 1901.

[125] H. Hotelling, "Analysis of a complex of statistical variables into principal components," *J. Educ. Psychol., 24*, pp. 417-441, 498-520, 1933.

Shen Yin, X. Steven, A. Naik, Pengcheng Deng and A. Haghani, "On PCA-based

[126] fault diagnosis techniques," *Conference on Control and Fault-Tolerant Systems*, pp. 179-184, 2010.

[127] Song Xue, Xiaolong Li and Zhiqiang Long, "Fault diagnosis for maglev system based on improved principal component analysis," *7th World Congress on Intelligent Control and Automation*, pp. 8563-8568, 2008.

[128] X. Wang, U. Kruger, G. W. Irwin, G. McCullough and N. McDowell, "Nonlinear PCA With the Local Approach for Diesel Engine Fault Detection and Diagnosis," *IEEE Transactions on Control Systems Technology*, vol. 16, no. 1, pp. 122-129, Jan. 2008.

[129] A. Roskovic, R. Grbic and D. Sliskovic, "Fault tolerant system in a process measurement system based on the PCA method," *Proceedings of the 34th Internacional Convention*, pp. 1646-1651, May 2011.

[130] I. T. Jolliffe, Principal Component Analysis, 2nd Edition, US: Springer, 2002.

[131] I. Sommerville, "System Models," [Online]. Available: cc.ee.ntu.edu.tw/~farn/courses/SE/ch8.ppt. [Accessed 18 September 2012].

132] D. Foito, P. Silva, T. Barbosa, J. Maia and V. M. J. Fernão Pires, "New Real Coordinates Model for an Asymmetrical Six-Phase Induction Machine," *ACEMP - Electromotion*, September 2011.

[133] S. Chen and R. Zivanovic, "Modeling and simulation of stator and rotor fault conditions in induction machines for testing fault diagnostic techniques," *European Transactions on Electrical Power*, vol. 20, no. 5, pp. 611-629, 2010.

Appendix A

```
%% Fault Detection and Identification in Three-Phase Induction Motors
(PCA)
% Copyright (c) Miguel Marques.
% All rigths reserved.
% Distributions are not allowed to source code or binary forms,
% with or without modifications.
% THIS IS UNPUBLISHED PROPRIETARY SOURCE CODE OF Miguel Marques.
clc
clear all
close all
%load variaton_torque_healthy
%load variaton_torque_sfa06
%load variaton_torque_sfa03
%load variaton_torque_sfb06
%load variaton_torque_sfb03
%load variaton_torque_sfc06
%load variaton_torque_sfc03
%load variaton_torque_brb07
%load variaton_torque_brb05
%% Initializations
ts = 0.001;                             %Sampling Time
fs = 1/ts;                              %Sampling Frequency
period=20;                              %PCA Computation Window
%% Data Acquisition
current_a1 = i_stator_brb05_0.signals.values(:,1);
current_b1 = i_stator_brb05_0.signals.values(:,2);
current_c1 = i_stator_brb05_0.signals.values(:,3);
total_length = length(current_a1);
startup_removal = total_length-300;  %Sample Threshold to remove the
startup condition
partial_length = total_length - startup_removal;
if partial_length <= 0
    disp('Startup Sampe Threshold > Total Length')
end
current_a = current_a1(startup_removal:total_length);
current_b = current_b1(startup_removal:total_length);
current_c = current_c1(startup_removal:total_length);
tamanho = floor(partial_length/periodo);
ialpha = zeros(periodo,1);          % αβ _transform direct component
ibeta = zeros(periodo,1);           % αβ _transform quadrature component
ialpha_filtered = zeros(partial_length,1); % αβ _transform in PU
ibeta_filtered = zeros(partial_length,1);  % αβ _transform in PU
counter = 0;
S_arra = zeros(partial_length,1);%Array to storage all the αβ direct
components
S_arrb = zeros(partial_length,1);%Array to storage all the αβ quadrature
components
S_final = zeros(partial_length,2);%Concatenation of S_arra and S_arrb
amax_arr = zeros(tamanho,1);      %Max Value of the αβ direct components
bmax_arr = zeros(tamanho,1);      %Max Value of the αβ quadrature
components
eigenarr1 = zeros(tamanho,1);    %Eigenvalue 1 array
eigenarr2 = zeros(tamanho,1);    %Eigenvalue 2 array
maxerrorarr = zeros(tamanho,1);  %Severity Factor Array
```

```
Sstarr = zeros(tamanho,1);
t = (0:partial_length)*ts;
%% PCA Computation
for index=1:periodo:partial_length
    for i=1:periodo
        ialpha(i)=sqrt(2/3)*current_a(i+index-1)-
(1/sqrt(6))*current_b(i+index-1)-(1/sqrt(6))*current_c(i+index-1);
        ibeta(i)=(1/sqrt(2))*current_b(i+index-1)-
(1/sqrt(2))*current_c(i+index-1);
        S_arra(i+index-1)= ialpha(i);
        S_arrb(i+index-1)= ibeta(i);
    end
    counter = counter+1;
    amax_arr(counter) = max(ialpha);
    bmax_arr(counter) = max(ibeta);
    S = [ialpha ibeta];
    E=(S'*S);
    [V,D] = eig(E);
    D=diag(D);
    eigenarr1(counter) = D(1,1);
    eigenarr2(counter) = D(2,1);
    mineig=min(D);
    maxeig=max(D);
    maxerrorarr(counter) = 1 - (mineig/maxeig);
    if (maxerrorarr(counter) >= 0.1)
        disp('\\STATOR WINDING FAULT//')
        %Severity Factor for stator faults
        Sstarr(counter)=maxerrorarr(counter);
    else
        disp('\\HEALTHY MOTOR//')
    end
end
amax = max(amax_arr);
bmax = max(bmax_arr);
if (amax > bmax)
    maxval = amax;
else
    maxval = bmax;
end
for j=1:partial_length
    ialpha_filtered(j)= S_arra(j)/amax;
    ibeta_filtered(j)= S_arrb(j)/bmax;
end
mineig_aux = min(eigenarr2);
maxeig_aux = max(eigenarr2);
maxerror_aux = 1 - (mineig_aux/maxeig_aux);
    if (maxerror_aux < 0.05)
        mineig_aux = maxeig_aux;
        disp('\\MAX ERROR < 5%//')
    else
        disp('\\BROKEN ROTOR BAR//');
    end
%% Plots
subplot(2,1,1)
plot(t,current_a);
hold on
plot(t,current_b,'g');
plot(t,current_c,'r');
xlabel('Time (s)  (A)');
ylabel('Amplitude (A)');
title('Stator Currents');
```

```
legend('Current A','Current B','Current C');
subplot(2,1,2)
plot(ialpha_filtered,ibeta_filtered);
axis equal;
xlabel('Id(pu)    (B)');
ylabel('Iq(pu)');
title('dq Pattern');
grid
hold on
plot([0 V(1,2)],[0 V(2,2)],'r-');    % first eigenvector
plot([0 V(1,1)],[0 V(2,1)],'g-');    % second eigenvector
```